



Underlying-event studies with strange hadrons in pp collisions at $\sqrt{s} = 13$ TeV with the ATLAS detector

The ATLAS Collaboration

Properties of the underlying-event in pp interactions are investigated primarily via the strange hadrons K_S^0 , Λ and $\bar{\Lambda}$, as reconstructed using the ATLAS detector at the LHC in minimum-bias pp collision data at $\sqrt{s} = 13$ TeV. The hadrons are reconstructed via the identification of the displaced two-particle vertices corresponding to the decay modes $K_S^0 \rightarrow \pi^+\pi^-$, $\Lambda \rightarrow \pi^-p$ and $\bar{\Lambda} \rightarrow \pi^+\bar{p}$. These are used in the construction of underlying-event observables in azimuthal regions computed relative to the leading charged-particle jet in the event. None of the hadronisation and underlying-event physics models considered can describe the data over the full kinematic range considered. Events with a leading charged-particle jet in the range of $10 < p_T \leq 40$ GeV are studied using the number of prompt charged particles in the transverse region. The ratio $N(\Lambda \rightarrow \pi^\mp p^\pm)/N(K_S^0 \rightarrow \pi^+\pi^-)$ as a function of the number of such charged particles varies only slightly over this range. This disagrees with the expectations of some of the considered Monte Carlo models.

Contents

1	Introduction	2
2	The ATLAS detector	4
3	Data and Monte Carlo samples	5
4	Object selections	6
5	Event selections	8
6	Event and particle correction factors	9
7	Analysis strategy	11
8	Uncertainties	11
9	Results	14
10	Conclusion	19

1 Introduction

The simulation of proton-proton (pp) collisions at the Large Hadron Collider (LHC) is divided into several stages. Typically there is the calculation of a hard interaction in perturbative quantum chromodynamics (QCD), which is followed by QCD-inspired parton shower models and then a phenomenological treatment of the hadronisation of the resulting partons. These hadronisation models, such as the Lund string [1] and cluster [2] models, attempt to act as universal solutions: part of the description of almost all pp collisions. The accuracy of these hadronisation models affects the interpretation of our measurements.

An extra complication is that partons from the pp interaction, in addition to those in the hard scattering, can undergo scattering in a process known as multi-parton interaction (MPI). These additional interactions are typically much softer than the hard interaction which, presumably, triggered the recording of the event.

Typical models of hadronisation have parameters that are tuned using data recorded in e^+e^- collisions from the LEP collider [3, 4], as well as from the LHC [5] and other experiments. Much of these data uses the properties of particles identified only as charged hadrons, but K_S^0 and $(\Lambda + \bar{\Lambda})$ yields, and properties of strange mesons and baryons in general have also been important in determining these parameters. The parameter sets are known as ‘tunes’ when applied to models using the Monte Carlo (MC) method and are made public by the experimenters using them. The increasing size of the high-precision LHC datasets demands ever higher precision in the modelling, and motivates an expanded set of measurements to help tune the models. New approaches may also highlight regions where some models do not provide an adequate description.

The mass of the strange quark is close to the divergent scale of perturbative QCD, $\Lambda_{\text{QCD}} \sim 250$ MeV, which makes for a subtle interplay between kinematic effects and long-distance (low-energy) QCD interactions.

The formation of baryons also presents additional sensitivity via the three-way colour reconnection required for baryon formation.

This paper presents spectra measurements within individual pp interactions of the strange neutral hadrons K_S^0 , Λ and $\bar{\Lambda}$, as measured in low pile-up pp data recorded in 2015 by the ATLAS experiment at the LHC during $\sqrt{s} = 13$ TeV collisions. These strange hadrons are reconstructed in this analysis via their displaced decay vertices, and these particle species are used extensively by LHC experiments to explore hadronisation and fragmentation in hadronic interactions; prior studies include Refs. [6–15].

The $(\Lambda + \bar{\Lambda})$ and K_S^0 yields are presented normalised to the total number of events or to the total number of prompt charged-particles, and the relative $(\Lambda + \bar{\Lambda})$ to K_S^0 yields are presented in addition. These ATLAS data are compared with MC predictions within a fiducial volume where ATLAS maintains both a high reconstruction efficiency and a low probability of fakes (a mis-reconstructed particle).

Measurements are made following a so called underlying-event (UE) formalism that originated in studies of $p\bar{p}$ collision in CDF [16]; many UE measurements are made based on LHC collision data with different particle species at different centre of mass energies, including ATLAS [17], ALICE [18] and CMS [19].

The charged-particle jet with the highest transverse momentum (p_T) in each event, denoted the ‘leading jet’, defines an axis in the plane transverse to the beam directions. The azimuth is split into three equal size regions defined by the leading jet as shown in Figure 1. The towards region contains the $2\pi/3$ of the azimuth centred on the leading jet, the away region is π away and typically contains most hadronic recoil. Finally the transverse region is formed from the two opposite-sided $\Delta\phi \simeq \pm\pi/2$ regions from the leading jet, each of size $\pi/3$. The transverse region is expected to be the most sensitive region in which to study hadronisation effects associated with MPI as it is minimally contaminated by any leading $2 \rightarrow 2$ scattering process in the event.

The multiplicity of reconstructed K_S^0 , of the combined sum of Λ and $\bar{\Lambda}$, and of prompt charged-particles is measured in each of the towards, transverse and away regions as a function of two variables. First, the multiplicities are measured against the p_T of the leading jet in the event. Second, they are measured against the multiplicity of prompt charged-particles in the transverse region ($N_{\text{ch,trans}}$). This variable exhibits sensitivity to per-event MPI fluctuations. This follows from the study performed in Ref. [20] and complements other related measurements such as those performed by ALICE in Refs. [13, 14, 18, 21].

These measurements test a set of fragmentation properties that ATLAS has not previously probed, allowing a range of predictions from different MC models to be compared with data. None of the models considered are entirely satisfactory over the observables, and these data could be used to improve future simulations. Other recent modelling improvements such as the baryonic colour reconnection model integrated into the HERWIG MC generator in Refs. [22, 23] are also expected to be sensitive to the results in this paper.

The following chapters describe the ATLAS detector (Section 2) and the data and simulation samples (Section 3). This is followed by the analysis’ selections (Sections 4 and 5), correction factors (Section 6), strategy (Section 7), uncertainties (Section 8), and ends with a set of results as compared with MC models (Section 9) and final conclusions (Section 10).

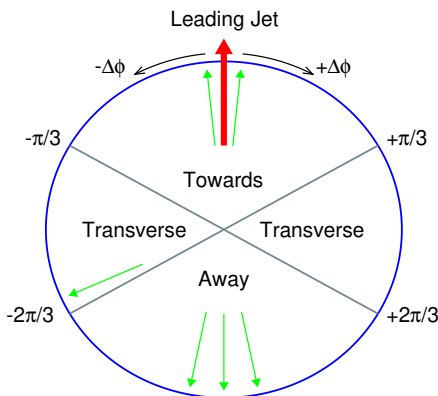


Figure 1: Illustration of the underlying-event regions relative to the leading jet.

2 The ATLAS detector

The ATLAS detector [24] at the LHC covers nearly the entire solid angle around the collision point.¹ It consists of an inner tracking detector surrounded by a thin superconducting solenoid, electromagnetic and hadronic calorimeters, and a muon spectrometer incorporating three large superconducting air-core toroidal magnets. The calorimeter and muon spectrometer detectors are not used by the analysis reported in this paper.

The inner-detector system (ID) is immersed in a 2 T axial magnetic field and provides charged-particle tracking in the range $|\eta| < 2.5$. The high-granularity silicon pixel detector covers the vertex region and typically provides four measurements per track, the first hit generally being in the insertable B-layer (IBL) installed before Run 2 [25, 26]. It is followed by the SemiConductor Tracker (SCT), which usually provides eight measurements per track. These silicon detectors are complemented by the transition radiation tracker (TRT), which enables radially extended track reconstruction up to $|\eta| = 2.0$. The TRT also provides electron identification information based on the fraction of hits (typically 30 in total) above a higher energy-deposit threshold corresponding to transition radiation.

The minimum-bias trigger scintillators (MBTS) [27] provide the trigger signal. These are mounted beyond the inner-detector volume at $z = \pm 3.56$ m and are segmented into two rings in pseudorapidity ($2.07 < |\eta| < 2.76$ and $2.76 < |\eta| < 3.86$), with eight azimuthal sectors in the inner ring and four in the outer.

Inelastic events are selected by the first-level trigger system implemented in custom hardware, followed by selections made by algorithms implemented in software in the high-level trigger [28]. The first-level trigger can accept events from the 40 MHz bunch crossings at a rate up to 100 kHz, but in the data sample used here it was pre-scaled to run at only about 1.5 kHz and all of the events were recorded without additional selection in the high-level trigger.

¹ ATLAS uses a right-handed coordinate system with its origin at the nominal interaction point (IP) in the centre of the detector and the z -axis along the beam pipe. The x -axis points from the IP to the centre of the LHC ring, and the y -axis points upwards. Polar coordinates (r, ϕ) are used in the transverse plane, ϕ being the azimuthal angle around the z -axis. The pseudorapidity is defined in terms of the polar angle θ as $\eta = -\ln \tan(\theta/2)$ and is equal to the rapidity $y = \frac{1}{2} \ln \left(\frac{E+p_z c}{E-p_z c} \right)$ in the relativistic limit. Angular distance is measured in units of $\Delta R \equiv \sqrt{(\Delta y)^2 + (\Delta \phi)^2}$.

A software suite [29] is used in data simulation, in the reconstruction and analysis of real and simulated data, in detector operations, and in the trigger and data acquisition systems of the experiment.

3 Data and Monte Carlo samples

Data from six LHC runs as recorded by the ATLAS detector in June 2015 are used. These runs had up to 29 colliding bunches with a large spatial separation between the colliding bunches, and with the probability of an inelastic interaction per bunch crossing being much smaller than one. Only data where the inner detector was operating nominally are included.

For five of the six runs, events were predominately recorded by a single-hemisphere primary trigger that required that at least one MBTS sector was above threshold. For a period during the sixth run, the primary trigger required at least one MBTS sector was above threshold in both the $+z$ and the $-z$ hemispheres of the detector. This two-hemisphere trigger selection introduces a slight bias towards events with a larger number of charged particles over a wider range of pseudorapidity. Events recorded by the two-hemisphere trigger are only used in the second part of the analysis that requires the event's leading jet to be in the range of $10 < p_T \leq 40$ GeV, as described in the following section. There are about 110M events recorded with the single-hemisphere trigger and an additional 20M events recorded exclusively with the two-hemisphere trigger.

All triggered events are required to be in coincidence with time windows in which proton bunches were present and colliding in both of the beams in ATLAS. The mean number of inelastic interactions per bunch-crossing, $\langle \mu \rangle$, varied over the runs between $0.003 < \langle \mu \rangle < 0.03$.

Three MC simulation samples are used: EPOS 3.4 [30] using the EPOS-LHC [31] tune, PYTHIA 8 inelastic [32] with the A2 [33] tune, and PYTHIA 8 inelastic with the Monash tune and modified colour-reconnection model [34] (which was used at particle level only). The ATLAS detector's response to the outputs of the EPOS-LHC and PYTHIA 8 A2 generators was simulated using GEANT4 [35, 36].

The EPOS MC provides an implementation of a parton-based Gribov-Regge theory [37], which is an effective QCD-inspired field theory describing the hard and soft scattering simultaneously. The treatment of string hadronisation in EPOS is dependent on the local density of string segments per unit volume relative to a critical-density parameter. Each string is classified as being in either a low density coronal region or in a high-density core region. Corona hadronisation proceeds via unmodified string fragmentation whereas the core is subjected to a hydrodynamic evolution, i.e. it is hadronised including additional contributions from longitudinal and radial flow effects [38]. This hydrodynamic collective flow approach to modelling MPI is contrasted against modelling in PYTHIA 8.

PYTHIA 8 inclusive pp non-diffractive events are dominated by t -channel gluon exchange whereas diffractive interactions are modelled via colour-singlet exchange. The modelling in PYTHIA 8 is based on leading-logarithmic initial- and final-state parton showers, a Lund-string hadronisation model, and particle-decays and soft-QCD modelling, in contrast to the hydrodynamic collective flow approach of EPOS. As the partonic cross-section for the t -channel gluon exchange exceeds the hadronic non-diffractive cross-section at low p_T , the existence of MPI is implied and included in PYTHIA 8 as an eikonal distribution of perturbative QCD scatterings, governed by impact-parameter and hadronic-overlap functions. The ATLAS minimum-bias tune A2 is used. This tune is based on the MSTW2008 leading order (LO) parton distribution function (PDF) set [39], and was tuned using ATLAS minimum-bias data at 7 TeV for the MPI parameters. It uses PYTHIA's MPI-based colour reconnection scheme, with mergers of colour flow between MPI systems

controlled by a reconnection-range parameter. It provides a good description of both the minimum-bias multiplicity and p_T distributions, and transverse energy-flow data [40].

The Monash [41] tune is used in combination with an alternate colour-reconnection model to provide an additional simulation parameterisation which is compared with data. This is latter referred to as PYTHIA 8 Monash+CR (Colour Reconnection). The Monash tune was constructed using Drell–Yan and underlying-event data from ATLAS, but also data from CMS, from the Super Proton Synchrotron, and from the Tevatron in order to constrain energy scaling. It uses the NNPDF 2.3 LO PDF set [42]. This tune gives an excellent description of the ATLAS 7, 8 and 13 TeV minimum-bias p_T spectra [43–45]. Monash is used in conjunction with the ‘Mode 2’ parameterisation of the colour-reconnection model from Ref. [34]. This model uses approximations to the full group-theoretical weights from SU(3) to compute probabilistic string topologies where short string lengths are favoured. This allows ‘string-junction’ structures to form, which provides a further source of baryon (and anti-baryon) production. This can arise at larger distances of order five femtometers, as compared with local baryon-production mechanisms.

4 Object selections

The following selections are imposed to identify candidate physics objects using the ATLAS inner-detector.

Prompt tracks: The prompt tracks selection only considers tracks reconstructed from the primary minimum bias tracking step, discussed in more detail in Ref. [46]. This step reconstructs tracks with a maximum transverse impact parameter of 10 mm. Prompt tracks are required to satisfy $p_T > 500$ MeV, $|\eta| < 2.5$, minimum hits requirements in the pixel and SCT, and a χ^2 requirement to remove mismeasured high- p_T tracks. Selected tracks are required to have both the transverse and longitudinal (multiplied by $\sin \theta$) absolute impact parameters relative to the primary vertex (see Section 5) of less than 1.5 mm. Tracks with $|\eta| < 2.5$ are used as input to jet reconstruction, with a requirement of $|\eta| < 2.1$ being later used to construct underlying-event observables. This minimises contamination from tracks originating from jets with $|\eta| \geq 2.1$.

Jets: The anti- k_t algorithm [47, 48] with a radius parameter of $R = 0.4$ is used to reconstruct charged-particle jets using the set of prompt tracks as input. The leading jet is defined as the highest- p_T jet satisfying $|\eta| < 2.1$; this η restriction prevents edge-effects by ensuring that tracks associated with the jet are all from within the tracking acceptance.

Large-radius tracks: ATLAS’ standard tracking is not optimised for the reconstruction of charged particles at large impact parameter; the large-radius tracking runs as a secondary tracking step to improve upon the reconstruction efficiency for these particles. The reconstruction of these tracks is important to maintain efficiency for low- p_T charged particles from strange hadron decay which can have large curvature. This secondary step forms tracks with space points that were not used in the primary minimum bias tracking step. The transverse (longitudinal) impact-parameter requirements applied during reconstruction are loosened significantly from 10 to 300 mm (250 to 1,500 mm) and the requirement of a pixel hit is dropped. Tracks reconstructed in the large-radius step are not used directly; instead they are supplied as additional inputs to a V^0 -finder algorithm.

Table 1: K_S^0 , Λ and $\bar{\Lambda}$ selection criteria.

	K_S^0	$\Lambda, \bar{\Lambda}$
$ \eta $	< 1.0	< 1.0
p_T	$> 400 \text{ MeV}$	$> 750 \text{ MeV}$
$\cos \theta$	> 0.9990	> 0.9998
R_{xy}	$4 \text{ mm} < R_{xy} \leq 300 \text{ mm}$	$15 \text{ mm} < R_{xy} \leq 300 \text{ mm}$
$M_{V^0}^{\text{err}}$	$< 15 \text{ MeV}$	$< 5 \text{ MeV}$
M_{V^0}	$ M_{V^0} - M_{K_S^0} < 20 \text{ MeV}$	$ M_{V^0} - M_{\Lambda} < 7 \text{ MeV}$

V^0 finder: Vertices reconstructed from a pair of oppositely-charged particle tracks are denoted ‘ V^0 ’. The V^0 -finder algorithm reconstructs candidate two-body decay vertices [8]. The algorithm iterates over all possible pairs of oppositely charged particle tracks in the combined sample of both the primary and the large-radius tracks; no quality selections are applied to the tracks before their use in the V^0 algorithm. The algorithm identifies two-particle vertex candidates with a χ^2 probability $> 1 \times 10^{-4}$. Candidates are rejected if the radius of the innermost space-point on either track is at a smaller radius than the V^0 candidate reconstructed position. The passing V^0 candidates form a preselection sample. They are fitted with each of the $K_S^0 \rightarrow \pi^+ \pi^-$, $\Lambda \rightarrow p \pi^-$ and $\bar{\Lambda} \rightarrow \bar{p} \pi^+$ particle hypothesis for the positive and negative charged-particle track.

Kaon and Lambda: The selection of K_S^0 , Λ and $\bar{\Lambda}$ candidates is made from the set of preselected V^0 . The selections favour a high-purity sample containing few fake V^0 . The selections are listed in Table 1; here θ is the angle in 3D between the direction of the candidate momentum and the line joining the primary and V^0 secondary vertices, R_{xy} is the decay length of the candidate projected on to the x, y plane, M_{V^0} is the candidate’s computed mass and $M_{V^0}^{\text{err}}$ is the uncertainty in this mass. Hadron masses are taken as $497.611 \pm 0.013 \text{ MeV}$ for K_S^0 and $1115.683 \pm 0.006 \text{ MeV}$ for Λ and $\bar{\Lambda}$ [49].

Candidates must also satisfy two subsequent cleaning selections. Pairs of selected V^0 of the same species are vetoed if they are less than a distance of $\Delta R < 0.1$ away from each other. This removes duplicate pairs of V^0 that reconstruct from a triplet of tracks. A V^0 is additionally vetoed if it simultaneously satisfies the K_S^0 and Λ , or K_S^0 and $\bar{\Lambda}$ selections, which removes ambiguous candidates. It is not possible for a V^0 to simultaneously satisfy the Λ and $\bar{\Lambda}$ selections.

Selected candidates are visualised in an Armenteros-Podolanski diagram [50] in Figure 2. In this 2D distribution the abscissa is used to plot the asymmetry of the momentum component of the V^0 ’s two tracks that is parallel to the V^0 ’s momentum vector, $\alpha = (p_{\parallel}^+ - p_{\parallel}^-)/(p_{\parallel}^+ + p_{\parallel}^-)$, and the ordinate to plot the momentum component of the two tracks that is perpendicular to the V^0 ’s momentum vector. K_S^0 have symmetric decays and hence a symmetric shape around $\alpha = 0.0$ whereas Λ populate the region near $\alpha = 0.5$ and $\bar{\Lambda}$ the region near $\alpha = -0.5$ as the p (or \bar{p}) takes a larger fraction of the decay momentum.

Particle-level selection: The particle level selection defines a fiducial volume, and the data are corrected and unfolded to match this definition. The particle level selection closely follows the reconstruction-level selection. Prompt particles are required to be stable (lifetime $\tau > 0.3 \times 10^{-10} \text{ s}$), to not be a charged baryon with lifetime $0.3 \times 10^{-10} < \tau \leq 3.0 \times 10^{-10}$ (see Ref. [46]), $|\eta| < 2.1$ (or $|\eta| < 2.5$, when being used as input to jet finding), have a non-zero charge and $p_T > 500 \text{ MeV}$.

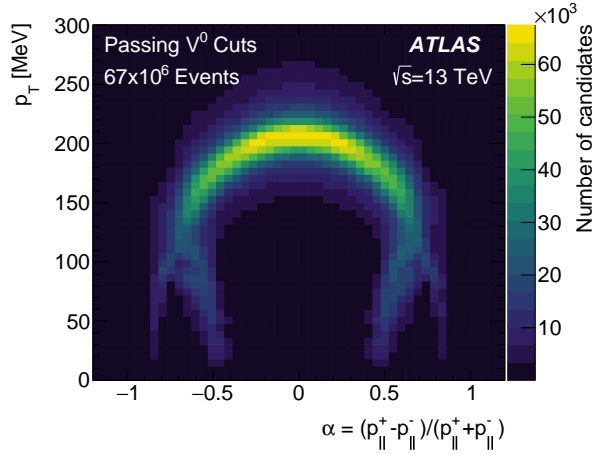


Figure 2: Armenteros-Podolanski diagram of all K_S^0 , Λ and $\bar{\Lambda}$ candidates in data, the ordinate has bin intervals of 6 MeV in p_T and the abscissa has bin intervals of 0.048 in α . See text for the definitions of the ordinate and abscissa.

The reconstruction of charged-particle jets at the particle-level is analogous to the jets selection above at the reconstruction-level.

Branching ratios are folded into the selection of weakly decaying strange hadrons. In addition to the $|\eta|$, p_T and R_{xy} requirements listed above in Table 1, selected K_S^0 , Λ and $\bar{\Lambda}$ are required to decay into $\pi^+\pi^-$, $p\pi^-$ and $\bar{p}\pi^+$, respectively. In all cases the two decay-children must satisfy $|\eta| < 2.5$, but there is no explicit p_T requirement on the children. Passing candidates of the same particle species that are less than a distance of $\Delta R < 0.1$ separation are vetoed to mirror the reconstruction-level selections.

5 Event selections

The following requirements are applied to select events for inclusion in the analysis. Physics objects as defined in Section 4 are used in the event selection.

Trigger: Data events are required to satisfy the trigger requirements detailed in Section 3.

Vertex: Data and MC events are required to contain a primary vertex reconstructed from two or more tracks with $p_T > 100$ MeV following the selection in Ref. [46]. Pile-up events are defined as data events containing two or more reconstructed primary vertices with four or more associated tracks each. These events are removed.

Track: Events are required to have at least one track with $p_T > 1$ GeV which passes the prompt tracking selection. Particle-level events similarly require at least one selected charged particle with $p_T > 1$ GeV.

Jet: Events where the leading jet satisfies $10 < p_T \leq 40$ GeV are classified as having satisfied the restricted leading-jet selection.

A total of 67M events satisfy the event selections in data, with a 1.4M event subset satisfying the restricted leading-jet selection. The available EPOS-LHC and PYTHIA 8 Monash+CR MC statistics are comparable in size to the data, whilst the PYTHIA 8 A2 sample is only around 25% of the size of the data.

6 Event and particle correction factors

Some detector effects are corrected for by the application of correction factors. These are applied as an event-level weight for the trigger, and as per-candidate weights for selected tracks and V^0 .

Data events selected by the single-hemisphere MBTS trigger are corrected to remove a small trigger inefficiency for low values of leading-jet p_T . This trigger is 98.8% efficient in events with a single track reconstructed relative to the beam spot with $p_T > 500$ MeV, and the efficiency quickly rises to 100% with five or more tracks. No trigger correction is applied to the two-hemisphere MBTS triggered sample due to this only being used in conjunction with a $10 < p_T \leq 40$ GeV requirement on the leading jet, for which the trigger is 100% efficient.

Selected prompt tracks and V^0 are corrected for detector effects by application of a per-track or per- V^0 weight. The initial computation of the weights with MC involves matching the selected prompt tracks and both of the decay tracks of the selected V^0 to particle level tracks. Inner-detector space points are associated with the charged particle that was found to produce the largest energy deposition. Reconstructed tracks are matched to charged particles based on the fraction of space points on the track that are common to both the reconstructed track and the particle-level particle.

The MC-derived average tracking efficiency for prompt charged pions with $p_T > 500$ MeV is 88% at central pseudorapidity, falling to 75% by $|\eta| = 2.1$. The track-correction weight includes efficiency corrections for charged particles that failed to be reconstructed, and corrections for reconstructed tracks that were not matched to particle level. The correction is assessed as a function of η and p_T . Details of the correction are found in Ref. [46].

V^0 are similarly corrected using MC-derived correction factors that are applied on a per- V^0 basis; the details are as follows.

The V^0 correction is factored into an efficiency correction, which is assessed as a function of p_T and R_{xy} , and a correction for fakes, which is quantified as a function of p_T , R_{xy} and $N_{\text{ch,local}}$. Here $N_{\text{ch,local}}$ counts the number of prompt selected tracks (i.e., from the primary vertex) within a cone of size $\Delta R = 0.2$ around the V^0 's momentum vector. It allows the probability of a selected V^0 arising due to combinatorial background or non-prompt strange-hadron production to be assessed as a function of the local charged-particle density. The probability that a Λ candidate is a fake rises from 15% for $N_{\text{ch,local}} = 0$ up to around 50% for $N_{\text{ch,local}} = 6$. The V^0 weight is the product of the efficiency weight ($w_\epsilon = 1/\epsilon$, $w_\epsilon \geq 1$) and the fakes weight ($w_f = 1 - \text{fake fraction}$, $w_f \leq 1$). Examples of the K_S^0 , Λ and $\bar{\Lambda}$ efficiency and fake distributions are presented in Figure 3.

The mean correction factor is found by integrating over the fiducial region. The EPOS-LHC reconstruction efficiency is $46.07 \pm 0.01\%$ for K_S^0 , $30.00 \pm 0.02\%$ for Λ , and $26.20 \pm 0.02\%$ $\bar{\Lambda}$. For comparison, the equivalent efficiency as computed with PYTHIA 8 A2 agrees to within $< 0.01\%$ (0.03%) for K_S^0 (Λ and $\bar{\Lambda}$). The quoted uncertainties include only the statistical error. The difference between Λ and $\bar{\Lambda}$ is due to the

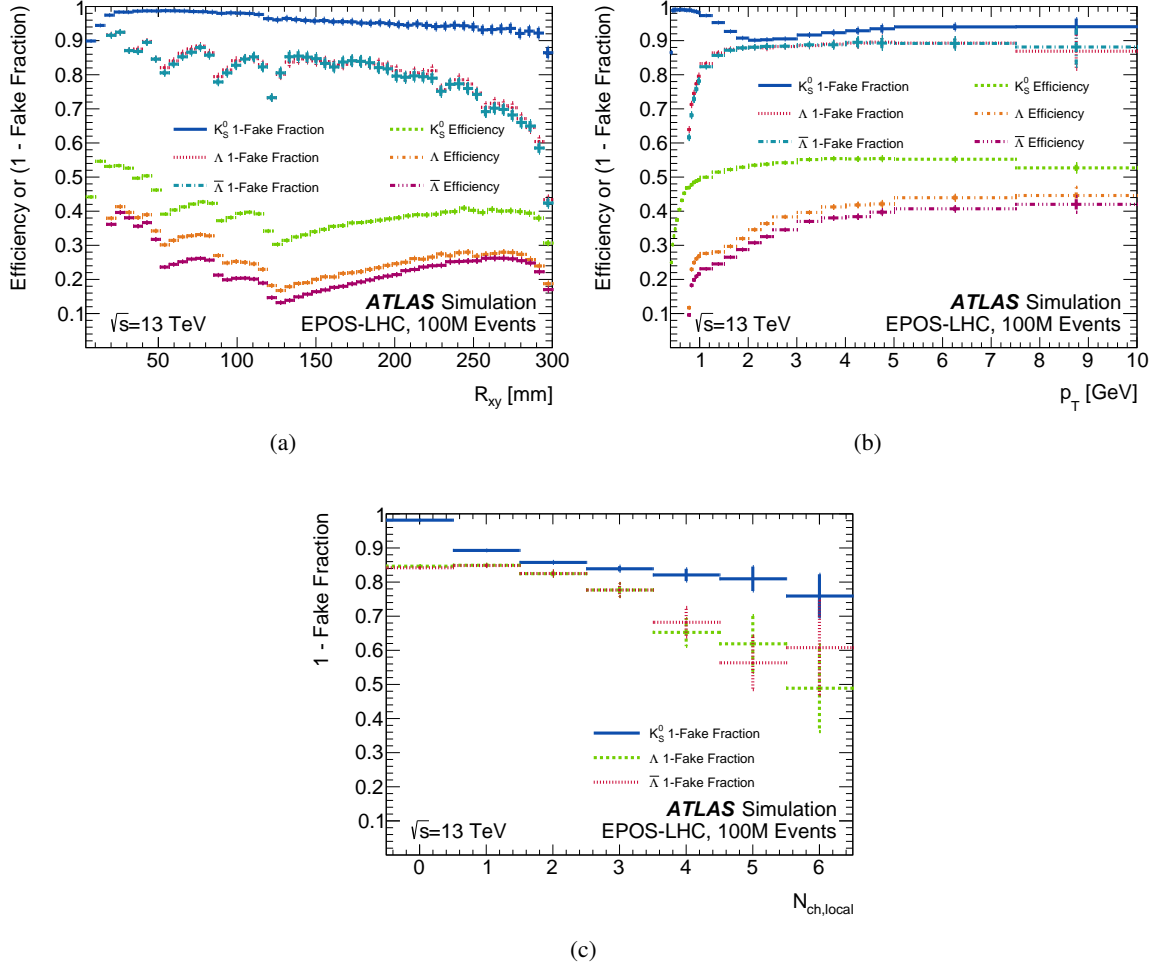


Figure 3: K_S^0 , Λ and $\bar{\Lambda}$ efficiency and (1-fake fraction) as computed from EPOS-LHC MC for (a) R_{xy} , (b) p_T , (c) $N_{ch,local}$. The structure as a function of R_{xy} displayed in (a) is due to the effect of pixel detector layers.

asymmetric momentum distribution in the decay together with the asymmetric efficiency of the ATLAS tracker relative to low-momentum charged-particles. The two MC simulations disagree in the fraction of selected V^0 for which the MC particle record does not contain a strange hadron. This was found to arise from PYTHIA 8 A2 underestimating the inclusive Λ and $\bar{\Lambda}$ yield by up to 50% whereas EPOS-LHC is within 10% of the data. Side-band studies were performed using the functional forms from Ref. [8] to fit the K_S^0 and $(\Lambda + \bar{\Lambda})$ line-shapes. These studies indicate that data and both of the MC simulations have comparable levels of combinatorial background. The combination of the comparable background with an under predicted yield results in PYTHIA 8 A2 predicting that on average 30% of the reconstructed Λ and $\bar{\Lambda}$ candidates fail to match against a selected particle-level hadron, versus 25% for EPOS-LHC. For K_S^0 it is around 4% for both of the MC simulations. EPOS-LHC is used to calculate the correction factors applied to the data due to its better agreement with data.

The strange-particle reconstruction efficiency was evaluated under systematically modified ATLAS geometry models derived from the studies in Ref. [51]. The largest effect was observed from a 5% increase in all non-silicon material volumes in the inner detector. The mean efficiency under this geometry model

was reduced by 0.7% for K_S^0 and 0.4% for $(\Lambda + \bar{\Lambda})$, with the largest reduction for V^0 at the low- p_T kinematic limit.

Systematic uncertainties are added for both the fake-fraction evaluation via side-bands and efficiency evaluation via material effects in simulation, as discussed in Section 8.

7 Analysis strategy

For data and MC simulated events, the leading jet in selected events is used to define the towards, transverse, and away regions of the event. The multiplicity is computed separately in each of these three regions for the selected K_S^0 candidates, the combined set of $(\Lambda + \bar{\Lambda})$ selected V^0 candidates, and for the selected prompt charged-particles. The per-candidate correction weights from Section 6 and Ref. [46] are applied when computing these observables. A further observable ‘event count’ is added; this observable is used to count the events in each bin of (e.g.) leading-jet p_T and therefore allows per-event normalised figures to be formed. Final results are obtained by taking the ratio either between pairs of multiplicity observables, or as a multiplicity observable normalised to the event observable. This normalisation step is performed at the end of the analysis after all events are processed.

Each of the observable’s distributions are unfolded before taking these ratios using an iterative method [52] with four iterations, after which the process is observed to converge. Simulation from EPOS-LHC is used for the response matrix in the unfolding. The unfolding procedure corrects for migrations between different p_T bins of the reconstructed and particle-level leading jet. It does not correct for strange hadron or prompt charged-particle reconstruction effects; these were corrected for by the application of the per-candidate weights incorporated into the observables.

The first set of results are presented as a function of leading-jet p_T . The K_S^0 and $(\Lambda + \bar{\Lambda})$ multiplicities are normalised to either the prompt charged-particle multiplicity in the same underlying-event region, or to the ‘event count’ observable to obtain the mean yield. These are shown below in Figures 5 and 6.

This analysis strategy is repeated for events satisfying the restricted leading-jet selection, $10 < p_T \leq 40$ GeV. There is less of a dependency on the leading-jet p_T in this regime of higher- p_T hard-interactions, hence the choice of plot abscissa is changed to be the multiplicity of prompt charged-particles in the transverse region ($N_{\text{ch,trans}}$).

Ratios are presented as a function of $N_{\text{ch,trans}}$ for the K_S^0 and $(\Lambda + \bar{\Lambda})$ multiplicities as normalised to the prompt charged-particle multiplicity in the towards region in Figures 7(a), 7(b), and of the relative yield of $(\Lambda + \bar{\Lambda})$ multiplicity to K_S^0 multiplicity in the towards and transverse regions in Figures 7(c) and 7(d).

8 Uncertainties

The following sources of systematic uncertainty are considered. They are assumed to be uncorrelated and are combined in quadrature. Unless noted, the systematic uncertainties are symmetrised around the central value. The unfolding prior, unfolding model, and non-closure systematic uncertainties below are all smoothed with a Gaussian kernel whose width is three times the width of the current bin, to mitigate the effect of statistical fluctuations.

Unfolding prior dependence: The dependence on the MC unfolding prior is evaluated using a reweighting method. The ratio is taken between MC simulation and data for each reconstructed observable and a spline-based interpolation between bins is used to convert this ratio into a weighting function. A reweighted variant of EPOS-LHC acting as pseudo-data is produced. For each event the reweighting function is evaluated based on the particle level leading-jet p_T or $N_{\text{ch,trans}}$, the weight is applied to the observable at both the particle and reconstruction levels. The EPOS-LHC pseudo-data are unfolded through the nominal EPOS-LHC response matrix with the nominal number of iterations. The percentage deviation of the unfolded EPOS-LHC pseudo-data with respect of the reweighed EPOS-LHC particle level distribution is taken as a source of uncertainty.

Unfolding model: Data are unfolded through response matrices constructed using the PYTHIA 8 A2 MC sample as opposed to the nominal EPOS-LHC MC sample. The per- V^0 correction factors applied to both the data and the PYTHIA 8 reconstructed V^0 still wholly originate from EPOS-LHC. This procedure checks for differences between EPOS and PYTHIA 8 in the modelling of the leading charged-particle (required to be greater than 1 GeV), the leading jet, and any differences between the modelling of event re-orientation (see below). It also checks against any residual effects from unfolding using a model with a different strange hadron yield, as PYTHIA 8 A2's $(\Lambda + \bar{\Lambda})$ yield is significantly smaller than in data. The percentage difference between data unfolded with an EPOS-LHC response matrix and a PYTHIA 8 A2 response matrix is taken as a source of uncertainty.

Strange-hadron correction systematic uncertainties: A study was performed in which the probability of selecting a fake V^0 was obtained by fitting the K_S^0 , Λ and $\bar{\Lambda}$ line-shapes as discussed in Section 6. Inside of the analysis' mass-window, the contribution of the fit associated with combinatorial background differs by a maximum of 2% between the EPOS-LHC MC simulation used to derive the correction factors and the data.

The effect of uncertainty in the material budget of the ATLAS detector model was also included in this systematic via a second study, as additionally discussed in Section 6. The efficiency correction factor is modified by a power law that acts to reduce the efficiency by 4% at a V^0 p_T of 400 MeV, and increase it by 2%, clamped, for $p_T \geq 8$ GeV.

Both the flat 2% variation in the associated per- V^0 fakes corrections weight and the power-law variation in the per- V^0 efficiency corrections weight are varied independently and included in the strange hadron correction systematic for all of K_S^0 , Λ and $\bar{\Lambda}$.

Final contributions in this category are derived from the statistical uncertainty in the evaluation of the efficiency and of the fake fraction. These two components of the V^0 correction weight were independently varied positively and negatively by the respective asymmetric statistical uncertainty.

Prompt-track systematic uncertainties: Systematic uncertainties on prompt tracks from Ref. [46] are included when the multiplicity of prompt tracks is evaluated. This includes the effects of inner-detector material uncertainty, the effect of the χ^2 requirement applied to high- p_T tracks, plus an additional flat 0.5% systematic.

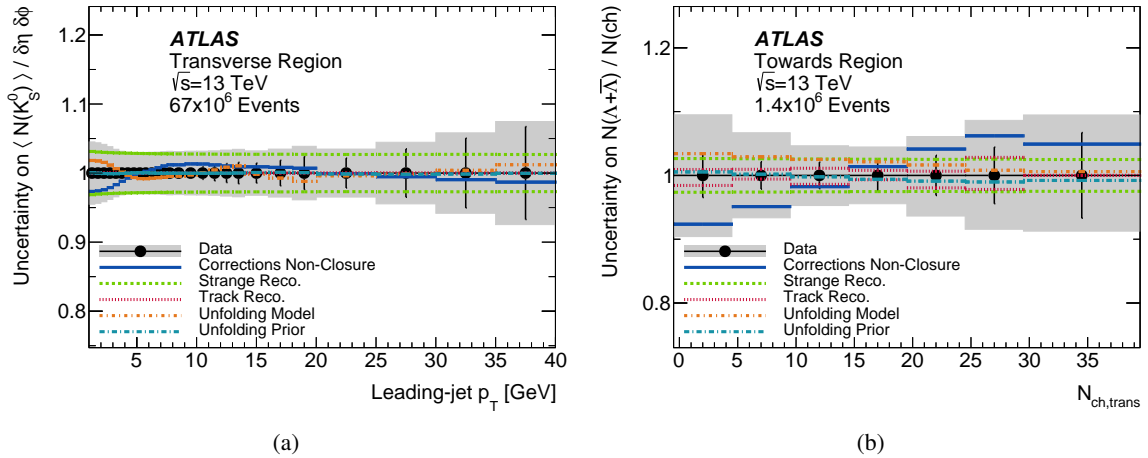


Figure 4: Breakdown of uncertainties in the measurement of (a) the event-normalised mean number of K_S^0 in the transverse region as a function of leading-jet p_T , and (b) for the $(\Lambda + \bar{\Lambda})$ multiplicity as normalised to the prompt charged-particle multiplicity in the towards region as a function of $N_{ch,trans}$. Error bars show the statistical error and the shaded bands show the total uncertainty. The ‘Model’, ‘Prior’ and ‘Non-closure’ systematic uncertainties are symmetrised.

Non-closure correction and systematic uncertainty: The EPOS-LHC reconstruction-level observables, including per-particle weighting, are unfolded through the EPOS-LHC response matrices. The term non-closure is used to refer to any residual differences that remain between a reconstruction level MC distribution that was fully corrected for all detector-effects and the corresponding particle level distribution from the same MC sample. Any non-closure is taken both as a correction factor, and as a conservative systematic uncertainty. The application of the correction is integrated into the bootstrap procedure. Many effects can cause this non-closure. Event re-orientation effects are where the ϕ of the leading reconstructed jet does not match the ϕ of the leading particle-level jet. This causes a misalignment of the three underlying-event regions between the particle level and the reconstruction level. The MC modelling of the effect is primarily encoded in the off-diagonal bins of the response matrices as it correlates with a mismatched jet p_T between particle level and reconstruction level. Other causes of non-closure effect arise from the V^0 efficiency correction. This correction is computed in bins of particle-level strange hadron kinematics and is then applied on a statistical basis as a correction to the set of reconstructed V^0 candidates.

Two illustrative breakdowns of the systematic uncertainties are shown in addition to the statistical uncertainty and the total uncertainty in Figure 4, where one breakdown is chosen for each of the two choices of plot abscissa from the following results section. These systematic uncertainties are representative of the final Figures 5, 6 and 7. All of these figures are obtained from the ratio of two unfolded observables. A bootstrap method [53] is used to obtain the statistical error in each bin. This bootstrap technique uses 500 pseudo-runs in both the data and the MC simulation, each differing as expected across observables due to correlated statistical fluctuations. These correlations are propagated to all of Figures 4, 5, 6 and 7. The statistical error for each bin in all final figures is taken as the root mean square over all pseudo-runs; the covariance between pairs of bins is computed at the same time.

9 Results

K_S^0 and $(\Lambda + \bar{\Lambda})$ multiplicities are presented in Figures 5 and 6 as a function of the leading-jet p_T , with two choices of normalisation. The event-normalised mean distributions show distinct soft and hard regimes, separated by a leading-jet p_T of around 10 GeV. The mean values in all distributions show a strong monotonic rise in the soft regime. In the hard regime the mean values either remain constant over the considered range, or continue to rise with a significantly smaller slope. This soft/hard transition is less distinct against the normalisation to the prompt charged-particle yield, here the strange-to-prompt yield is suppressed at low values of leading-jet p_T for $(\Lambda + \bar{\Lambda})$ and for K_S^0 in the transverse region. However for K_S^0 in the towards and away regions it is enhanced. The soft regime is discussed first, followed by the hard regime.

No model gives a perfect description of the data, but the EPOS-LHC model gives the best overall performance in the soft regime for both of the choices of normalisation. At a leading-jet p_T of around 5 GeV, EPOS-LHC is observed to correctly model the normalisation for both of the K_S^0 and $(\Lambda + \bar{\Lambda})$ mean multiplicities over all underlying-event regions, the agreement is not as good when normalised to prompt charged-particles but EPOS-LHC remains in best or joint-best agreement. At very low leading-jet p_T , EPOS-LHC has a tendency to underestimate, especially for relative baryon yields. Similar and indeed larger trends are observed in the other models. An exception however is the Monash+CR model of the K_S^0 and $(\Lambda + \bar{\Lambda})$ relative yields in the towards region, as shown in Figures 5(c), 5(d), 6(c) and 6(d). The Monash+CR model generally performs as well or better than EPOS-LHC here in the towards region at low leading-jet p_T .

The PYTHIA 8 A2 model makes predictions that are significantly too low in all distributions in the soft regime. The underestimation is large in magnitude, up to 40% for the K_S^0 distributions in Figure 5 and up to 60% for the $(\Lambda + \bar{\Lambda})$ distributions in Figure 6. The PYTHIA 8 Monash+CR model performs better than the A2 model for all distributions.

The distributions show a much weaker dependence on the leading-jet p_T in the hard regime. Here the pp interactions are predominately non-diffractive and at low impact parameter, the activity observed is hence driven by the multiple soft and semi-hard interactions occurring in each event that constitute the underlying-event. The towards and away regions maintain a tendency for the event-normalised mean multiplicity to rise as a function of increasing leading-jet p_T whereas it falls for the prompt-charged normalised cases. The slope is however considerably shallower in the hard regime for both of the choices of normalisation. The transverse region in data is predominately flat over the considered range of the hard regime between $10 < p_T \leq 40$ GeV. This is in part by construction, as this region of the azimuth is minimally affected by any leading partonic $2 \rightarrow 2$ scattering interaction. It is noted that while the event-normalised mean is observed to have only a small dependence on the leading-jet p_T , individual events may show large deviations from the mean, as explored below.

The EPOS-LHC model does not do as well in the hard regime as it did in the soft regime, likely a consequence of it lacking a hard-scattering model. A common characteristic seen in all event-normalised EPOS-LHC distributions is a decrease in the mean multiplicity above approximately 8 GeV in the leading-jet p_T , and a slower increase above 13 GeV. This deviation from a monotonic rise over the transition from a soft to a hard event structure is not observed in the other considered models, nor would such a dip hypothesis be drawn from the data. After this dip, the EPOS-LHC model predicts a slow monotonic rise in the event normalised yield and slow monotonic fall in the prompt charged-particle normalised yield, the shape of which are generally in good agreement with data. The overall normalisation following the dip

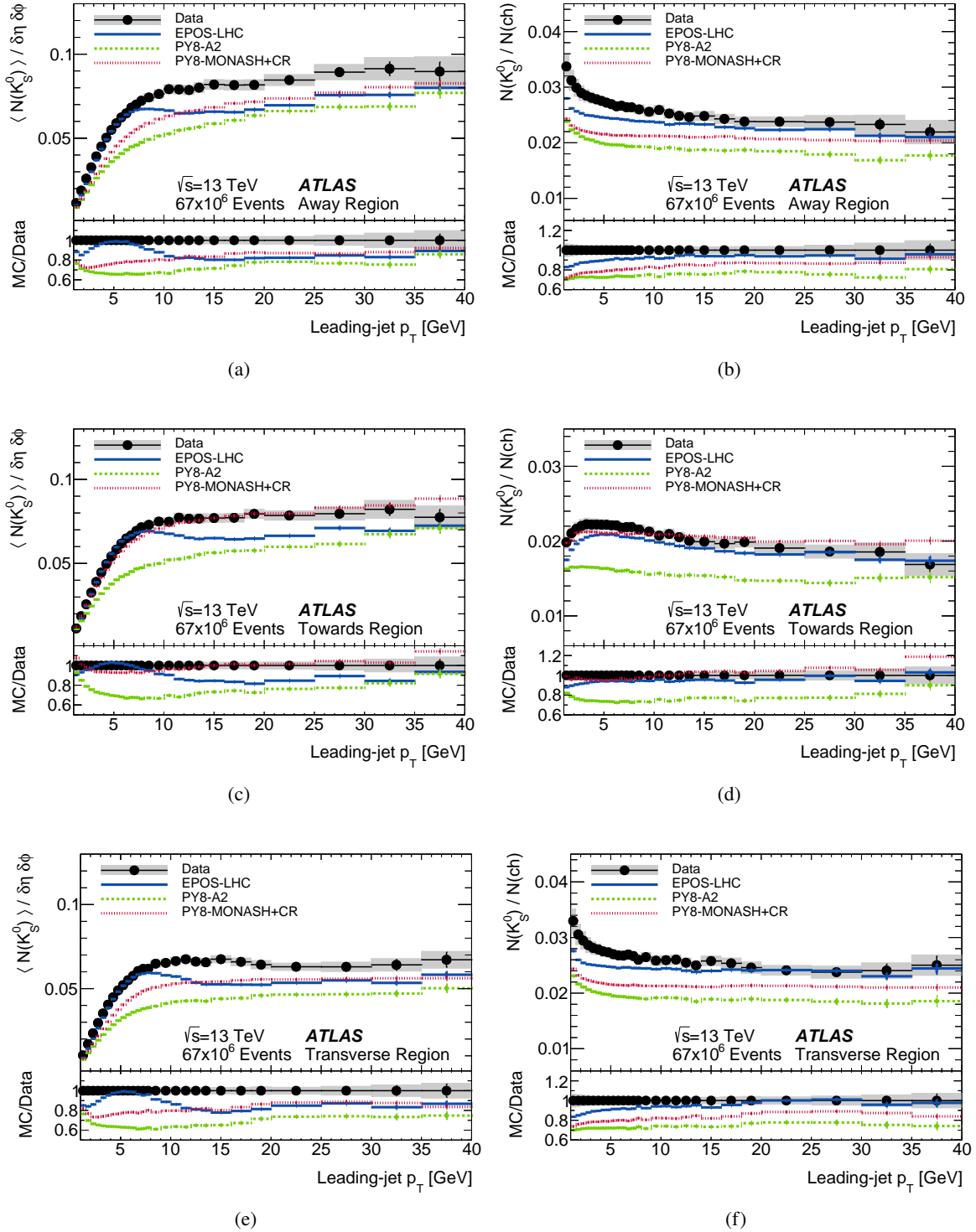


Figure 5: (Left) Per event and per unit (η, ϕ) normalised and (right) prompt charged-particle normalised K_S^0 yields as a function of leading-jet p_T in the (a, b) away, (c, d) towards and (e, f) transverse regions. Error bars show the statistical error and the shaded bands show the total uncertainty.

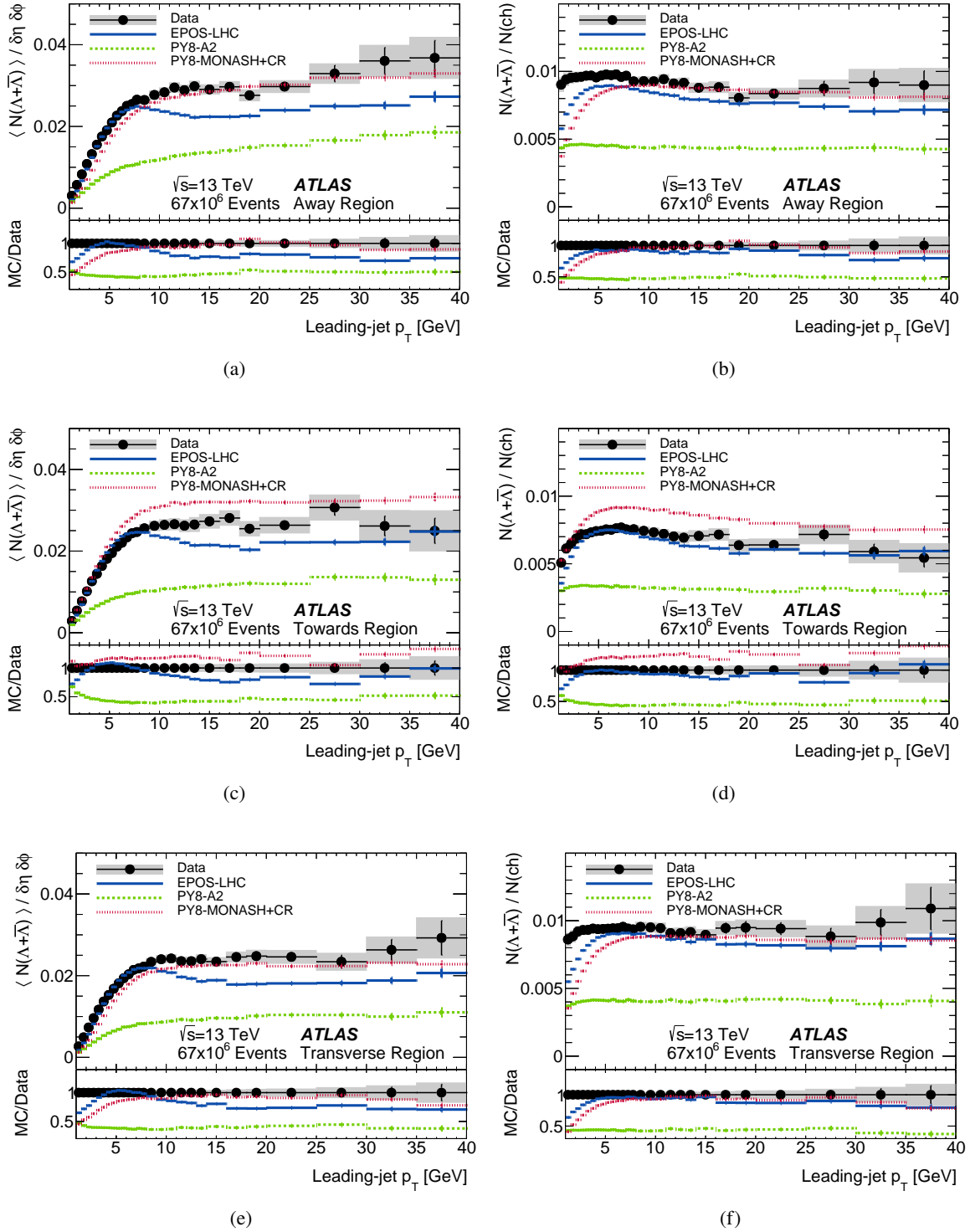


Figure 6: (Left) Per event and per unit (η, ϕ) normalised and (right) prompt charged-particle normalised $(\Lambda + \bar{\Lambda})$ yields as a function of leading-jet p_T in the (a, b) away, (c, d) towards and (e, f) transverse regions. Error bars show the statistical error and the shaded bands show the total uncertainty.

region remains too low, however, in the event normalised sample when compared with data. EPOS-LHC under predicts the data by up to 20% in the hard regime.

The PYTHIA 8 A2 model performs well in modelling the shape of the distributions in the hard regime. However, the large under predictions from the soft regime carry forward and the A2 model continues to under predict by 20%–40% for K_S^0 distributions, and by 40%–60% for $(\Lambda + \bar{\Lambda})$ distributions for both of the choices of normalisation. The shape of the PYTHIA 8 Monash+CR distribution is comparable to A2; however the Monash+CR model is shown to more accurately model an overall higher observed multiplicity in the hard regime. The PYTHIA 8 Monash+CR model is observed to be in good agreement with data when modelling the mean multiplicity of K_S^0 in the toward region, and of $(\Lambda + \bar{\Lambda})$ in both the away and transverse regions, for both of the choices of normalisation.

For a comparable UE measurement using only prompt charged particles such as Ref. [17], the agreement between data and MC simulation is typically 20% or better, whereas for the strange-particle species in this analysis, differences between data and MC simulation exceeding 50% are observed for some distributions.

The data discussed so far as being in the hard regime are explored further in Figure 7. The sample of events whose leading jet lies inside $10 < p_T \leq 40$ GeV are included in these figures, with the per-event number of prompt charged-particles in the transverse region ($N_{\text{ch,trans}}$) used to define the plot abscissa. $N_{\text{ch,trans}}$ is used as a proxy for the number of soft and semi-hard interactions within the pp collision in this subset of events.

The K_S^0 and $(\Lambda + \bar{\Lambda})$ yields as normalised to the charged-particle yield are shown in Figures 7(a) and 7(b) in the towards region. The model disagreement is worse at small values of $N_{\text{ch,trans}}$ which correspond to events with little activity in the transverse region. EPOS-LHC performs the best here, with the PYTHIA 8 A2 model continuing to underestimate the yield while better modelling the shape. The PYTHIA 8 Monash+CR model predicts no dependence on the relative K_S^0 yield with $N_{\text{ch,trans}}$ in the towards region, which is not in agreement with the data.

In Figures 7(c) and 7(d) the ratio of $(\Lambda + \bar{\Lambda})$ to K_S^0 multiplicity is presented in the towards and transverse regions. The data show only a weak dependence on the $(\Lambda + \bar{\Lambda})$ to K_S^0 ratio in the transverse region as a function of $N_{\text{ch,trans}}$. Of the considered models, only the more simplistic (with regards to the modelling of strange production in the underlying-event) PYTHIA 8 A2 model correctly predicts that the $(\Lambda + \bar{\Lambda})$ to K_S^0 ratios are largely insensitive to the $N_{\text{ch,trans}}$ activity levels in the event. However, the absolute value of the ratio from the PYTHIA 8 A2 model is under predicted by around 40%, due to the underproduction of $(\Lambda + \bar{\Lambda})$ hadrons in the A2 model relative to data.

These trends may be contrasted with the ALICE measurement in Ref. [13]. A similar enhancement of the strange yield relative to prompt charged-particles is observed by ALICE with respect to prompt charged pions for K_S^0 and $(\Lambda + \bar{\Lambda})$. This is seen here in Figures 7(a), 7(b) in the towards region of events at higher values of $N_{\text{ch,trans}}$. This is the opposite trend than what was observed above in Figures 5(d) and 6(d) where the equivalent strange-particle yields in the towards region were decreasing as a function of increasing leading-jet p_T . This highlights the importance of considering both of the choices of abscissa when investigating the modelling of colour-reconnection effects.

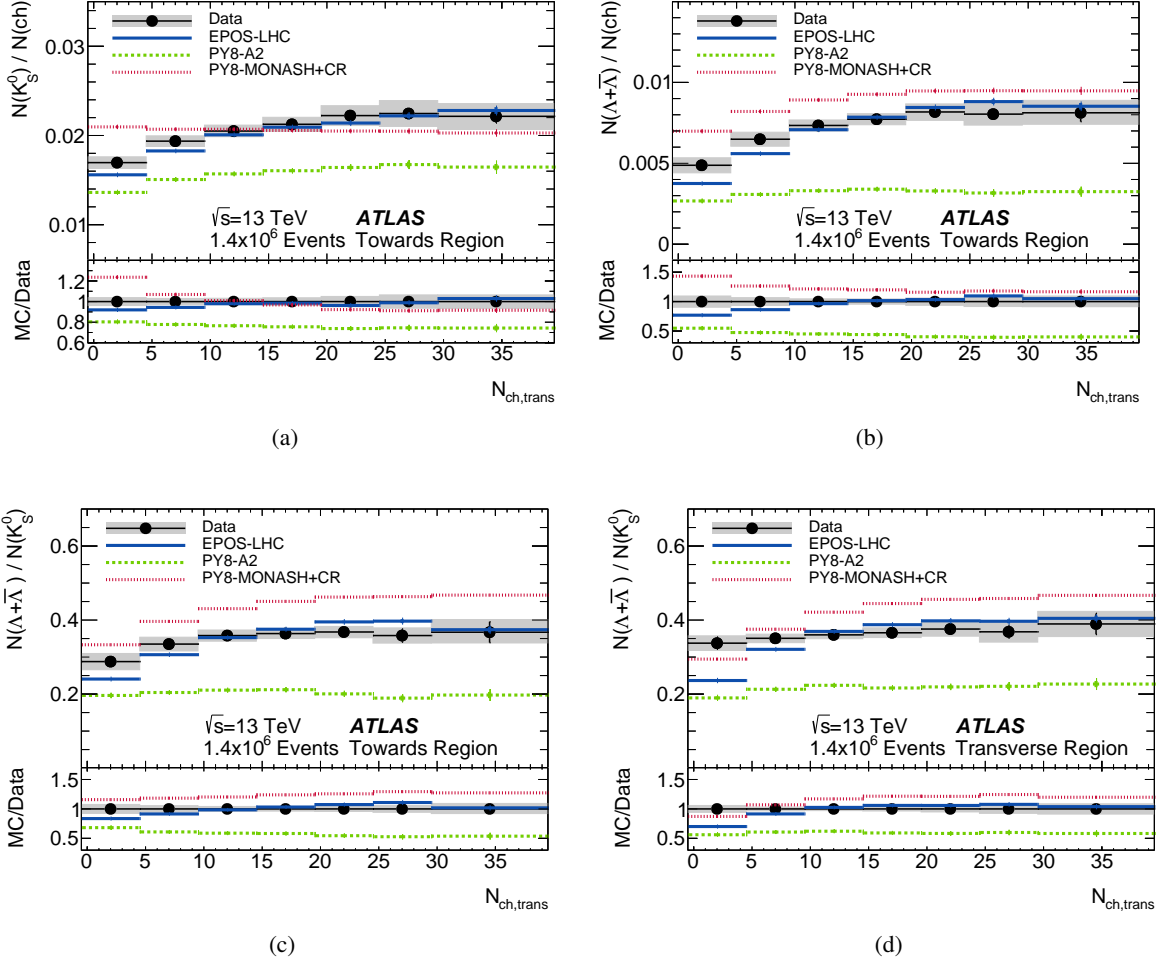


Figure 7: Comparison between data and MC simulation for several multiplicity ratios as a function of $N_{\text{ch,trans}}$ in events with leading jet $10 < p_T \leq 40$ GeV. Shown are the prompt charged-particle normalised (a) K_S^0 and (b) $(\Lambda + \bar{\Lambda})$ multiplicity yields in the towards region, and relative yields of $(\Lambda + \bar{\Lambda})$ to K_S^0 in the (c) towards and (d) transverse regions. Error bars show the statistical error and the shaded bands show the total uncertainty.

10 Conclusion

Properties of the underlying-event are investigated via the strange hadrons K_S^0 , Λ and $\bar{\Lambda}$ in ATLAS minimum-bias pp collision data at $\sqrt{s} = 13$ TeV. The hadrons are reconstructed via the identification of the displaced two-particle vertices corresponding to the decay modes $K_S^0 \rightarrow \pi^+\pi^-$, $\Lambda \rightarrow \pi^-p$ and $\bar{\Lambda} \rightarrow \pi^+\bar{p}$.

K_S^0 , Λ and $\bar{\Lambda}$ multiplicity ratios are constructed normalised to the number of events, or to the prompt charged-particle multiplicity in the underlying event ‘toward’, ‘transverse’ and ‘away’ regions relative to the azimuthal angle ϕ of the leading charged-particle jet. They are compared to different MC simulation models.

PYTHIA 8 A2 is able to describe the dependence of these observables on the leading-jet p_T for both of the K_S^0 and $(\Lambda + \bar{\Lambda})$ distributions, but underestimates the yields by around 40%–50%. PYTHIA 8 Monash+CR displays an enhanced K_S^0 yield and a significantly enhanced $(\Lambda + \bar{\Lambda})$ yield bringing it more in alignment with data. EPOS-LHC is better able to model the rise with leading-jet p_T , however it typically plateaus out too early – and even decreases in some event-normalised observables at yet higher leading-jet p_T . This is counter to what was observed in the data.

A further selection takes events whose leading jet has $10 < p_T \leq 40$ GeV. The Λ/K_S^0 ratio is observed to have little dependence of the number of prompt charged-particles in the transverse region, which acts here as a proxy for the number of multi-parton interactions in the event. An enhancement of the K_S^0 and $(\Lambda + \bar{\Lambda})$ to prompt charged-particles ratios in the towards region is observed for larger values of the number of prompt charged-particles in the transverse region. The EPOS-LHC model is in best agreement with these data.

These data measurements are particularly sensitive to the theoretical modelling and MC tuning of strange and baryon production during hadronisation and may be used to constrain theoretical modelling of non-perturbative effects within individual pp interactions.

Acknowledgements

We thank CERN for the very successful operation of the LHC and its injectors, as well as the support staff at CERN and at our institutions worldwide without whom ATLAS could not be operated efficiently.

The crucial computing support from all WLCG partners is acknowledged gratefully, in particular from CERN, the ATLAS Tier-1 facilities at TRIUMF/SFU (Canada), NDGF (Denmark, Norway, Sweden), CC-IN2P3 (France), KIT/GridKA (Germany), INFN-CNAF (Italy), NL-T1 (Netherlands), PIC (Spain), RAL (UK) and BNL (USA), the Tier-2 facilities worldwide and large non-WLCG resource providers. Major contributors of computing resources are listed in Ref. [54].

We gratefully acknowledge the support of ANPCyT, Argentina; YerPhI, Armenia; ARC, Australia; BMWFW and FWF, Austria; ANAS, Azerbaijan; CNPq and FAPESP, Brazil; NSERC, NRC and CFI, Canada; CERN; ANID, Chile; CAS, MOST and NSFC, China; Minciencias, Colombia; MEYS CR, Czech Republic; D NRF and DNSRC, Denmark; IN2P3-CNRS and CEA-DRF/IRFU, France; SRNSFG, Georgia; BMBF, HGF and MPG, Germany; GSRI, Greece; RGC and Hong Kong SAR, China; ISF and Benoziy Center, Israel; INFN, Italy; MEXT and JSPS, Japan; CNRST, Morocco; NWO, Netherlands; RCN, Norway; MNiSW, Poland; FCT, Portugal; MNE/IFA, Romania; MESTD, Serbia; MSSR, Slovakia; ARRS and

MIZŠ, Slovenia; DSI/NRF, South Africa; MICINN, Spain; SRC and Wallenberg Foundation, Sweden; SERI, SNSF and Cantons of Bern and Geneva, Switzerland; MOST, Taipei; TENMAK, Türkiye; STFC, United Kingdom; DOE and NSF, United States of America.

Individual groups and members have received support from BCKDF, CANARIE, CRC and DRAC, Canada; PRIMUS 21/SCI/017, CERN-CZ and FORTE, Czech Republic; COST, ERC, ERDF, Horizon 2020, ICSC-NextGenerationEU and Marie Skłodowska-Curie Actions, European Union; Investissements d’Avenir Labex, Investissements d’Avenir Idex and ANR, France; DFG and AvH Foundation, Germany; Herakleitos, Thales and Aristeia programmes co-financed by EU-ESF and the Greek NSRF, Greece; BSF-NSF and MINERVA, Israel; Norwegian Financial Mechanism 2014-2021, Norway; NCN and NAWA, Poland; La Caixa Banking Foundation, CERCA Programme Generalitat de Catalunya and PROMETEO and GenT Programmes Generalitat Valenciana, Spain; Göran Gustafssons Stiftelse, Sweden; The Royal Society and Leverhulme Trust, United Kingdom.

In addition, individual members wish to acknowledge support from CERN: European Organization for Nuclear Research (CERN PIAS); Chile: Agencia Nacional de Investigación y Desarrollo (FONDECYT 1190886, FONDECYT 1210400, FONDECYT 1230987); China: National Natural Science Foundation of China (NSFC - 12175119, NSFC 12275265, NSFC-12075060); Czech Republic: Czech Science Foundation (GACR - 24-11373S), Ministry of Education Youth and Sports (FORTE CZ.02.01.01/00/22_008/0004632); European Union: European Research Council (ERC - 948254, ERC 101089007), Horizon 2020 Framework Programme (MUCCA - CHIST-ERA-19-XAI-00), Italian Center for High Performance Computing, Big Data and Quantum Computing (ICSC, NextGenerationEU); France: Agence Nationale de la Recherche (ANR-20-CE31-0013, ANR-21-CE31-0013, ANR-21-CE31-0022), Investissements d’Avenir Labex (ANR-11-LABX-0012); Germany: Baden-Württemberg Stiftung (BW Stiftung-Postdoc Eliteprogramme), Deutsche Forschungsgemeinschaft (DFG - 469666862, DFG - CR 312/5-2); Italy: Istituto Nazionale di Fisica Nucleare (ICSC, NextGenerationEU); Japan: Japan Society for the Promotion of Science (JSPS KAKENHI Grant No. 22KK0227, JSPS KAKENHI JP21H05085, JSPS KAKENHI JP22H01227, JSPS KAKENHI JP22H04944); Netherlands: Netherlands Organisation for Scientific Research (NWO Veni 2020 - VI.Veni.202.179); Norway: Research Council of Norway (RCN-314472); Poland: Polish National Agency for Academic Exchange (PPN/PPO/2020/1/00002/U/00001), Polish National Science Centre (NCN 2021/42/E/ST2/00350, NCN OPUS nr 2022/47/B/ST2/03059, NCN UMO-2019/34/E/ST2/00393, UMO-2020/37/B/ST2/01043, UMO-2021/40/C/ST2/00187, UMO-2022/47/O/ST2/00148, UMO-2023/49/B/ST2/04085); Slovenia: Slovenian Research Agency (ARIS grant J1-3010); Spain: Generalitat Valenciana (Artemisa, FEDER, IDIFEDER/2018/048), Ministry of Science and Innovation (MCIN & NextGenEU -PCI2022-135018-2, MICIN & FEDER -PID2021-125273NB, RYC2019-028510-I, RYC2020-030254-I), PROMETEO and GenT Programmes Generalitat Valenciana (CIDEAGENT/2019/023, CIDEAGENT/2019/027); Sweden: Swedish Research Council (VR 2018-00482, VR 2022-03845, VR 2022-04683, VR 2023-03403, VR grant 2021-03651), Knut and Alice Wallenberg Foundation (KAW 2018.0157, KAW 2018.0458, KAW 2019.0447, KAW 2022.0358); Switzerland: Swiss National Science Foundation (SNSF - PCEFP2_194658); United Kingdom: Leverhulme Trust (Leverhulme Trust RPG-2020-004), Royal Society (NIF-R1-231091); United States of America: Neubauer Family Foundation.

References

- [1] B. Andersson, G. Gustafson, G. Ingelman and T. Sjöstrand, *Parton fragmentation and string dynamics*, [Phys. Rept. **97** \(1983\) 31](#).

- [2] G. Marchesini et al., *HERWIG 5.1 - a Monte Carlo event generator for simulating hadron emission reactions with interfering gluons*, *Comput. Phys. Commun.* **67** (1992) 465.
- [3] K. Ackerstaff et al., *Measurements of flavour-dependent fragmentation functions in $Z^0 \rightarrow q\bar{q}$ events*, *Eur. Phys. J. C* **7** (1999) 369, arXiv: [hep-ex/9807004](#).
- [4] G. Alexander et al., *A Study of b quark fragmentation into B^0 and B^+ mesons at LEP*, *Phys. Lett. B* **364** (1995) 93.
- [5] ATLAS Collaboration, *Properties of jet fragmentation using charged particles measured with the ATLAS detector in pp collisions at $\sqrt{s} = 13$ TeV*, *Phys. Rev. D* **100** (2019) 052011, arXiv: [1906.09254 \[hep-ex\]](#).
- [6] CMS Collaboration, *Strange Particle Production in pp Collisions at $\sqrt{s} = 0.9$ and 7 TeV*, *JHEP* **05** (2011) 064, arXiv: [1102.4282 \[hep-ex\]](#).
- [7] CMS Collaboration, *Measurement of neutral strange particle production in the underlying event in proton–proton collisions at $\sqrt{s} = 7$ TeV*, *Phys. Rev. D* **88** (2013) 052001, arXiv: [1305.6016 \[hep-ex\]](#).
- [8] ATLAS Collaboration, *K_S^0 and Λ production in pp interactions at $\sqrt{s} = 0.9$ and 7 TeV measured with the ATLAS detector at the LHC*, *Phys. Rev. D* **85** (2012) 012001, arXiv: [1111.1297 \[hep-ex\]](#).
- [9] CMS Collaboration, *Observation of sequential Υ suppression in PbPb collisions*, *Phys. Rev. Lett.* **109** (2012) 222301, arXiv: [1208.2826 \[hep-ex\]](#).
- [10] ALICE Collaboration, *K_S^0 - and (anti-) Λ -hadron correlations in pp collisions at $\sqrt{s} = 13$ TeV*, *Eur. Phys. J. C* **81** (2021) 945, arXiv: [2107.11209 \[nucl-ex\]](#).
- [11] ALICE Collaboration, *Production of Λ and K_S^0 in jets in p -Pb collisions at $\sqrt{s_{NN}}=5.02$ TeV and pp collisions at $\sqrt{s}=7$ TeV*, *Phys. Lett. B* **827** (2022) 136984, arXiv: [2105.04890 \[nucl-ex\]](#).
- [12] ALICE Collaboration, *Production of light-flavor hadrons in pp collisions at $\sqrt{s} = 7$ and $\sqrt{s} = 13$ TeV*, *Eur. Phys. J. C* **81** (2021) 256, arXiv: [2005.11120 \[nucl-ex\]](#).
- [13] ALICE Collaboration, *Enhanced production of multi-strange hadrons in high-multiplicity proton-proton collisions*, *Nature Phys.* **13** (2017) 535, arXiv: [1606.07424 \[nucl-ex\]](#).
- [14] ALICE Collaboration, *Multiplicity dependence of π , K , and p production in pp collisions at $\sqrt{s} = 13$ TeV*, *Eur. Phys. J. C* **80** (2020) 693, arXiv: [2003.02394 \[nucl-ex\]](#).
- [15] ATLAS Collaboration, *Measurement of K_S^0 and Λ^0 production in $t\bar{t}$ dileptonic events in pp collisions at $\sqrt{s} = 7$ TeV with the ATLAS detector*, *Eur. Phys. J. C* **79** (2019) 1017, arXiv: [1907.10862 \[hep-ex\]](#).
- [16] CDF Collaboration, *Underlying event in hard interactions at the Fermilab Tevatron $\bar{p}p$ collider*, *Phys. Rev. D* **70** (7 2004) 072002.
- [17] ATLAS Collaboration, *Measurement of charged-particle distributions sensitive to the underlying event in $\sqrt{s} = 13$ TeV proton–proton collisions with the ATLAS detector at the LHC*, *JHEP* **03** (2017) 157, arXiv: [1701.05390 \[hep-ex\]](#).

- [18] ALICE Collaboration, *Underlying event properties in pp collisions at $\sqrt{s} = 13$ TeV*, *JHEP* **04** (2020) 192, arXiv: [1910.14400 \[nucl-ex\]](#).
- [19] CMS Collaboration, *Measurement of the underlying event in the Drell-Yan process in proton-proton collisions at $\sqrt{s} = 7$ TeV*, *Eur. Phys. J. C* **72** (2012) 2080, arXiv: [1204.1411 \[hep-ex\]](#).
- [20] T. Martin, P. Skands and S. Farrington, *Probing collective effects in hadronisation with the extremes of the underlying event*, *Eur. Phys. J. C* **76** (2016) 299, arXiv: [1603.05298 \[hep-ph\]](#).
- [21] ALICE Collaboration, *Measurements of long-range two-particle correlation over a wide pseudorapidity range in p-Pb collisions at $\sqrt{s_{NN}} = 5.02$ TeV*, *JHEP* **01** (2024) 199, arXiv: [2310.07490 \[nucl-ex\]](#).
- [22] J. Bellm et al., *Herwig 7.2 release note*, *Eur. Phys. J. C* **80** (2020) 452, arXiv: [1912.06509 \[hep-ph\]](#).
- [23] S. Gieseke, P. Kirchga ber and S. Pl tzer, *Baryon production from cluster hadronisation*, *Eur. Phys. J. C* **78** (2018) 99, arXiv: [1710.10906 \[hep-ph\]](#).
- [24] ATLAS Collaboration, *The ATLAS Experiment at the CERN Large Hadron Collider*, *JINST* **3** (2008) S08003.
- [25] ATLAS Collaboration, *ATLAS Insertable B-Layer: Technical Design Report*, ATLAS-TDR-19; CERN-LHCC-2010-013, 2010, URL: <https://cds.cern.ch/record/1291633>, Addendum: ATLAS-TDR-19-ADD-1; CERN-LHCC-2012-009, 2012, URL: <https://cds.cern.ch/record/1451888>.
- [26] B. Abbott et al., *Production and integration of the ATLAS Insertable B-Layer*, *JINST* **13** (2018) T05008, arXiv: [1803.00844 \[physics.ins-det\]](#).
- [27] ATLAS Collaboration, *Performance of the Minimum Bias Trigger in pp collisions at $\sqrt{s} = 7$ TeV*, ATLAS-CONF-2010-068, 2010, URL: <https://cds.cern.ch/record/1281343>.
- [28] ATLAS Collaboration, *Performance of the ATLAS trigger system in 2015*, *Eur. Phys. J. C* **77** (2017) 317, arXiv: [1611.09661 \[hep-ex\]](#).
- [29] ATLAS Collaboration, *Software and computing for Run 3 of the ATLAS experiment at the LHC*, (2024), arXiv: [2404.06335 \[hep-ex\]](#).
- [30] T. Pierog and K. Werner, *EPOS Model and Ultra High Energy Cosmic Rays*, *Nucl. Phys. B Proc. Suppl.* **196** (2009) 102, ed. by J.-N. Capdevielle, R. Engel and B. Pattison, arXiv: [0905.1198 \[hep-ph\]](#).
- [31] T. Pierog, I. Karpenko, J. M. Katzy, E. Yatsenko and K. Werner, *EPOS LHC: Test of collective hadronization with data measured at the CERN Large Hadron Collider*, *Phys. Rev. C* **92** (2015) 034906, arXiv: [1306.0121 \[hep-ph\]](#).
- [32] T. Sj strand et al., *An introduction to PYTHIA 8.2*, *Comput. Phys. Commun.* **191** (2015) 159, arXiv: [1410.3012 \[hep-ph\]](#).
- [33] ATLAS Collaboration, *Further ATLAS tunes of PYTHIA 6 and Pythia 8*, ATL-PHYS-PUB-2011-014, 2011, URL: <https://cds.cern.ch/record/1400677>.
- [34] J. R. Christiansen and P. Z. Skands, *String formation beyond leading colour*, *JHEP* **08** (2015) 003, arXiv: [1505.01681 \[hep-ph\]](#).
- [35] S. Agostinelli et al., *GEANT4 – a simulation toolkit*, *Nucl. Instrum. Meth. A* **506** (2003) 250.

- [36] ATLAS Collaboration, *The ATLAS Simulation Infrastructure*, *Eur. Phys. J. C* **70** (2010) 823, arXiv: [1005.4568 \[physics.ins-det\]](#).
- [37] H. J. Drescher, M. Hladik, S. Ostapchenko, T. Pierog and K. Werner, *Parton-based Gribov-Regge theory*, *Phys. Rept.* **350** (2001) 93, arXiv: [hep-ph/0007198](#).
- [38] K. Werner, *Core-corona separation in ultra-relativistic heavy ion collisions*, *Phys. Rev. Lett.* **98** (2007) 152301, arXiv: [0704.1270 \[nucl-th\]](#).
- [39] A. D. Martin, W. J. Stirling, R. S. Thorne and G. Watt, *Parton distributions for the LHC*, *Eur. Phys. J. C* **63** (2009) 189, arXiv: [0901.0002 \[hep-ph\]](#).
- [40] ATLAS Collaboration, *Measurements of the pseudorapidity dependence of the total transverse energy in proton–proton collisions at $\sqrt{s} = 7$ TeV with ATLAS*, *JHEP* **11** (2012) 033, arXiv: [1208.6256 \[hep-ex\]](#).
- [41] P. Skands, S. Carrazza and J. Rojo, *Tuning PYTHIA 8.1: the Monash 2013 Tune*, *Eur. Phys. J. C* **74** (2014) 3024, arXiv: [1404.5630 \[hep-ph\]](#).
- [42] NNPDF Collaboration, R. D. Ball et al., *Parton distributions with LHC data*, *Nucl. Phys. B* **867** (2013) 244, arXiv: [1207.1303 \[hep-ph\]](#).
- [43] ATLAS Collaboration, *Charged-particle distributions in $\sqrt{s} = 13$ TeV pp interactions measured with the ATLAS detector at the LHC*, *Phys. Lett. B* **758** (2016) 67, arXiv: [1602.01633 \[hep-ex\]](#).
- [44] ATLAS Collaboration, *Charged-particle multiplicities in pp interactions measured with the ATLAS detector at the LHC*, *New J. Phys.* **13** (2011) 053033, arXiv: [1012.5104 \[hep-ex\]](#).
- [45] ATLAS Collaboration, *Charged-particle distributions in pp interactions at $\sqrt{s} = 8$ TeV measured with the ATLAS detector*, *Eur. Phys. J. C* **76** (2016) 403, arXiv: [1603.02439 \[hep-ex\]](#).
- [46] ATLAS Collaboration, *Charged-particle distributions at low transverse momentum in $\sqrt{s} = 13$ TeV pp interactions measured with the ATLAS detector at the LHC*, *Eur. Phys. J. C* **76** (2016) 502, arXiv: [1606.01133 \[hep-ex\]](#).
- [47] M. Cacciari, G. P. Salam and G. Soyez, *The anti- k_t jet clustering algorithm*, *JHEP* **04** (2008) 063, arXiv: [0802.1189 \[hep-ph\]](#).
- [48] M. Cacciari, G. P. Salam and G. Soyez, *FastJet user manual*, *Eur. Phys. J. C* **72** (2012) 1896, arXiv: [1111.6097 \[hep-ph\]](#).
- [49] P. A. Zyla et al., *Review of Particle Physics*, *PTEP* **2020** (2020) 083C01.
- [50] J. Podolanski and R. Armenteros, *III. Analysis of V-events*, *Lond. Edinb. Dubl. Phil. Mag.* **45** (1954) 13.
- [51] ATLAS Collaboration, *Studies of the ATLAS Inner Detector material using $\sqrt{s} = 13$ TeV pp collision data*, ATL-PHYS-PUB-2015-050, 2015, URL: <https://cds.cern.ch/record/2109010>.
- [52] G. D’Agostini, *A multidimensional unfolding method based on Bayes’ theorem*, *Nucl. Instrum. Meth. A* **362** (1995) 487.
- [53] ATLAS Collaboration, *Evaluating statistical uncertainties and correlations using the bootstrap method*, ATL-PHYS-PUB-2021-011, 2021, URL: <https://cds.cern.ch/record/2759945>.

- [54] ATLAS Collaboration, *ATLAS Computing Acknowledgements*, ATL-SOFT-PUB-2023-001, 2023,
URL: <https://cds.cern.ch/record/2869272>.

The ATLAS Collaboration

G. Aad ¹⁰³, E. Aakvaag ¹⁶, B. Abbott ¹²¹, S. Abdelhameed ^{117a}, K. Abeling ⁵⁵, N.J. Abicht ⁴⁹, S.H. Abidi ²⁹, M. Aboeela ⁴⁴, A. Aboulhorma ^{35e}, H. Abramowicz ¹⁵², H. Abreu ¹⁵¹, Y. Abulaiti ¹¹⁸, B.S. Acharya ^{69a,69b,k}, A. Ackermann ^{63a}, C. Adam Bourdarios ⁴, L. Adamczyk ^{86a}, S.V. Addepalli ²⁶, M.J. Addison ¹⁰², J. Adelman ¹¹⁶, A. Adiguzel ^{21c}, T. Adye ¹³⁵, A.A. Affolder ¹³⁷, Y. Afik ³⁹, M.N. Agaras ¹³, J. Agarwala ^{73a,73b}, A. Aggarwal ¹⁰¹, C. Agheorghiesei ^{27c}, A. Ahmad ³⁶, F. Ahmadov ^{38,x}, W.S. Ahmed ¹⁰⁵, S. Ahuja ⁹⁶, X. Ai ^{62e}, G. Aielli ^{76a,76b}, A. Aikot ¹⁶⁴, M. Ait Tamliah ^{35e}, B. Aitbenchikh ^{35a}, M. Akbiyik ¹⁰¹, T.P.A. Åkesson ⁹⁹, A.V. Akimov ³⁷, D. Akiyama ¹⁶⁹, N.N. Akolkar ²⁴, S. Aktas ^{21a}, K. Al Houry ⁴¹, G.L. Alberghi ^{23b}, J. Albert ¹⁶⁶, P. Albicocco ⁵³, G.L. Albouy ⁶⁰, S. Alderweireldt ⁵², Z.L. Alegria ¹²², M. Aleksa ³⁶, I.N. Aleksandrov ³⁸, C. Alexa ^{27b}, T. Alexopoulos ¹⁰, F. Alfonsi ^{23b}, M. Algren ⁵⁶, M. Alhroob ¹⁶⁸, B. Ali ¹³³, H.M.J. Ali ⁹², S. Ali ³¹, S.W. Alibocus ⁹³, M. Aliev ^{33c}, G. Alimonti ^{71a}, W. Alkahi ⁵⁵, C. Allaire ⁶⁶, B.M.M. Allbrooke ¹⁴⁷, J.F. Allen ⁵², C.A. Allendes Flores ^{138f}, P.P. Allport ²⁰, A. Aloisio ^{72a,72b}, F. Alonso ⁹¹, C. Alpigiani ¹³⁹, Z.M.K. Alsolami ⁹², M. Alvarez Estevez ¹⁰⁰, A. Alvarez Fernandez ¹⁰¹, M. Alves Cardoso ⁵⁶, M.G. Alvigi ^{72a,72b}, M. Aly ¹⁰², Y. Amaral Coutinho ^{83b}, A. Ambler ¹⁰⁵, C. Amelung ³⁶, M. Amerl ¹⁰², C.G. Ames ¹¹⁰, D. Amidei ¹⁰⁷, K.J. Amirie ¹⁵⁶, S.P. Amor Dos Santos ^{131a}, K.R. Amos ¹⁶⁴, S. An ⁸⁴, V. Ananiev ¹²⁶, C. Anastopoulos ¹⁴⁰, T. Andeen ¹¹, J.K. Anders ³⁶, S.Y. Andrean ^{47a,47b}, A. Andreazza ^{71a,71b}, S. Angelidakis ⁹, A. Angerami ^{41,z}, A.V. Anisenkov ³⁷, A. Annovi ^{74a}, C. Antel ⁵⁶, E. Antipov ¹⁴⁶, M. Antonelli ⁵³, F. Anulli ^{75a}, M. Aoki ⁸⁴, T. Aoki ¹⁵⁴, M.A. Aparo ¹⁴⁷, L. Aperio Bella ⁴⁸, C. Appelt ¹⁸, A. Apyan ²⁶, S.J. Arbiol Val ⁸⁷, C. Arcangeletti ⁵³, A.T.H. Arce ⁵¹, E. Arena ⁹³, J-F. Arguin ¹⁰⁹, S. Argyropoulos ⁵⁴, J.-H. Arling ⁴⁸, O. Arnaez ⁴, H. Arnold ¹¹⁵, G. Artoni ^{75a,75b}, H. Asada ¹¹², K. Asai ¹¹⁹, S. Asai ¹⁵⁴, N.A. Asbah ³⁶, K. Assamagan ²⁹, R. Astalos ^{28a}, K.S.V. Astrand ⁹⁹, S. Atashi ¹⁶⁰, R.J. Atkin ^{33a}, M. Atkinson ¹⁶³, H. Atmani ^{35f}, P.A. Atmasiddha ¹²⁹, K. Augsten ¹³³, S. Auricchio ^{72a,72b}, A.D. Auriol ²⁰, V.A. Austrup ¹⁰², G. Avolio ³⁶, K. Axiotis ⁵⁶, G. Azuelos ^{109,ad}, D. Babal ^{28b}, H. Bachacou ¹³⁶, K. Bachas ^{153,o}, A. Bachi ³⁴, F. Backman ^{47a,47b}, A. Badea ³⁹, T.M. Baer ¹⁰⁷, P. Bagnaia ^{75a,75b}, M. Bahmani ¹⁸, D. Bahner ⁵⁴, K. Bai ¹²⁴, J.T. Baines ¹³⁵, L. Baines ⁹⁵, O.K. Baker ¹⁷³, E. Bakos ¹⁵, D. Bakshi Gupta ⁸, V. Balakrishnan ¹²¹, R. Balasubramanian ¹¹⁵, E.M. Baldin ³⁷, P. Balek ^{86a}, E. Ballabene ^{23b,23a}, F. Balli ¹³⁶, L.M. Baltos ^{63a}, W.K. Balunas ³², J. Balz ¹⁰¹, I. Bamwidhi ^{117b}, E. Banas ⁸⁷, M. Bandieramonte ¹³⁰, A. Bandyopadhyay ²⁴, S. Bansal ²⁴, L. Barak ¹⁵², M. Barakat ⁴⁸, E.L. Barberio ¹⁰⁶, D. Barberis ^{57b,57a}, M. Barbero ¹⁰³, M.Z. Barel ¹¹⁵, K.N. Barends ^{33a}, T. Barillari ¹¹¹, M-S. Barisits ³⁶, T. Barklow ¹⁴⁴, P. Baron ¹²³, D.A. Baron Moreno ¹⁰², A. Baroncelli ^{62a}, G. Barone ²⁹, A.J. Barr ¹²⁷, J.D. Barr ⁹⁷, F. Barreiro ¹⁰⁰, J. Barreiro Guimarães da Costa ^{14a}, U. Barron ¹⁵², M.G. Barros Teixeira ^{131a}, S. Barsov ³⁷, F. Bartels ^{63a}, R. Bartoldus ¹⁴⁴, A.E. Barton ⁹², P. Bartos ^{28a}, A. Basan ¹⁰¹, M. Baselga ⁴⁹, A. Bassalat ^{66,b}, M.J. Basso ^{157a}, R. Bate ¹⁶⁵, R.L. Bates ⁵⁹, S. Batlamous ¹⁰⁰, B. Batool ¹⁴², M. Battaglia ¹³⁷, D. Battulga ¹⁸, M. Baucé ^{75a,75b}, M. Bauer ³⁶, P. Bauer ²⁴, L.T. Bazzano Hurrell ³⁰, J.B. Beacham ⁵¹, T. Beau ¹²⁸, J.Y. Beaucamp ⁹¹, P.H. Beauchemin ¹⁵⁹, P. Bechtel ²⁴, H.P. Beck ^{19,n}, K. Becker ¹⁶⁸, A.J. Beddall ⁸², V.A. Bednyakov ³⁸, C.P. Bee ¹⁴⁶, L.J. Beemster ¹⁵, T.A. Beermann ³⁶, M. Begalli ^{83d}, M. Beger ²⁹, A. Behera ¹⁴⁶, J.K. Behr ⁴⁸, J.F. Beirer ³⁶, F. Beisiegel ²⁴, M. Belfkir ^{117b}, G. Bella ¹⁵², L. Bellagamba ^{23b}, A. Bellerive ³⁴, P. Bellos ²⁰, K. Beloborodov ³⁷, D. Benckekroun ^{35a}, F. Bendebba ^{35a}, Y. Benhammou ¹⁵²,

K.C. Benkendorfer ⁶¹, L. Beresford ⁴⁸, M. Beretta ⁵³, E. Bergeaas Kuutmann ¹⁶², N. Berger ⁴,
 B. Bergmann ¹³³, J. Beringer ^{17a}, G. Bernardi ⁵, C. Bernius ¹⁴⁴, F.U. Bernlochner ²⁴,
 F. Bernon ^{36,103}, A. Berrocal Guardia ¹³, T. Berry ⁹⁶, P. Berta ¹³⁴, A. Berthold ⁵⁰, S. Bethke ¹¹¹,
 A. Betti ^{75a,75b}, A.J. Bevan ⁹⁵, N.K. Bhalla ⁵⁴, M. Bhamjee ^{33c}, S. Bhatta ¹⁴⁶,
 D.S. Bhattacharya ¹⁶⁷, P. Bhattarai ¹⁴⁴, K.D. Bhide ⁵⁴, V.S. Bhopatkar ¹²², R.M. Bianchi ¹³⁰,
 G. Bianco ^{23b,23a}, O. Biebel ¹¹⁰, R. Bielski ¹²⁴, M. Biglietti ^{77a}, C.S. Billingsley ⁴⁴, M. Bindi ⁵⁵,
 A. Bingul ^{21b}, C. Bini ^{75a,75b}, A. Biondini ⁹³, C.J. Birch-sykes ¹⁰², G.A. Bird ³², M. Birman ¹⁷⁰,
 M. Biros ¹³⁴, S. Biryukov ¹⁴⁷, T. Bisanz ⁴⁹, E. Bisceglie ^{43b,43a}, J.P. Biswal ¹³⁵, D. Biswas ¹⁴²,
 I. Bloch ⁴⁸, A. Blue ⁵⁹, U. Blumenschein ⁹⁵, J. Blumenthal ¹⁰¹, V.S. Bobrovnikov ³⁷,
 M. Boehler ⁵⁴, B. Boehm ¹⁶⁷, D. Bogavac ³⁶, A.G. Bogdanchikov ³⁷, C. Bohm ^{47a},
 V. Boisvert ⁹⁶, P. Bokan ³⁶, T. Bold ^{86a}, M. Bomben ⁵, M. Bona ⁹⁵, M. Boonekamp ¹³⁶,
 C.D. Booth ⁹⁶, A.G. Borbély ⁵⁹, I.S. Bordulev ³⁷, H.M. Borecka-Bielska ¹⁰⁹, G. Borissov ⁹²,
 D. Bortoletto ¹²⁷, D. Boscherini ^{23b}, M. Bosman ¹³, J.D. Bossio Sola ³⁶, K. Bouaouda ^{35a},
 N. Bouchhar ¹⁶⁴, L. Boudet ⁴, J. Boudreau ¹³⁰, E.V. Bouhova-Thacker ⁹², D. Boumediene ⁴⁰,
 R. Bouquet ^{57b,57a}, A. Boveia ¹²⁰, J. Boyd ³⁶, D. Boye ²⁹, I.R. Boyko ³⁸, L. Bozianu ⁵⁶,
 J. Bracinik ²⁰, N. Brahimi ⁴, G. Brandt ¹⁷², O. Brandt ³², F. Braren ⁴⁸, B. Brau ¹⁰⁴,
 J.E. Brau ¹²⁴, R. Brenner ¹⁷⁰, L. Brenner ¹¹⁵, R. Brenner ¹⁶², S. Bressler ¹⁷⁰, D. Britton ⁵⁹,
 D. Britzger ¹¹¹, I. Brock ²⁴, G. Brooijmans ⁴¹, E. Brost ²⁹, L.M. Brown ¹⁶⁶, L.E. Bruce ⁶¹,
 T.L. Bruckler ¹²⁷, P.A. Bruckman de Renstrom ⁸⁷, B. Brüers ⁴⁸, A. Bruni ^{23b}, G. Bruni ^{23b},
 M. Bruschi ^{23b}, N. Bruscinò ^{75a,75b}, T. Buanes ¹⁶, Q. Buat ¹³⁹, D. Buchin ¹¹¹, A.G. Buckley ⁵⁹,
 O. Bulekov ³⁷, B.A. Bullard ¹⁴⁴, S. Burdin ⁹³, C.D. Burgard ⁴⁹, A.M. Burger ³⁶,
 B. Burghgrave ⁸, O. Burlayenko ⁵⁴, J.T.P. Burr ³², J.C. Burzynski ¹⁴³, E.L. Busch ⁴¹,
 V. Büscher ¹⁰¹, P.J. Bussey ⁵⁹, J.M. Butler ²⁵, C.M. Buttar ⁵⁹, J.M. Butterworth ⁹⁷,
 W. Buttinger ¹³⁵, C.J. Buxo Vazquez ¹⁰⁸, A.R. Buzykaev ³⁷, S. Cabrera Urbán ¹⁶⁴,
 L. Cadamuro ⁶⁶, D. Caforio ⁵⁸, H. Cai ¹³⁰, Y. Cai ^{14a,14e}, Y. Cai ^{14c}, V.M.M. Cairo ³⁶,
 O. Cakir ^{3a}, N. Calace ³⁶, P. Calafiura ^{17a}, G. Calderini ¹²⁸, P. Calfayan ⁶⁸, G. Callea ⁵⁹,
 L.P. Caloba ^{83b}, D. Calvet ⁴⁰, S. Calvet ⁴⁰, M. Calvetti ^{74a,74b}, R. Camacho Toro ¹²⁸,
 S. Camarda ³⁶, D. Camarero Munoz ²⁶, P. Camarri ^{76a,76b}, M.T. Camerlingo ^{72a,72b},
 D. Cameron ³⁶, C. Camincher ¹⁶⁶, M. Campanelli ⁹⁷, A. Camplani ⁴², V. Canale ^{72a,72b},
 A.C. Canbay ^{3a}, E. Canonero ⁹⁶, J. Cantero ¹⁶⁴, Y. Cao ¹⁶³, F. Capocasa ²⁶, M. Capua ^{43b,43a},
 A. Carbone ^{71a,71b}, R. Cardarelli ^{76a}, J.C.J. Cardenas ⁸, G. Carducci ^{43b,43a}, T. Carli ³⁶,
 G. Carlino ^{72a}, J.I. Carlotto ¹³, B.T. Carlson ^{130,p}, E.M. Carlson ^{166,157a}, J. Carmignani ⁹³,
 L. Carminati ^{71a,71b}, A. Carnelli ¹³⁶, M. Carnesale ^{75a,75b}, S. Caron ¹¹⁴, E. Carquin ^{138f},
 S. Carrá ^{71a}, G. Carratta ^{23b,23a}, A.M. Carroll ¹²⁴, T.M. Carter ⁵², M.P. Casado ^{13,h},
 M. Caspar ⁴⁸, F.L. Castillo ⁴, L. Castillo Garcia ¹³, V. Castillo Gimenez ¹⁶⁴, N.F. Castro ^{131a,131e},
 A. Catinaccio ³⁶, J.R. Catmore ¹²⁶, T. Cavaliere ⁴, V. Cavaliere ²⁹, N. Cavalli ^{23b,23a},
 Y.C. Cekmecelioglu ⁴⁸, E. Celebi ^{21a}, S. Cella ³⁶, F. Celli ¹²⁷, M.S. Centonze ^{70a,70b},
 V. Cepaitis ⁵⁶, K. Cerny ¹²³, A.S. Cerqueira ^{83a}, A. Cerri ¹⁴⁷, L. Cerrito ^{76a,76b}, F. Cerutti ^{17a},
 B. Cervato ¹⁴², A. Cervelli ^{23b}, G. Cesarini ⁵³, S.A. Cetin ⁸², D. Chakraborty ¹¹⁶, J. Chan ^{17a},
 W.Y. Chan ¹⁵⁴, J.D. Chapman ³², E. Chapon ¹³⁶, B. Chargeishvili ^{150b}, D.G. Charlton ²⁰,
 M. Chatterjee ¹⁹, C. Chauhan ¹³⁴, Y. Che ^{14c}, S. Chekanov ⁶, S.V. Chekulaev ^{157a},
 G.A. Chelkov ^{38,a}, A. Chen ¹⁰⁷, B. Chen ¹⁵², B. Chen ¹⁶⁶, H. Chen ^{14c}, H. Chen ²⁹,
 J. Chen ^{62c}, J. Chen ¹⁴³, M. Chen ¹²⁷, S. Chen ¹⁵⁴, S.J. Chen ^{14c}, X. Chen ^{62c,136},
 X. Chen ^{14b,ac}, Y. Chen ^{62a}, C.L. Cheng ¹⁷¹, H.C. Cheng ^{64a}, S. Cheong ¹⁴⁴, A. Cheplakov ³⁸,
 E. Cheremushkina ⁴⁸, E. Cherepanova ¹¹⁵, R. Cherkaoui El Moursli ^{35e}, E. Cheu ⁷, K. Cheung ⁶⁵,
 L. Chevalier ¹³⁶, V. Chiarella ⁵³, G. Chiarelli ^{74a}, N. Chiedde ¹⁰³, G. Chiodini ^{70a},
 A.S. Chisholm ²⁰, A. Chitan ^{27b}, M. Chitishvili ¹⁶⁴, M.V. Chizhov ³⁸, K. Choi ¹¹, Y. Chou ¹³⁹,

E.Y.S. Chow ¹¹⁴, K.L. Chu ¹⁷⁰, M.C. Chu ^{64a}, X. Chu ^{14a,14c}, J. Chudoba ¹³²,
 J.J. Chwastowski ⁸⁷, D. Cieri ¹¹¹, K.M. Ciesla ^{86a}, V. Cindro ⁹⁴, A. Ciocio ^{17a}, F. Ciroto ^{72a,72b},
 Z.H. Citron ¹⁷⁰, M. Citterio ^{71a}, D.A. Ciubotaru ^{27b}, A. Clark ⁵⁶, P.J. Clark ⁵², C. Clarry ¹⁵⁶,
 J.M. Clavijo Columbie ⁴⁸, S.E. Clawson ⁴⁸, C. Clement ^{47a,47b}, J. Clercx ⁴⁸, Y. Coadou ¹⁰³,
 M. Cobal ^{69a,69c}, A. Coccaro ^{57b}, R.F. Coelho Barrue ^{131a}, R. Coelho Lopes De Sa ¹⁰⁴,
 S. Coelli ^{71a}, B. Cole ⁴¹, J. Collot ⁶⁰, P. Conde Muiño ^{131a,131g}, M.P. Connell ^{33c},
 S.H. Connell ^{33c}, E.I. Conroy ¹²⁷, F. Conventi ^{72a,ae}, H.G. Cooke ²⁰, A.M. Cooper-Sarkar ¹²⁷,
 F.A. Corchia ^{23b,23a}, A. Cordeiro Oudot Choi ¹²⁸, L.D. Corpe ⁴⁰, M. Corradi ^{75a,75b},
 F. Corriveau ^{105,v}, A. Cortes-Gonzalez ¹⁸, M.J. Costa ¹⁶⁴, F. Costanza ⁴, D. Costanzo ¹⁴⁰,
 B.M. Cote ¹²⁰, J. Couthures ⁴, G. Cowan ⁹⁶, K. Cranmer ¹⁷¹, D. Cremonini ^{23b,23a},
 S. Crépe-Renaudin ⁶⁰, F. Crescioli ¹²⁸, M. Cristinziani ¹⁴², M. Cristoforetti ^{78a,78b}, V. Croft ¹¹⁵,
 J.E. Crosby ¹²², G. Crosetti ^{43b,43a}, A. Cueto ¹⁰⁰, Z. Cui ⁷, W.R. Cunningham ⁵⁹, F. Curcio ¹⁶⁴,
 J.R. Curran ⁵², P. Czodrowski ³⁶, M.M. Czurylo ³⁶, M.J. Da Cunha Sargedas De Sousa ^{57b,57a},
 J.V. Da Fonseca Pinto ^{83b}, C. Da Via ¹⁰², W. Dabrowski ^{86a}, T. Dado ⁴⁹, S. Dahbi ¹⁴⁹,
 T. Dai ¹⁰⁷, D. Dal Santo ¹⁹, C. Dallapiccola ¹⁰⁴, M. Dam ⁴², G. D'amen ²⁹, V. D'Amico ¹¹⁰,
 J. Damp ¹⁰¹, J.R. Dandoy ³⁴, D. Dannheim ³⁶, M. Danninger ¹⁴³, V. Dao ³⁶, G. Darbo ^{57b},
 S.J. Das ^{29,af}, F. Dattola ⁴⁸, S. D'Auria ^{71a,71b}, A. D'avanzo ^{72a,72b}, C. David ^{33a}, T. Davidek ¹³⁴,
 I. Dawson ⁹⁵, H.A. Day-hall ¹³³, K. De ⁸, R. De Asmundis ^{72a}, N. De Biase ⁴⁸,
 S. De Castro ^{23b,23a}, N. De Groot ¹¹⁴, P. de Jong ¹¹⁵, H. De la Torre ¹¹⁶, A. De Maria ^{14c},
 A. De Salvo ^{75a}, U. De Sanctis ^{76a,76b}, F. De Santis ^{70a,70b}, A. De Santo ¹⁴⁷,
 J.B. De Vivie De Regie ⁶⁰, D.V. Dedovich ³⁸, J. Degens ⁹³, A.M. Deiana ⁴⁴, F. Del Corso ^{23b,23a},
 J. Del Peso ¹⁰⁰, F. Del Rio ^{63a}, L. Delagrangé ¹²⁸, F. Deliot ¹³⁶, C.M. Delitzsch ⁴⁹,
 M. Della Pietra ^{72a,72b}, D. Della Volpe ⁵⁶, A. Dell'Acqua ³⁶, L. Dell'Asta ^{71a,71b}, M. Delmastro ⁴,
 P.A. Delsart ⁶⁰, S. Demers ¹⁷³, M. Demichev ³⁸, S.P. Denisov ³⁷, L. D'Eramo ⁴⁰,
 D. Derendarz ⁸⁷, F. Derue ¹²⁸, P. Dervan ⁹³, K. Desch ²⁴, C. Deutsch ²⁴, F.A. Di Bello ^{57b,57a},
 A. Di Ciaccio ^{76a,76b}, L. Di Ciaccio ⁴, A. Di Domenico ^{75a,75b}, C. Di Donato ^{72a,72b},
 A. Di Girolamo ³⁶, G. Di Gregorio ³⁶, A. Di Luca ^{78a,78b}, B. Di Micco ^{77a,77b}, R. Di Nardo ^{77a,77b},
 M. Diamantopoulou ³⁴, F.A. Dias ¹¹⁵, T. Dias Do Vale ¹⁴³, M.A. Diaz ^{138a,138b},
 F.G. Diaz Capriles ²⁴, M. Didenko ¹⁶⁴, E.B. Diehl ¹⁰⁷, S. Díez Cornell ⁴⁸, C. Diez Pardo ¹⁴²,
 C. Dimitriadi ^{162,24}, A. Dimitrievska ²⁰, J. Dingfelder ²⁴, I-M. Dinu ^{27b}, S.J. Dittmeier ^{63b},
 F. Dittus ³⁶, M. Divisek ¹³⁴, F. Djama ¹⁰³, T. Djobava ^{150b}, C. Doglioni ^{102,99},
 A. Dohnalova ^{28a}, J. Dolejsi ¹³⁴, Z. Dolezal ¹³⁴, K. Domijan ^{86a}, K.M. Dona ³⁹,
 M. Donadelli ^{83c}, B. Dong ¹⁰⁸, J. Donini ⁴⁰, A. D'Onofrio ^{72a,72b}, M. D'Onofrio ⁹³,
 J. Dopke ¹³⁵, A. Doria ^{72a}, N. Dos Santos Fernandes ^{131a}, P. Dougan ¹⁰², M.T. Dova ⁹¹,
 A.T. Doyle ⁵⁹, M.A. Dragnet ¹²⁷, E. Dreyer ¹⁷⁰, I. Drivas-koulouris ¹⁰, M. Drnevich ¹¹⁸,
 M. Drozdova ⁵⁶, D. Du ^{62a}, T.A. du Pree ¹¹⁵, F. Dubinin ³⁷, M. Dubovsky ^{28a}, E. Duchovni ¹⁷⁰,
 G. Duckeck ¹¹⁰, O.A. Ducu ^{27b}, D. Duda ⁵², A. Dudarev ³⁶, E.R. Duden ²⁶, M. D'uffizi ¹⁰²,
 L. Duflost ⁶⁶, M. Dührssen ³⁶, I. Duminica ^{27g}, A.E. Dumitriu ^{27b}, M. Dunford ^{63a}, S. Dungs ⁴⁹,
 K. Dunne ^{47a,47b}, A. Duperrin ¹⁰³, H. Duran Yildiz ^{3a}, M. Düren ⁵⁸, A. Durglishvili ^{150b},
 B.L. Dwyer ¹¹⁶, G.I. Dyckes ^{17a}, M. Dyndal ^{86a}, B.S. Dziedzic ³⁶, Z.O. Earnshaw ¹⁴⁷,
 G.H. Eberwein ¹²⁷, B. Eckerova ^{28a}, S. Eggebrecht ⁵⁵, E. Egidio Purcino De Souza ¹²⁸,
 L.F. Ehrke ⁵⁶, G. Eigen ¹⁶, K. Einsweiler ^{17a}, T. Ekelof ¹⁶², P.A. Ekman ⁹⁹, S. El Farkh ^{35b},
 Y. El Ghazali ^{35b}, H. El Jarrari ³⁶, A. El Moussaouy ¹⁰⁹, V. Ellajosyula ¹⁶², M. Ellert ¹⁶²,
 F. Ellinghaus ¹⁷², N. Ellis ³⁶, J. Elmsheuser ²⁹, M. Elsayy ^{117a}, M. Elsing ³⁶,
 D. Emelianov ¹³⁵, Y. Enari ¹⁵⁴, I. Ene ^{17a}, S. Epari ¹³, P.A. Erland ⁸⁷, M. Errenst ¹⁷²,
 M. Escalier ⁶⁶, C. Escobar ¹⁶⁴, E. Etzion ¹⁵², G. Evans ^{131a}, H. Evans ⁶⁸, L.S. Evans ⁹⁶,
 A. Ezhilov ³⁷, S. Ezzarqtouni ^{35a}, F. Fabbri ^{23b,23a}, L. Fabbri ^{23b,23a}, G. Facini ⁹⁷,

V. Fadeyev [id](#)¹³⁷, R.M. Fakhruddinov [id](#)³⁷, D. Fakoudis [id](#)¹⁰¹, S. Falciano [id](#)^{75a},
L.F. Falda Ulhoa Coelho [id](#)³⁶, F. Fallavollita [id](#)¹¹¹, J. Faltova [id](#)¹³⁴, C. Fan [id](#)¹⁶³, Y. Fan [id](#)^{14a},
Y. Fang [id](#)^{14a,14e}, M. Fanti [id](#)^{71a,71b}, M. Faraj [id](#)^{69a,69b}, Z. Farazpay [id](#)⁹⁸, A. Farbin [id](#)⁸, A. Farilla [id](#)^{77a},
T. Farooque [id](#)¹⁰⁸, S.M. Farrington [id](#)⁵², F. Fassi [id](#)^{35e}, D. Fassouliotis [id](#)⁹, M. Faucci Giannelli [id](#)^{76a,76b},
W.J. Fawcett [id](#)³², L. Fayard [id](#)⁶⁶, P. Federic [id](#)¹³⁴, P. Federicova [id](#)¹³², O.L. Fedin [id](#)^{37,a}, M. Feickert [id](#)¹⁷¹,
L. Feligioni [id](#)¹⁰³, D.E. Fellers [id](#)¹²⁴, C. Feng [id](#)^{62b}, M. Feng [id](#)^{14b}, Z. Feng [id](#)¹¹⁵, M.J. Fenton [id](#)¹⁶⁰,
L. Ferencz [id](#)⁴⁸, R.A.M. Ferguson [id](#)⁹², S.I. Fernandez Luengo [id](#)^{138f}, P. Fernandez Martinez [id](#)¹³,
M.J.V. Fernoux [id](#)¹⁰³, J. Ferrando [id](#)⁹², A. Ferrari [id](#)¹⁶², P. Ferrari [id](#)^{115,114}, R. Ferrari [id](#)^{73a}, D. Ferrere [id](#)⁵⁶,
C. Ferretti [id](#)¹⁰⁷, F. Fiedler [id](#)¹⁰¹, P. Fiedler [id](#)¹³³, A. Filipčič [id](#)⁹⁴, E.K. Filmer [id](#)¹, F. Filthaut [id](#)¹¹⁴,
M.C.N. Fiolhais [id](#)^{131a,131c,c}, L. Fiorini [id](#)¹⁶⁴, W.C. Fisher [id](#)¹⁰⁸, T. Fitschen [id](#)¹⁰², P.M. Fitzhugh [id](#)¹³⁶,
I. Fleck [id](#)¹⁴², P. Fleischmann [id](#)¹⁰⁷, T. Flick [id](#)¹⁷², M. Flores [id](#)^{33d,aa}, L.R. Flores Castillo [id](#)^{64a},
L. Flores Sanz De Acedo [id](#)³⁶, F.M. Follega [id](#)^{78a,78b}, N. Fomin [id](#)¹⁶, J.H. Foo [id](#)¹⁵⁶, A. Formica [id](#)¹³⁶,
A.C. Forti [id](#)¹⁰², E. Fortin [id](#)³⁶, A.W. Fortman [id](#)^{17a}, M.G. Foti [id](#)^{17a}, L. Fountas [id](#)^{9,i}, D. Fournier [id](#)⁶⁶,
H. Fox [id](#)⁹², P. Francavilla [id](#)^{74a,74b}, S. Francescato [id](#)⁶¹, S. Franchellucci [id](#)⁵⁶, M. Franchini [id](#)^{23b,23a},
S. Franchino [id](#)^{63a}, D. Francis [id](#)³⁶, L. Franco [id](#)¹¹⁴, V. Franco Lima [id](#)³⁶, L. Franconi [id](#)⁴⁸, M. Franklin [id](#)⁶¹,
G. Frattari [id](#)²⁶, Y.Y. Frid [id](#)¹⁵², J. Friend [id](#)⁵⁹, N. Fritzsche [id](#)⁵⁰, A. Froch [id](#)⁵⁴, D. Froidevaux [id](#)³⁶,
J.A. Frost [id](#)¹²⁷, Y. Fu [id](#)^{62a}, S. Fuenzalida Garrido [id](#)^{138f}, M. Fujimoto [id](#)¹⁰³, K.Y. Fung [id](#)^{64a},
E. Furtado De Simas Filho [id](#)^{83e}, M. Furukawa [id](#)¹⁵⁴, J. Fuster [id](#)¹⁶⁴, A. Gabrielli [id](#)^{23b,23a},
A. Gabrielli [id](#)¹⁵⁶, P. Gadow [id](#)³⁶, G. Gagliardi [id](#)^{57b,57a}, L.G. Gagnon [id](#)^{17a}, S. Gaid [id](#)¹⁶¹,
S. Galantzan [id](#)¹⁵², E.J. Gallas [id](#)¹²⁷, B.J. Gallop [id](#)¹³⁵, K.K. Gan [id](#)¹²⁰, S. Ganguly [id](#)¹⁵⁴, Y. Gao [id](#)⁵²,
F.M. Garay Walls [id](#)^{138a,138b}, B. Garcia [id](#)²⁹, C. García [id](#)¹⁶⁴, A. Garcia Alonso [id](#)¹¹⁵,
A.G. Garcia Caffaro [id](#)¹⁷³, J.E. García Navarro [id](#)¹⁶⁴, M. Garcia-Sciveres [id](#)^{17a}, G.L. Gardner [id](#)¹²⁹,
R.W. Gardner [id](#)³⁹, N. Garelli [id](#)¹⁵⁹, D. Garg [id](#)⁸⁰, R.B. Garg [id](#)¹⁴⁴, J.M. Gargan [id](#)⁵², C.A. Garner [id](#)¹⁵⁶,
C.M. Garvey [id](#)^{33a}, V.K. Gassmann [id](#)¹⁵⁹, G. Gaudio [id](#)^{73a}, V. Gautam [id](#)¹³, P. Gauzzi [id](#)^{75a,75b},
I.L. Gavrilenko [id](#)³⁷, A. Gavrilyuk [id](#)³⁷, C. Gay [id](#)¹⁶⁵, G. Gaycken [id](#)⁴⁸, E.N. Gazis [id](#)¹⁰, A.A. Geanta [id](#)^{27b},
C.M. Gee [id](#)¹³⁷, A. Gekow [id](#)¹²⁰, C. Gemme [id](#)^{57b}, M.H. Genest [id](#)⁶⁰, A.D. Gentry [id](#)¹¹³, S. George [id](#)⁹⁶,
W.F. George [id](#)²⁰, T. Geralis [id](#)⁴⁶, P. Gessinger-Befurt [id](#)³⁶, M.E. Geyik [id](#)¹⁷², M. Ghani [id](#)¹⁶⁸,
K. Ghorbanian [id](#)⁹⁵, A. Ghosal [id](#)¹⁴², A. Ghosh [id](#)¹⁶⁰, A. Ghosh [id](#)⁷, B. Giacobbe [id](#)^{23b}, S. Giagu [id](#)^{75a,75b},
T. Giani [id](#)¹¹⁵, P. Giannetti [id](#)^{74a}, A. Giannini [id](#)^{62a}, S.M. Gibson [id](#)⁹⁶, M. Gignac [id](#)¹³⁷, D.T. Gil [id](#)^{86b},
A.K. Gilbert [id](#)^{86a}, B.J. Gilbert [id](#)⁴¹, D. Gillberg [id](#)³⁴, G. Gilles [id](#)¹¹⁵, L. Ginabat [id](#)¹²⁸,
D.M. Gingrich [id](#)^{2,ad}, M.P. Giordani [id](#)^{69a,69c}, P.F. Giraud [id](#)¹³⁶, G. Giugliarelli [id](#)^{69a,69c}, D. Giugni [id](#)^{71a},
F. Giuli [id](#)³⁶, I. Gkialas [id](#)^{9,i}, L.K. Gladilin [id](#)³⁷, C. Glasman [id](#)¹⁰⁰, G.R. Gledhill [id](#)¹²⁴, G. Glemža [id](#)⁴⁸,
M. Glisic [id](#)¹²⁴, I. Gnesi [id](#)^{43b,e}, Y. Go [id](#)²⁹, M. Goblirsch-Kolb [id](#)³⁶, B. Gocke [id](#)⁴⁹, D. Godin [id](#)¹⁰⁹,
B. Gokturk [id](#)^{21a}, S. Goldfarb [id](#)¹⁰⁶, T. Golling [id](#)⁵⁶, M.G.D. Gololo [id](#)^{33g}, D. Golubkov [id](#)³⁷,
J.P. Gombas [id](#)¹⁰⁸, A. Gomes [id](#)^{131a,131b}, G. Gomes Da Silva [id](#)¹⁴², A.J. Gomez Delegido [id](#)¹⁶⁴,
R. Gonçalves [id](#)^{131a}, L. Gonella [id](#)²⁰, A. Gongadze [id](#)^{150c}, F. Gonnella [id](#)²⁰, J.L. Gonski [id](#)¹⁴⁴,
R.Y. González Andana [id](#)⁵², S. González de la Hoz [id](#)¹⁶⁴, R. Gonzalez Lopez [id](#)⁹³,
C. Gonzalez Renteria [id](#)^{17a}, M.V. Gonzalez Rodrigues [id](#)⁴⁸, R. Gonzalez Suarez [id](#)¹⁶²,
S. Gonzalez-Sevilla [id](#)⁵⁶, L. Goossens [id](#)³⁶, B. Gorini [id](#)³⁶, E. Gorini [id](#)^{70a,70b}, A. Gorišek [id](#)⁹⁴,
T.C. Gosart [id](#)¹²⁹, A.T. Goshaw [id](#)⁵¹, M.I. Gostkin [id](#)³⁸, S. Goswami [id](#)¹²², C.A. Gottardo [id](#)³⁶,
S.A. Gotz [id](#)¹¹⁰, M. Gouighri [id](#)^{35b}, V. Goumarre [id](#)⁴⁸, A.G. Goussiou [id](#)¹³⁹, N. Govender [id](#)^{33c},
I. Grabowska-Bold [id](#)^{86a}, K. Graham [id](#)³⁴, E. Gramstad [id](#)¹²⁶, S. Grancagnolo [id](#)^{70a,70b}, C.M. Grant [id](#)^{1,136},
P.M. Gravila [id](#)^{27f}, F.G. Gravili [id](#)^{70a,70b}, H.M. Gray [id](#)^{17a}, M. Greco [id](#)^{70a,70b}, C. Grefe [id](#)²⁴,
A.S. Grefsrud [id](#)¹⁶, I.M. Gregor [id](#)⁴⁸, K.T. Greif [id](#)¹⁶⁰, P. Grenier [id](#)¹⁴⁴, S.G. Grewe [id](#)¹¹¹, A.A. Grillo [id](#)¹³⁷,
K. Grimm [id](#)³¹, S. Grinstein [id](#)^{13,r}, J.-F. Grivaz [id](#)⁶⁶, E. Gross [id](#)¹⁷⁰, J. Grosse-Knetter [id](#)⁵⁵,
J.C. Grundy [id](#)¹²⁷, L. Guan [id](#)¹⁰⁷, J.G.R. Guerrero Rojas [id](#)¹⁶⁴, G. Guerrieri [id](#)^{69a,69c}, F. Guescini [id](#)¹¹¹,
R. Gugel [id](#)¹⁰¹, J.A.M. Guhit [id](#)¹⁰⁷, A. Guida [id](#)¹⁸, E. Guilloton [id](#)¹⁶⁸, S. Guindon [id](#)³⁶, F. Guo [id](#)^{14a,14e},

J. Guo ^{62c}, L. Guo ⁴⁸, Y. Guo ¹⁰⁷, R. Gupta ¹³⁰, S. Gurbuz ²⁴, S.S. Gurdasani ⁵⁴,
 G. Gustavino ³⁶, M. Guth ⁵⁶, P. Gutierrez ¹²¹, L.F. Gutierrez Zagazeta ¹²⁹, M. Gutsche ⁵⁰,
 C. Gutschow ⁹⁷, C. Gwenlan ¹²⁷, C.B. Gwilliam ⁹³, E.S. Haaland ¹²⁶, A. Haas ¹¹⁸,
 M. Habedank ⁴⁸, C. Haber ^{17a}, H.K. Hadavand ⁸, A. Hadeef ⁵⁰, S. Hadzic ¹¹¹, A.I. Hagan ⁹²,
 J.J. Hahn ¹⁴², E.H. Haines ⁹⁷, M. Haleem ¹⁶⁷, J. Haley ¹²², J.J. Hall ¹⁴⁰, G.D. Hallewell ¹⁰³,
 L. Halser ¹⁹, K. Hamano ¹⁶⁶, M. Hamer ²⁴, G.N. Hamity ⁵², E.J. Hampshire ⁹⁶, J. Han ^{62b},
 K. Han ^{62a}, L. Han ^{14c}, L. Han ^{62a}, S. Han ^{17a}, Y.F. Han ¹⁵⁶, K. Hanagaki ⁸⁴, M. Hance ¹³⁷,
 D.A. Hangal ⁴¹, H. Hanif ¹⁴³, M.D. Hank ¹²⁹, J.B. Hansen ⁴², P.H. Hansen ⁴², K. Hara ¹⁵⁸,
 D. Harada ⁵⁶, T. Harenberg ¹⁷², S. Harkusha ³⁷, M.L. Harris ¹⁰⁴, Y.T. Harris ¹²⁷, J. Harrison ¹³,
 N.M. Harrison ¹²⁰, P.F. Harrison ¹⁶⁸, N.M. Hartman ¹¹¹, N.M. Hartmann ¹¹⁰, R.Z. Hasan ^{96,135},
 Y. Hasegawa ¹⁴¹, S. Hassan ¹⁶, R. Hauser ¹⁰⁸, C.M. Hawkes ²⁰, R.J. Hawkings ³⁶,
 Y. Hayashi ¹⁵⁴, S. Hayashida ¹¹², D. Hayden ¹⁰⁸, C. Hayes ¹⁰⁷, R.L. Hayes ¹¹⁵, C.P. Hays ¹²⁷,
 J.M. Hays ⁹⁵, H.S. Hayward ⁹³, F. He ^{62a}, M. He ^{14a,14e}, Y. He ¹⁵⁵, Y. He ⁴⁸, Y. He ⁹⁷,
 N.B. Heatley ⁹⁵, V. Hedberg ⁹⁹, A.L. Heggelund ¹²⁶, N.D. Hehir ^{95,*}, C. Heidegger ⁵⁴,
 K.K. Heidegger ⁵⁴, W.D. Heidorn ⁸¹, J. Heilman ³⁴, S. Heim ⁴⁸, T. Heim ^{17a}, J.G. Heinlein ¹²⁹,
 J.J. Heinrich ¹²⁴, L. Heinrich ^{111,ab}, J. Hejbal ¹³², A. Held ¹⁷¹, S. Hellesund ¹⁶,
 C.M. Helling ¹⁶⁵, S. Hellman ^{47a,47b}, R.C.W. Henderson ⁹², L. Henkelmann ³²,
 A.M. Henriques Correia ³⁶, H. Herde ⁹⁹, Y. Hernández Jiménez ¹⁴⁶, L.M. Herrmann ²⁴,
 T. Herrmann ⁵⁰, G. Herten ⁵⁴, R. Hertenberger ¹¹⁰, L. Hervas ³⁶, M.E. Hespings ¹⁰¹,
 N.P. Hesse ^{157a}, M. Hidaoui ^{35b}, E. Hill ¹⁵⁶, S.J. Hillier ²⁰, J.R. Hinds ¹⁰⁸, F. Hinterkeuser ²⁴,
 M. Hirose ¹²⁵, S. Hirose ¹⁵⁸, D. Hirschbuehl ¹⁷², T.G. Hitchings ¹⁰², B. Hiti ⁹⁴, J. Hobbs ¹⁴⁶,
 R. Hobincu ^{27e}, N. Hod ¹⁷⁰, M.C. Hodgkinson ¹⁴⁰, B.H. Hodgkinson ¹²⁷, A. Hoecker ³⁶,
 D.D. Hofer ¹⁰⁷, J. Hofer ⁴⁸, T. Holm ²⁴, M. Holzbock ¹¹¹, L.B.A.H. Hommels ³²,
 B.P. Honan ¹⁰², J.J. Hong ⁶⁸, J. Hong ^{62c}, T.M. Hong ¹³⁰, B.H. Hooberman ¹⁶³,
 W.H. Hopkins ⁶, M.C. Hoppesch ¹⁶³, Y. Horii ¹¹², S. Hou ¹⁴⁹, A.S. Howard ⁹⁴, J. Howarth ⁵⁹,
 J. Hoya ⁶, M. Hrabovsky ¹²³, A. Hrynevich ⁴⁸, T. Hryn'ova ⁴, P.J. Hsu ⁶⁵, S.-C. Hsu ¹³⁹,
 T. Hsu ⁶⁶, M. Hu ^{17a}, Q. Hu ^{62a}, S. Huang ^{64b}, X. Huang ^{14a,14e}, Y. Huang ¹⁴⁰, Y. Huang ¹⁰¹,
 Y. Huang ^{14a}, Z. Huang ¹⁰², Z. Hubacek ¹³³, M. Huebner ²⁴, F. Hugging ²⁴, T.B. Huffman ¹²⁷,
 C.A. Hugli ⁴⁸, M. Huhtinen ³⁶, S.K. Huiberts ¹⁶, R. Hulsken ¹⁰⁵, N. Huseynov ¹², J. Huston ¹⁰⁸,
 J. Huth ⁶¹, R. Hyneman ¹⁴⁴, G. Iacobucci ⁵⁶, G. Iakovidis ²⁹, L. Iconomidou-Fayard ⁶⁶,
 J.P. Iddon ³⁶, P. Iengo ^{72a,72b}, R. Iguchi ¹⁵⁴, T. Iizawa ¹²⁷, Y. Ikegami ⁸⁴, N. Ilic ¹⁵⁶,
 H. Imam ^{35a}, M. Ince Lezki ⁵⁶, T. Ingebretsen Carlson ^{47a,47b}, G. Introzzi ^{73a,73b}, M. Iodice ^{77a},
 V. Ippolito ^{75a,75b}, R.K. Irwin ⁹³, M. Ishino ¹⁵⁴, W. Islam ¹⁷¹, C. Issever ^{18,48}, S. Istin ^{21a,ah},
 H. Ito ¹⁶⁹, R. Iuppa ^{78a,78b}, A. Ivina ¹⁷⁰, J.M. Izen ⁴⁵, V. Izzo ^{72a}, P. Jacka ¹³², P. Jackson ¹,
 C.S. Jagfeld ¹¹⁰, G. Jain ^{157a}, P. Jain ⁴⁸, K. Jakobs ⁵⁴, T. Jakoubek ¹⁷⁰, J. Jamieson ⁵⁹,
 M. Javurkova ¹⁰⁴, L. Jeanty ¹²⁴, J. Jejelava ^{150a,y}, P. Jenni ^{54,f}, C.E. Jessiman ³⁴, C. Jia ^{62b},
 J. Jia ¹⁴⁶, X. Jia ⁶¹, X. Jia ^{14a,14e}, Z. Jia ^{14c}, C. Jiang ⁵², S. Jiggins ⁴⁸, J. Jimenez Pena ¹³,
 S. Jin ^{14c}, A. Jinaru ^{27b}, O. Jinnouchi ¹⁵⁵, P. Johansson ¹⁴⁰, K.A. Johns ⁷, J.W. Johnson ¹³⁷,
 D.M. Jones ¹⁴⁷, E. Jones ⁴⁸, P. Jones ³², R.W.L. Jones ⁹², T.J. Jones ⁹³, H.L. Joos ^{55,36},
 R. Joshi ¹²⁰, J. Jovicevic ¹⁵, X. Ju ^{17a}, J.J. Junggeburth ¹⁰⁴, T. Junkermann ^{63a},
 A. Juste Rozas ^{13,r}, M.K. Juzek ⁸⁷, S. Kabana ^{138e}, A. Kaczmarek ⁸⁷, M. Kado ¹¹¹,
 H. Kagan ¹²⁰, M. Kagan ¹⁴⁴, A. Kahn ¹²⁹, C. Kahra ¹⁰¹, T. Kaji ¹⁵⁴, E. Kajomovitz ¹⁵¹,
 N. Kakati ¹⁷⁰, I. Kalaitzidou ⁵⁴, C.W. Kalderon ²⁹, N.J. Kang ¹³⁷, D. Kar ^{33g}, K. Karava ¹²⁷,
 M.J. Kareem ^{157b}, E. Karentzos ⁵⁴, O. Karkout ¹¹⁵, S.N. Karpov ³⁸, Z.M. Karpova ³⁸,
 V. Kartvelishvili ⁹², A.N. Karyukhin ³⁷, E. Kasimi ¹⁵³, J. Katzy ⁴⁸, S. Kaur ³⁴, K. Kawade ¹⁴¹,
 M.P. Kawale ¹²¹, C. Kawamoto ⁸⁸, T. Kawamoto ^{62a}, E.F. Kay ³⁶, F.I. Kaya ¹⁵⁹, S. Kazakos ¹⁰⁸,
 V.F. Kazanin ³⁷, Y. Ke ¹⁴⁶, J.M. Keaveney ^{33a}, R. Keeler ¹⁶⁶, G.V. Kehris ⁶¹, J.S. Keller ³⁴,

A.S. Kelly⁹⁷, J.J. Kempster¹⁴⁷, P.D. Kennedy¹⁰¹, O. Kepka¹³², B.P. Kerridge¹³⁵, S. Kersten¹⁷², B.P. Kerševan⁹⁴, L. Keszezhova^{28a}, S. Ketabchi Haghighat¹⁵⁶, R.A. Khan¹³⁰, A. Khanov¹²², A.G. Kharlamov³⁷, T. Kharlamova³⁷, E.E. Khoda¹³⁹, M. Kholodenko³⁷, T.J. Khoo¹⁸, G. Khorauli¹⁶⁷, J. Khubua^{150b}, Y.A.R. Khwaira¹²⁸, B. Kibirige^{33g}, D.W. Kim^{47a,47b}, Y.K. Kim³⁹, N. Kimura⁹⁷, M.K. Kingston⁵⁵, A. Kirchhoff⁵⁵, C. Kirfel²⁴, F. Kirfel²⁴, J. Kirk¹³⁵, A.E. Kiryunin¹¹¹, C. Kitsaki¹⁰, O. Kivernyk²⁴, M. Klassen¹⁵⁹, C. Klein³⁴, L. Klein¹⁶⁷, M.H. Klein⁴⁴, S.B. Klein⁵⁶, U. Klein⁹³, P. Klimek³⁶, A. Klimentov²⁹, T. Klioutchnikova³⁶, P. Kluit¹¹⁵, S. Kluth¹¹¹, E. Kneringer⁷⁹, T.M. Knight¹⁵⁶, A. Knue⁴⁹, R. Kobayashi⁸⁸, D. Kobylanskii¹⁷⁰, S.F. Koch¹²⁷, M. Kocian¹⁴⁴, P. Kodyš¹³⁴, D.M. Koeck¹²⁴, P.T. Koenig²⁴, T. Koffas³⁴, O. Kolay⁵⁰, I. Koletsou⁴, T. Komarek¹²³, K. Köneke⁵⁴, A.X.Y. Kong¹, T. Kono¹¹⁹, N. Konstantinidis⁹⁷, P. Kontaxakis⁵⁶, B. Konya⁹⁹, R. Kopeliansky⁴¹, S. Koperny^{86a}, K. Korcyl⁸⁷, K. Kordas^{153,d}, A. Korn⁹⁷, S. Korn⁵⁵, I. Korolkov¹³, N. Korotkova³⁷, B. Kortman¹¹⁵, O. Kortner¹¹¹, S. Kortner¹¹¹, W.H. Kostecka¹¹⁶, V.V. Kostyukhin¹⁴², A. Kotsokechagia¹³⁶, A. Kotwal⁵¹, A. Koulouris³⁶, A. Kourkoumeli-Charalampidi^{73a,73b}, C. Kourkoumelis⁹, E. Kourlitis^{111,ab}, O. Kovanda¹²⁴, R. Kowalewski¹⁶⁶, W. Kozanecki¹³⁶, A.S. Kozhin³⁷, V.A. Kramarenko³⁷, G. Kramberger⁹⁴, P. Kramer¹⁰¹, M.W. Krasny¹²⁸, A. Krasznahorkay³⁶, J.W. Kraus¹⁷², J.A. Kremer⁴⁸, T. Kresse⁵⁰, J. Kretschmar⁹³, K. Kreul¹⁸, P. Krieger¹⁵⁶, S. Krishnamurthy¹⁰⁴, M. Krivos¹³⁴, K. Krizka²⁰, K. Kroeninger⁴⁹, H. Kroha¹¹¹, J. Kroll¹³², J. Kroll¹²⁹, K.S. Krowpman¹⁰⁸, U. Kruchonak³⁸, H. Krüger²⁴, N. Krumnack⁸¹, M.C. Kruse⁵¹, O. Kuchinskaia³⁷, S. Kuday^{3a}, S. Kuehn³⁶, R. Kuesters⁵⁴, T. Kuhl⁴⁸, V. Kukhtin³⁸, Y. Kulchitsky^{37,a}, S. Kuleshov^{138d,138b}, M. Kumar^{33g}, N. Kumari⁴⁸, P. Kumari^{157b}, A. Kupco¹³², T. Kupfer⁴⁹, A. Kupich³⁷, O. Kuprash⁵⁴, H. Kurashige⁸⁵, L.L. Kurchaninov^{157a}, O. Kurdysh⁶⁶, Y.A. Kurochkin³⁷, A. Kurova³⁷, M. Kuze¹⁵⁵, A.K. Kvam¹⁰⁴, J. Kvita¹²³, T. Kwan¹⁰⁵, N.G. Kyriacou¹⁰⁷, L.A.O. Laatu¹⁰³, C. Lacasta¹⁶⁴, F. Lacava^{75a,75b}, H. Lacker¹⁸, D. Lacour¹²⁸, N.N. Lad⁹⁷, E. Ladygin³⁸, A. Lafarge⁴⁰, B. Laforge¹²⁸, T. Lagouri¹⁷³, F.Z. Lahbabi^{35a}, S. Lai⁵⁵, J.E. Lambert¹⁶⁶, S. Lammers⁶⁸, W. Lampl⁷, C. Lampoudis^{153,d}, G. Lamprinoudis¹⁰¹, A.N. Lancaster¹¹⁶, E. Lançon²⁹, U. Landgraf⁵⁴, M.P.J. Landon⁹⁵, V.S. Lang⁵⁴, O.K.B. Langrekken¹²⁶, A.J. Lankford¹⁶⁰, F. Lanni³⁶, K. Lantzschi²⁴, A. Lanza^{73a}, J.F. Laporte¹³⁶, T. Lari^{71a}, F. Lasagni Manghi^{23b}, M. Lassnig³⁶, V. Latonova¹³², A. Laudrain¹⁰¹, A. Laurier¹⁵¹, S.D. Lawlor¹⁴⁰, Z. Lawrence¹⁰², R. Lazaridou¹⁶⁸, M. Lazzaroni^{71a,71b}, B. Le¹⁰², E.M. Le Boulicaut⁵¹, L.T. Le Pottier^{17a}, B. Leban^{23b,23a}, A. Lebedev⁸¹, M. LeBlanc¹⁰², F. Ledroit-Guillon⁶⁰, S.C. Lee¹⁴⁹, S. Lee^{47a,47b}, T.F. Lee⁹³, L.L. Leeuw^{33c}, H.P. Lefebvre⁹⁶, M. Lefebvre¹⁶⁶, C. Leggett^{17a}, G. Lehmann Miotto³⁶, M. Leigh⁵⁶, W.A. Leight¹⁰⁴, W. Leinonen¹¹⁴, A. Leisos^{153,q}, M.A.L. Leite^{83c}, C.E. Leitgeb¹⁸, R. Leitner¹³⁴, K.J.C. Leney⁴⁴, T. Lenz²⁴, S. Leone^{74a}, C. Leonidopoulos⁵², A. Leopold¹⁴⁵, C. Leroy¹⁰⁹, R. Les¹⁰⁸, C.G. Lester³², M. Levchenko³⁷, J. Levêque⁴, L.J. Levinson¹⁷⁰, G. Levrini^{23b,23a}, M.P. Lewicki⁸⁷, C. Lewis¹³⁹, D.J. Lewis⁴, A. Li⁵, B. Li^{62b}, C. Li^{62a}, C-Q. Li¹¹¹, H. Li^{62a}, H. Li^{62b}, H. Li^{14c}, H. Li^{14b}, H. Li^{62b}, J. Li^{62c}, K. Li¹³⁹, L. Li^{62c}, M. Li^{14a,14e}, S. Li^{14a,14e}, S. Li^{62d,62c}, T. Li⁵, X. Li¹⁰⁵, Z. Li¹²⁷, Z. Li¹⁵⁴, Z. Li^{14a,14e}, S. Liang^{14a,14e}, Z. Liang^{14a}, M. Liberatore¹³⁶, B. Liberti^{76a}, K. Lie^{64c}, J. Lieber Marin^{83e}, H. Lien⁶⁸, H. Lin¹⁰⁷, K. Lin¹⁰⁸, R.E. Lindley⁷, J.H. Lindon², E. Lipeles¹²⁹, A. Lipniacka¹⁶, A. Lister¹⁶⁵, J.D. Little⁴, B. Liu^{14a}, B.X. Liu^{14d}, D. Liu^{62d,62c}, E.H.L. Liu²⁰, J.B. Liu^{62a}, J.K.K. Liu³², K. Liu^{62d}, K. Liu^{62d,62c}, M. Liu^{62a}, M.Y. Liu^{62a}, P. Liu^{14a}, Q. Liu^{62d,139,62c}, X. Liu^{62a}, X. Liu^{62b}, Y. Liu^{14d,14e}, Y.L. Liu^{62b}, Y.W. Liu^{62a}, J. Llorente Merino¹⁴³, S.L. Lloyd⁹⁵, E.M. Lobodzinska⁴⁸, P. Loch⁷, T. Lohse¹⁸, K. Lohwasser¹⁴⁰, E. Loiacono⁴⁸,

M. Lokajicek ^{132,*}, J.D. Lomas ²⁰, J.D. Long ¹⁶³, I. Longarini ¹⁶⁰, R. Longo ¹⁶³,
I. Lopez Paz ⁶⁷, A. Lopez Solis ⁴⁸, N. Lorenzo Martinez ⁴, A.M. Lory ¹¹⁰, M. Losada ^{117a},
G. Löschcke Centeno ¹⁴⁷, O. Loseva ³⁷, X. Lou ^{47a,47b}, X. Lou ^{14a,14e}, A. Lounis ⁶⁶,
P.A. Love ⁹², G. Lu ^{14a,14e}, M. Lu ⁶⁶, S. Lu ¹²⁹, Y.J. Lu ⁶⁵, H.J. Lubatti ¹³⁹, C. Luci ^{75a,75b},
F.L. Lucio Alves ^{14c}, F. Luehring ⁶⁸, I. Luise ¹⁴⁶, O. Lukianchuk ⁶⁶, O. Lundberg ¹⁴⁵,
B. Lund-Jensen ¹⁴⁵, N.A. Luongo ⁶, M.S. Lutz ³⁶, A.B. Lux ²⁵, D. Lynn ²⁹, R. Lysak ¹³²,
E. Lytken ⁹⁹, V. Lyubushkin ³⁸, T. Lyubushkina ³⁸, M.M. Lyukova ¹⁴⁶, M.Firdaus M. Soberi ⁵²,
H. Ma ²⁹, K. Ma ^{62a}, L.L. Ma ^{62b}, W. Ma ^{62a}, Y. Ma ¹²², G. Maccarrone ⁵³,
J.C. MacDonald ¹⁰¹, P.C. Machado De Abreu Farias ^{83e}, R. Madar ⁴⁰, T. Madula ⁹⁷, J. Maeda ⁸⁵,
T. Maeno ²⁹, H. Maguire ¹⁴⁰, V. Maiboroda ¹³⁶, A. Maio ^{131a,131b,131d}, K. Maj ^{86a},
O. Majersky ⁴⁸, S. Majewski ¹²⁴, N. Makovec ⁶⁶, V. Maksimovic ¹⁵, B. Malaescu ¹²⁸,
Pa. Malecki ⁸⁷, V.P. Maleev ³⁷, F. Malek ^{60,m}, M. Mali ⁹⁴, D. Malito ⁹⁶, U. Mallik ⁸⁰,
S. Maltezos ¹⁰, S. Malyukov ³⁸, J. Mamuzic ¹³, G. Mancini ⁵³, M.N. Mancini ²⁶, G. Manco ^{73a,73b},
J.P. Mandalia ⁹⁵, I. Mandić ⁹⁴, L. Manhaes de Andrade Filho ^{83a}, I.M. Maniatis ¹⁷⁰,
J. Manjarres Ramos ⁹⁰, D.C. Mankad ¹⁷⁰, A. Mann ¹¹⁰, S. Manzoni ³⁶, L. Mao ^{62c},
X. Mapekula ^{33c}, A. Marantis ^{153,q}, G. Marchiori ⁵, M. Marcisovsky ¹³², C. Marcon ^{71a},
M. Marinescu ²⁰, S. Marium ⁴⁸, M. Marjanovic ¹²¹, A. Markhoos ⁵⁴, M. Markovitch ⁶⁶,
E.J. Marshall ⁹², Z. Marshall ^{17a}, S. Marti-Garcia ¹⁶⁴, T.A. Martin ¹³⁵, V.J. Martin ⁵²,
B. Martin dit Latour ¹⁶, L. Martinelli ^{75a,75b}, M. Martinez ^{13,r}, P. Martinez Agullo ¹⁶⁴,
V.I. Martinez Outschoorn ¹⁰⁴, P. Martinez Suarez ¹³, S. Martin-Haugh ¹³⁵, G. Martinovicova ¹³⁴,
V.S. Martoiu ^{27b}, A.C. Martyniuk ⁹⁷, A. Marzin ³⁶, D. Mascione ^{78a,78b}, L. Masetti ¹⁰¹,
T. Mashimo ¹⁵⁴, J. Masik ¹⁰², A.L. Maslennikov ³⁷, P. Massarotti ^{72a,72b}, P. Mastrandrea ^{74a,74b},
A. Mastroberardino ^{43b,43a}, T. Masubuchi ¹⁵⁴, T. Mathisen ¹⁶², J. Matousek ¹³⁴, N. Matsuzawa ¹⁵⁴,
J. Maurer ^{27b}, A.J. Maury ⁶⁶, B. Maček ⁹⁴, D.A. Maximov ³⁷, A.E. May ¹⁰², R. Mazini ¹⁴⁹,
I. Maznas ¹¹⁶, M. Mazza ¹⁰⁸, S.M. Mazza ¹³⁷, E. Mazzeo ^{71a,71b}, C. Mc Ginn ²⁹,
J.P. Mc Gowan ¹⁶⁶, S.P. Mc Kee ¹⁰⁷, C.C. McCracken ¹⁶⁵, E.F. McDonald ¹⁰⁶,
A.E. McDougall ¹¹⁵, J.A. Mcfayden ¹⁴⁷, R.P. McGovern ¹²⁹, G. Mchedlidze ^{150b},
R.P. Mckenzie ^{33g}, T.C. Mclachlan ⁴⁸, D.J. Mclaughlin ⁹⁷, S.J. McMahon ¹³⁵,
C.M. Mcpartland ⁹³, R.A. McPherson ^{166,v}, S. Mehlhase ¹¹⁰, A. Mehta ⁹³, D. Melini ¹⁶⁴,
B.R. Mellado Garcia ^{33g}, A.H. Melo ⁵⁵, F. Meloni ⁴⁸, A.M. Mendes Jacques Da Costa ¹⁰²,
H.Y. Meng ¹⁵⁶, L. Meng ⁹², S. Menke ¹¹¹, M. Mentink ³⁶, E. Meoni ^{43b,43a}, G. Mercado ¹¹⁶,
S. Merianos ¹⁵³, C. Merlassino ^{69a,69c}, L. Merola ^{72a,72b}, C. Meroni ^{71a,71b}, J. Metcalfe ⁶,
A.S. Mete ⁶, E. Meuser ¹⁰¹, C. Meyer ⁶⁸, J-P. Meyer ¹³⁶, R.P. Middleton ¹³⁵, L. Mijović ⁵²,
G. Mikenberg ¹⁷⁰, M. Mikestikova ¹³², M. Mikuž ⁹⁴, H. Mildner ¹⁰¹, A. Milic ³⁶,
D.W. Miller ³⁹, E.H. Miller ¹⁴⁴, L.S. Miller ³⁴, A. Milov ¹⁷⁰, D.A. Milstead ^{47a,47b}, T. Min ^{14c},
A.A. Minaenko ³⁷, I.A. Minashvili ^{150b}, L. Mince ⁵⁹, A.I. Mincer ¹¹⁸, B. Mindur ^{86a},
M. Mineev ³⁸, Y. Mino ⁸⁸, L.M. Mir ¹³, M. Miralles Lopez ⁵⁹, M. Mironova ^{17a}, A. Mishima ¹⁵⁴,
M.C. Missio ¹¹⁴, A. Mitra ¹⁶⁸, V.A. Mitsou ¹⁶⁴, Y. Mitsumori ¹¹², O. Miu ¹⁵⁶,
P.S. Miyagawa ⁹⁵, T. Mkrtychyan ^{63a}, M. Mlinarevic ⁹⁷, T. Mlinarevic ⁹⁷, M. Mlynarikova ³⁶,
S. Mobius ¹⁹, P. Mogg ¹¹⁰, M.H. Mohamed Farook ¹¹³, A.F. Mohammed ^{14a,14e}, S. Mohapatra ⁴¹,
G. Mokgatitswane ^{33g}, L. Moleri ¹⁷⁰, B. Mondal ¹⁴², S. Mondal ¹³³, K. Mönig ⁴⁸,
E. Monnier ¹⁰³, L. Monsonis Romero ¹⁶⁴, J. Montejo Berlingen ¹³, M. Montella ¹²⁰,
F. Montekali ^{77a,77b}, F. Monticelli ⁹¹, S. Monzani ^{69a,69c}, N. Morange ⁶⁶,
A.L. Moreira De Carvalho ⁴⁸, M. Moreno Llácer ¹⁶⁴, C. Moreno Martinez ⁵⁶, P. Morettini ^{57b},
S. Morgenstern ³⁶, M. Morii ⁶¹, M. Morinaga ¹⁵⁴, F. Morodei ^{75a,75b}, L. Morvaj ³⁶,
P. Moschovakos ³⁶, B. Moser ³⁶, M. Mosidze ^{150b}, T. Moskalets ⁵⁴, P. Moskvitina ¹¹⁴,
J. Moss ^{31,j}, P. Moszkowicz ^{86a}, A. Moussa ^{35d}, E.J.W. Moyse ¹⁰⁴, O. Mtintsilana ^{33g},

S. Muanza ¹⁰³, J. Mueller ¹³⁰, D. Muenstermann ⁹², R. Müller ¹⁹, G.A. Mullier ¹⁶², A.J. Mullin ³², J.J. Mullin ¹²⁹, D.P. Mungo ¹⁵⁶, D. Munoz Perez ¹⁶⁴, F.J. Munoz Sanchez ¹⁰², M. Murin ¹⁰², W.J. Murray ^{168,135}, M. Muškinja ⁹⁴, C. Mwewa ²⁹, A.G. Myagkov ^{37,a}, A.J. Myers ⁸, G. Myers ¹⁰⁷, M. Myska ¹³³, B.P. Nachman ^{17a}, O. Nackenhorst ⁴⁹, K. Nagai ¹²⁷, K. Nagano ⁸⁴, J.L. Nagle ^{29,af}, E. Nagy ¹⁰³, A.M. Nairz ³⁶, Y. Nakahama ⁸⁴, K. Nakamura ⁸⁴, K. Nakkalil ⁵, H. Nanjo ¹²⁵, E.A. Narayanan ¹¹³, I. Naryshkin ³⁷, L. Nasella ^{71a,71b}, M. Naseri ³⁴, S. Nasri ^{117b}, C. Nass ²⁴, G. Navarro ^{22a}, J. Navarro-Gonzalez ¹⁶⁴, R. Nayak ¹⁵², A. Nayaz ¹⁸, P.Y. Nechaeva ³⁷, S. Nechaeva ^{23b,23a}, F. Nechansky ⁴⁸, L. Nedic ¹²⁷, T.J. Neep ²⁰, A. Negri ^{73a,73b}, M. Negrini ^{23b}, C. Nellist ¹¹⁵, C. Nelson ¹⁰⁵, K. Nelson ¹⁰⁷, S. Nemecek ¹³², M. Nessi ^{36,g}, M.S. Neubauer ¹⁶³, F. Neuhaus ¹⁰¹, J. Neundorf ⁴⁸, P.R. Newman ²⁰, C.W. Ng ¹³⁰, Y.W.Y. Ng ⁴⁸, B. Ngair ^{117a}, H.D.N. Nguyen ¹⁰⁹, R.B. Nickerson ¹²⁷, R. Nicolaidou ¹³⁶, J. Nielsen ¹³⁷, M. Niemeyer ⁵⁵, J. Niermann ⁵⁵, N. Nikiforou ³⁶, V. Nikolaenko ^{37,a}, I. Nikolic-Audit ¹²⁸, K. Nikolopoulos ²⁰, P. Nilsson ²⁹, I. Ninca ⁴⁸, G. Ninio ¹⁵², A. Nisati ^{75a}, N. Nishu ², R. Nisius ¹¹¹, J-E. Nitschke ⁵⁰, E.K. Nkadimeng ^{33g}, T. Nobe ¹⁵⁴, T. Nommensen ¹⁴⁸, M.B. Norfolk ¹⁴⁰, R.R.B. Norisam ⁹⁷, B.J. Norman ³⁴, M. Noury ^{35a}, J. Novak ⁹⁴, T. Novak ⁹⁴, L. Novotny ¹³³, R. Novotny ¹¹³, L. Nozka ¹²³, K. Ntekas ¹⁶⁰, N.M.J. Nunes De Moura Junior ^{83b}, J. Ocariz ¹²⁸, A. Ochi ⁸⁵, I. Ochoa ^{131a}, S. Oerdek ^{48,s}, J.T. Offermann ³⁹, A. Ogrodnik ¹³⁴, A. Oh ¹⁰², C.C. Ohm ¹⁴⁵, H. Oide ⁸⁴, R. Oishi ¹⁵⁴, M.L. Ojeda ⁴⁸, Y. Okumura ¹⁵⁴, L.F. Oleiro Seabra ^{131a}, S.A. Olivares Pino ^{138d}, G. Oliveira Correa ¹³, D. Oliveira Damazio ²⁹, D. Oliveira Goncalves ^{83a}, J.L. Oliver ¹⁶⁰, Ö.O. Öncel ⁵⁴, A.P. O'Neill ¹⁹, A. Onofre ^{131a,131e}, P.U.E. Onyisi ¹¹, M.J. Oreglia ³⁹, G.E. Orellana ⁹¹, D. Orestano ^{77a,77b}, N. Orlando ¹³, R.S. Orr ¹⁵⁶, V. O'Shea ⁵⁹, L.M. Osojnak ¹²⁹, R. Ospanov ^{62a}, G. Otero y Garzon ³⁰, H. Otono ⁸⁹, P.S. Ott ^{63a}, G.J. Ottino ^{17a}, M. Ouchrif ^{35d}, F. Ould-Saada ¹²⁶, T. Ovsiannikova ¹³⁹, M. Owen ⁵⁹, R.E. Owen ¹³⁵, V.E. Ozcan ^{21a}, F. Ozturk ⁸⁷, N. Ozturk ⁸, S. Ozturk ⁸², H.A. Pacey ¹²⁷, A. Pacheco Pages ¹³, C. Padilla Aranda ¹³, G. Padovano ^{75a,75b}, S. Pagan Griso ^{17a}, G. Palacino ⁶⁸, A. Palazzo ^{70a,70b}, J. Pampel ²⁴, J. Pan ¹⁷³, T. Pan ^{64a}, D.K. Panchal ¹¹, C.E. Pandini ¹¹⁵, J.G. Panduro Vazquez ¹³⁵, H.D. Pandya ¹, H. Pang ^{14b}, P. Pani ⁴⁸, G. Panizzo ^{69a,69c}, L. Panwar ¹²⁸, L. Paolozzi ⁵⁶, S. Parajuli ¹⁶³, A. Paramonov ⁶, C. Paraskevopoulos ⁵³, D. Paredes Hernandez ^{64b}, A. Pareti ^{73a,73b}, K.R. Park ⁴¹, T.H. Park ¹⁵⁶, M.A. Parker ³², F. Parodi ^{57b,57a}, E.W. Parrish ¹¹⁶, V.A. Parrish ⁵², J.A. Parsons ⁴¹, U. Parzefall ⁵⁴, B. Pascual Dias ¹⁰⁹, L. Pascual Dominguez ¹⁰⁰, E. Pasqualucci ^{75a}, S. Passaggio ^{57b}, F. Pastore ⁹⁶, P. Patel ⁸⁷, U.M. Patel ⁵¹, J.R. Pater ¹⁰², T. Pauly ³⁶, C.I. Pazos ¹⁵⁹, J. Pearkes ¹⁴⁴, M. Pedersen ¹²⁶, R. Pedro ^{131a}, S.V. Peleganchuk ³⁷, O. Penc ³⁶, E.A. Pender ⁵², G.D. Penn ¹⁷³, K.E. Pensi ¹¹⁰, M. Penzin ³⁷, B.S. Peralva ^{83d}, A.P. Pereira Peixoto ¹³⁹, L. Pereira Sanchez ¹⁴⁴, D.V. Perepelitsa ^{29,af}, E. Perez Codina ^{157a}, M. Perganti ¹⁰, H. Pernegger ³⁶, S. Perrella ^{75a,75b}, O. Perrin ⁴⁰, K. Peters ⁴⁸, R.F.Y. Peters ¹⁰², B.A. Petersen ³⁶, T.C. Petersen ⁴², E. Petit ¹⁰³, V. Petousis ¹³³, C. Petridou ^{153,d}, T. Petru ¹³⁴, A. Petrukhin ¹⁴², M. Pettee ^{17a}, N.E. Pettersson ³⁶, A. Petukhov ³⁷, K. Petukhova ¹³⁴, R. Pezoa ^{138f}, L. Pezzotti ³⁶, G. Pezzullo ¹⁷³, T.M. Pham ¹⁷¹, T. Pham ¹⁰⁶, P.W. Phillips ¹³⁵, G. Piacquadio ¹⁴⁶, E. Pianori ^{17a}, F. Piazza ¹²⁴, R. Piegai ³⁰, D. Pietreanu ^{27b}, A.D. Pilkington ¹⁰², M. Pinamonti ^{69a,69c}, J.L. Pinfeld ², B.C. Pinheiro Pereira ^{131a}, A.E. Pinto Pinoargote ^{136,136}, L. Pintucci ^{69a,69c}, K.M. Piper ¹⁴⁷, A. Pirttikoski ⁵⁶, D.A. Pizzi ³⁴, L. Pizzimento ^{64b}, A. Pizzini ¹¹⁵, M.-A. Pleier ²⁹, V. Pleskot ¹³⁴, E. Plotnikova ³⁸, G. Poddar ⁹⁵, R. Poettgen ⁹⁹, L. Poggioli ¹²⁸, I. Pokharel ⁵⁵, S. Polacek ¹³⁴, G. Polesello ^{73a}, A. Poley ^{143,157a}, A. Polini ^{23b}, C.S. Pollard ¹⁶⁸, Z.B. Pollock ¹²⁰, E. Pompa Pacchi ^{75a,75b}, N.I. Pond ⁹⁷, D. Ponomarenko ¹¹⁴, L. Pontecorvo ³⁶, S. Popa ^{27a}, G.A. Popeneciu ^{27d}, A. Poreba ³⁶,

D.M. Portillo Quintero [ID157a](#), S. Pospisil [ID133](#), M.A. Postill [ID140](#), P. Postolache [ID27c](#), K. Potamianos [ID168](#), P.A. Potepa [ID86a](#), I.N. Potrap [ID38](#), C.J. Potter [ID32](#), H. Potti [ID1](#), J. Poveda [ID164](#), M.E. Pozo Astigarraga [ID36](#), A. Prades Ibanez [ID164](#), J. Pretel [ID54](#), D. Price [ID102](#), M. Primavera [ID70a](#), M.A. Principe Martin [ID100](#), R. Privara [ID123](#), T. Procter [ID59](#), M.L. Proffitt [ID139](#), N. Proklova [ID129](#), K. Prokofiev [ID64c](#), G. Proto [ID111](#), J. Proudfoot [ID6](#), M. Przybycien [ID86a](#), W.W. Przygoda [ID86b](#), A. Psallidas [ID46](#), J.E. Puddefoot [ID140](#), D. Pudzha [ID37](#), D. Pyatiizbyantseva [ID37](#), J. Qian [ID107](#), D. Qichen [ID102](#), Y. Qin [ID13](#), T. Qiu [ID52](#), A. Quadt [ID55](#), M. Queitsch-Maitland [ID102](#), G. Quetant [ID56](#), R.P. Quinn [ID165](#), G. Rabanal Bolanos [ID61](#), D. Rafanoharana [ID54](#), F. Raffaelli [ID76a,76b](#), F. Ragusa [ID71a,71b](#), J.L. Rainbolt [ID39](#), J.A. Raine [ID56](#), S. Rajagopalan [ID29](#), E. Ramakoti [ID37](#), I.A. Ramirez-Berend [ID34](#), K. Ran [ID48,14e](#), N.P. Rapheeha [ID33g](#), H. Rasheed [ID27b](#), V. Raskina [ID128](#), D.F. Rassloff [ID63a](#), A. Rastogi [ID17a](#), S. Rave [ID101](#), B. Ravina [ID55](#), I. Ravinovich [ID170](#), M. Raymond [ID36](#), A.L. Read [ID126](#), N.P. Readioff [ID140](#), D.M. Rebuzzi [ID73a,73b](#), G. Redlinger [ID29](#), A.S. Reed [ID111](#), K. Reeves [ID26](#), J.A. Reidelsturz [ID172](#), D. Reikher [ID152](#), A. Rej [ID49](#), C. Rembser [ID36](#), M. Renda [ID27b](#), M.B. Rendel [ID111](#), F. Renner [ID48](#), A.G. Rennie [ID160](#), A.L. Rescia [ID48](#), S. Resconi [ID71a](#), M. Ressegotti [ID57b,57a](#), S. Rettie [ID36](#), J.G. Reyes Rivera [ID108](#), E. Reynolds [ID17a](#), O.L. Rezanova [ID37](#), P. Reznicek [ID134](#), H. Riani [ID35d](#), N. Ribaric [ID92](#), E. Ricci [ID78a,78b](#), R. Richter [ID111](#), S. Richter [ID47a,47b](#), E. Richter-Was [ID86b](#), M. Ridel [ID128](#), S. Ridouani [ID35d](#), P. Rieck [ID118](#), P. Riedler [ID36](#), E.M. Riefel [ID47a,47b](#), J.O. Rieger [ID115](#), M. Rijssenbeek [ID146](#), M. Rimoldi [ID36](#), L. Rinaldi [ID23b,23a](#), T.T. Rinn [ID29](#), M.P. Rinnagel [ID110](#), G. Ripellino [ID162](#), I. Riu [ID13](#), J.C. Rivera Vergara [ID166](#), F. Rizatdinova [ID122](#), E. Rizvi [ID95](#), B.R. Roberts [ID17a](#), S.H. Robertson [ID105,v](#), D. Robinson [ID32](#), C.M. Robles Gajardo [ID138f](#), M. Robles Manzano [ID101](#), A. Robson [ID59](#), A. Rocchi [ID76a,76b](#), C. Roda [ID74a,74b](#), S. Rodriguez Bosca [ID36](#), Y. Rodriguez Garcia [ID22a](#), A. Rodriguez Rodriguez [ID54](#), A.M. Rodríguez Vera [ID116](#), S. Roe [ID36](#), J.T. Roemer [ID160](#), A.R. Roepe-Gier [ID137](#), J. Roggel [ID172](#), O. Røhne [ID126](#), R.A. Rojas [ID104](#), C.P.A. Roland [ID128](#), J. Roloff [ID29](#), A. Romaniouk [ID37](#), E. Romano [ID73a,73b](#), M. Romano [ID23b](#), A.C. Romero Hernandez [ID163](#), N. Rompotis [ID93](#), L. Roos [ID128](#), S. Rosati [ID75a](#), B.J. Rosser [ID39](#), E. Rossi [ID127](#), E. Rossi [ID72a,72b](#), L.P. Rossi [ID61](#), L. Rossini [ID54](#), R. Rosten [ID120](#), M. Rotaru [ID27b](#), B. Rottler [ID54](#), C. Rougier [ID90](#), D. Rousseau [ID66](#), D. Rouso [ID48](#), A. Roy [ID163](#), S. Roy-Garand [ID156](#), A. Rozanov [ID103](#), Z.M.A. Rozario [ID59](#), Y. Rozen [ID151](#), A. Rubio Jimenez [ID164](#), A.J. Ruby [ID93](#), V.H. Ruelas Rivera [ID18](#), T.A. Ruggeri [ID1](#), A. Ruggiero [ID127](#), A. Ruiz-Martinez [ID164](#), A. Rummler [ID36](#), Z. Rurikova [ID54](#), N.A. Rusakovich [ID38](#), H.L. Russell [ID166](#), G. Russo [ID75a,75b](#), J.P. Rutherford [ID7](#), S. Rutherford Colmenares [ID32](#), M. Rybar [ID134](#), E.B. Rye [ID126](#), A. Ryzhov [ID44](#), J.A. Sabater Iglesias [ID56](#), P. Sabatini [ID164](#), H.F.W. Sadrozinski [ID137](#), F. Safai Tehrani [ID75a](#), B. Safarzadeh Samani [ID135](#), S. Saha [ID1](#), M. Sahinsoy [ID111](#), A. Saibel [ID164](#), M. Saimpert [ID136](#), M. Saito [ID154](#), T. Saito [ID154](#), A. Sala [ID71a,71b](#), D. Salamani [ID36](#), A. Salnikov [ID144](#), J. Salt [ID164](#), A. Salvador Salas [ID152](#), D. Salvatore [ID43b,43a](#), F. Salvatore [ID147](#), A. Salzburger [ID36](#), D. Sammel [ID54](#), E. Sampson [ID92](#), D. Sampsonidis [ID153,d](#), D. Sampsonidou [ID124](#), J. Sánchez [ID164](#), V. Sanchez Sebastian [ID164](#), H. Sandaker [ID126](#), C.O. Sander [ID48](#), J.A. Sandesara [ID104](#), M. Sandhoff [ID172](#), C. Sandoval [ID22b](#), L. Sanfilippo [ID63a](#), D.P.C. Sankey [ID135](#), T. Sano [ID88](#), A. Sansoni [ID53](#), L. Santi [ID75a,75b](#), C. Santoni [ID40](#), H. Santos [ID131a,131b](#), A. Santra [ID170](#), E. Sanzani [ID23b,23a](#), K.A. Saoucha [ID161](#), J.G. Saraiva [ID131a,131d](#), J. Sardain [ID7](#), O. Sasaki [ID84](#), K. Sato [ID158](#), C. Sauer [ID63b](#), E. Sauvan [ID4](#), P. Savard [ID156,ad](#), R. Sawada [ID154](#), C. Sawyer [ID135](#), L. Sawyer [ID98](#), C. Sbarra [ID23b](#), A. Sbrizzi [ID23b,23a](#), T. Scanlon [ID97](#), J. Schaarschmidt [ID139](#), U. Schäfer [ID101](#), A.C. Schaffer [ID66,44](#), D. Schaile [ID110](#), R.D. Schamberger [ID146](#), C. Scharf [ID18](#), M.M. Schefer [ID19](#), V.A. Schegelsky [ID37](#), D. Scheirich [ID134](#), M. Schernau [ID160](#), C. Scheulen [ID55](#), C. Schiavi [ID57b,57a](#), M. Schioppa [ID43b,43a](#), B. Schlag [ID144,1](#), K.E. Schleicher [ID54](#), S. Schlenker [ID36](#), J. Schmeing [ID172](#), M.A. Schmidt [ID172](#), K. Schmieden [ID101](#), C. Schmitt [ID101](#), N. Schmitt [ID101](#), S. Schmitt [ID48](#), L. Schoeffel [ID136](#), A. Schoening [ID63b](#), P.G. Scholer [ID34](#), E. Schopf [ID127](#), M. Schott [ID24](#), J. Schovancova [ID36](#), S. Schramm [ID56](#), T. Schroer [ID56](#), H-C. Schultz-Coulon [ID63a](#), M. Schumacher [ID54](#), B.A. Schumm [ID137](#), Ph. Schune [ID136](#), A.J. Schuy [ID139](#),

H.R. Schwartz ¹³⁷, A. Schwartzman ¹⁴⁴, T.A. Schwarz ¹⁰⁷, Ph. Schwemling ¹³⁶,
 R. Schwienhorst ¹⁰⁸, A. Sciandra ²⁹, G. Sciolla ²⁶, F. Scuri ^{74a}, C.D. Sebastiani ⁹³,
 K. Sedlaczek ¹¹⁶, S.C. Seidel ¹¹³, A. Seiden ¹³⁷, B.D. Seidlitz ⁴¹, C. Seitz ⁴⁸, J.M. Seixas ^{83b},
 G. Sekhniaidze ^{72a}, L. Selem ⁶⁰, N. Semprini-Cesari ^{23b,23a}, D. Sengupta ⁵⁶, V. Senthilkumar ¹⁶⁴,
 L. Serin ⁶⁶, M. Sessa ^{76a,76b}, H. Severini ¹²¹, F. Sforza ^{57b,57a}, A. Sfyrta ⁵⁶, Q. Sha ^{14a},
 E. Shabalina ⁵⁵, A.H. Shah ³², R. Shaheen ¹⁴⁵, J.D. Shahinian ¹²⁹, D. Shaked Renous ¹⁷⁰,
 L.Y. Shan ^{14a}, M. Shapiro ^{17a}, A. Sharma ³⁶, A.S. Sharma ¹⁶⁵, P. Sharma ⁸⁰, P.B. Shatalov ³⁷,
 K. Shaw ¹⁴⁷, S.M. Shaw ¹⁰², Q. Shen ^{62c,5}, D.J. Sheppard ¹⁴³, P. Sherwood ⁹⁷, L. Shi ⁹⁷,
 X. Shi ^{14a}, C.O. Shimmin ¹⁷³, J.D. Shinner ⁹⁶, I.P.J. Shipsey ¹²⁷, S. Shirabe ⁸⁹,
 M. Shiyakova ^{38,t}, M.J. Shochet ³⁹, J. Shojaii ¹⁰⁶, D.R. Shope ¹²⁶, B. Shrestha ¹²¹,
 S. Shrestha ^{120,ag}, M.J. Shroff ¹⁶⁶, P. Sicho ¹³², A.M. Sickles ¹⁶³, E. Sideras Haddad ^{33g},
 A.C. Sidley ¹¹⁵, A. Sidoti ^{23b}, F. Siegert ⁵⁰, Dj. Sijacki ¹⁵, F. Sili ⁹¹, J.M. Silva ⁵²,
 M.V. Silva Oliveira ²⁹, S.B. Silverstein ^{47a}, S. Simion ⁶⁶, R. Simoniello ³⁶, E.L. Simpson ¹⁰²,
 H. Simpson ¹⁴⁷, L.R. Simpson ¹⁰⁷, N.D. Simpson ⁹⁹, S. Simsek ⁸², S. Sindhu ⁵⁵, P. Sinervo ¹⁵⁶,
 S. Singh ¹⁵⁶, S. Sinha ⁴⁸, S. Sinha ¹⁰², M. Sioli ^{23b,23a}, I. Siral ³⁶, E. Sitnikova ⁴⁸,
 J. Sjölin ^{47a,47b}, A. Skaf ⁵⁵, E. Skorda ²⁰, P. Skubic ¹²¹, M. Slawinska ⁸⁷, V. Smakhtin ¹⁷⁰,
 B.H. Smart ¹³⁵, S.Yu. Smirnov ³⁷, Y. Smirnov ³⁷, L.N. Smirnova ^{37,a}, O. Smirnova ⁹⁹,
 A.C. Smith ⁴¹, D.R. Smith ¹⁶⁰, E.A. Smith ³⁹, H.A. Smith ¹²⁷, J.L. Smith ¹⁰², R. Smith ¹⁴⁴,
 M. Smizanska ⁹², K. Smolek ¹³³, A.A. Snesarev ³⁷, S.R. Snider ¹⁵⁶, H.L. Snoek ¹¹⁵,
 S. Snyder ²⁹, R. Sobie ^{166,v}, A. Soffer ¹⁵², C.A. Solans Sanchez ³⁶, E.Yu. Soldatov ³⁷,
 U. Soldevila ¹⁶⁴, A.A. Solodkov ³⁷, S. Solomon ²⁶, A. Soloshenko ³⁸, K. Solovieva ⁵⁴,
 O.V. Solovyanov ⁴⁰, P. Sommer ³⁶, A. Sonay ¹³, W.Y. Song ^{157b}, A. Sopczak ¹³³, A.L. Soppio ⁹⁷,
 F. Sopkova ^{28b}, J.D. Sorenson ¹¹³, I.R. Sotarriva Alvarez ¹⁵⁵, V. Sothilingam ^{63a},
 O.J. Soto Sandoval ^{138c,138b}, S. Sottocornola ⁶⁸, R. Soualah ¹⁶¹, Z. Soumami ^{35e}, D. South ⁴⁸,
 N. Soybelman ¹⁷⁰, S. Spagnolo ^{70a,70b}, M. Spalla ¹¹¹, D. Sperlich ⁵⁴, G. Spigo ³⁶, S. Spinali ⁹²,
 D.P. Spiteri ⁵⁹, M. Spousta ¹³⁴, E.J. Staats ³⁴, R. Stamen ^{63a}, A. Stampeki ²⁰, M. Standke ²⁴,
 E. Stanecka ⁸⁷, W. Stanek-Maslouska ⁴⁸, M.V. Stange ⁵⁰, B. Stanislaus ^{17a}, M.M. Stanitzki ⁴⁸,
 B. Stapf ⁴⁸, E.A. Starchenko ³⁷, G.H. Stark ¹³⁷, J. Stark ⁹⁰, P. Staroba ¹³², P. Starovoitov ^{63a},
 S. Stärz ¹⁰⁵, R. Staszewski ⁸⁷, G. Stavropoulos ⁴⁶, J. Steentoft ¹⁶², P. Steinberg ²⁹,
 B. Stelzer ^{143,157a}, H.J. Stelzer ¹³⁰, O. Stelzer-Chilton ^{157a}, H. Stenzel ⁵⁸, T.J. Stevenson ¹⁴⁷,
 G.A. Stewart ³⁶, J.R. Stewart ¹²², M.C. Stockton ³⁶, G. Stoicea ^{27b}, M. Stolarski ^{131a},
 S. Stonjek ¹¹¹, A. Straessner ⁵⁰, J. Strandberg ¹⁴⁵, S. Strandberg ^{47a,47b}, M. Stratmann ¹⁷²,
 M. Strauss ¹²¹, T. Streblor ¹⁰³, P. Strizenec ^{28b}, R. Ströhmer ¹⁶⁷, D.M. Strom ¹²⁴,
 R. Stroynowski ⁴⁴, A. Strubig ^{47a,47b}, S.A. Stucci ²⁹, B. Stugu ¹⁶, J. Stupak ¹²¹, N.A. Styles ⁴⁸,
 D. Su ¹⁴⁴, S. Su ^{62a}, W. Su ^{62d}, X. Su ^{62a}, D. Suchy ^{28a}, K. Sugizaki ¹⁵⁴, V.V. Sulin ³⁷,
 M.J. Sullivan ⁹³, D.M.S. Sultan ¹²⁷, L. Sultanaliyeva ³⁷, S. Sultansoy ^{3b}, T. Sumida ⁸⁸,
 S. Sun ¹⁰⁷, S. Sun ¹⁷¹, O. Sunneborn Gudnadottir ¹⁶², N. Sur ¹⁰³, M.R. Sutton ¹⁴⁷,
 H. Suzuki ¹⁵⁸, M. Svatos ¹³², M. Swiatlowski ^{157a}, T. Swirski ¹⁶⁷, I. Sykora ^{28a}, M. Sykora ¹³⁴,
 T. Sykora ¹³⁴, D. Ta ¹⁰¹, K. Tackmann ^{48,s}, A. Taffard ¹⁶⁰, R. Tafirout ^{157a},
 J.S. Tafuya Vargas ⁶⁶, Y. Takubo ⁸⁴, M. Talby ¹⁰³, A.A. Talyshev ³⁷, K.C. Tam ^{64b},
 N.M. Tamir ¹⁵², A. Tanaka ¹⁵⁴, J. Tanaka ¹⁵⁴, R. Tanaka ⁶⁶, M. Tanasini ¹⁴⁶, Z. Tao ¹⁶⁵,
 S. Tapia Araya ^{138f}, S. Tapprogge ¹⁰¹, A. Tarek Abouelfadl Mohamed ¹⁰⁸, S. Tarem ¹⁵¹,
 K. Tariq ^{14a}, G. Tarna ^{27b}, G.F. Tartarelli ^{71a}, M.J. Tartarin ⁹⁰, P. Tas ¹³⁴, M. Tasevsky ¹³²,
 E. Tassi ^{43b,43a}, A.C. Tate ¹⁶³, G. Tateno ¹⁵⁴, Y. Tayalati ^{35e,u}, G.N. Taylor ¹⁰⁶, W. Taylor ^{157b},
 A.S. Tee ¹⁷¹, R. Teixeira De Lima ¹⁴⁴, P. Teixeira-Dias ⁹⁶, J.J. Teoh ¹⁵⁶, K. Terashi ¹⁵⁴,
 J. Terron ¹⁰⁰, S. Terzo ¹³, M. Testa ⁵³, R.J. Teuscher ^{156,v}, A. Thaler ⁷⁹, O. Theiner ⁵⁶,
 N. Themistokleous ⁵², T. Thevenaux-Pelzer ¹⁰³, O. Thielmann ¹⁷², D.W. Thomas ⁹⁶,

J.P. Thomas ²⁰, E.A. Thompson ^{17a}, P.D. Thompson ²⁰, E. Thomson ¹²⁹, R.E. Thornberry ⁴⁴, C. Tian ^{62a}, Y. Tian ⁵⁵, V. Tikhomirov ^{37,a}, Yu.A. Tikhonov ³⁷, S. Timoshenko ³⁷, D. Timoshyn ¹³⁴, E.X.L. Ting ¹, P. Tipton ¹⁷³, A. Tishelman-Charny ²⁹, S.H. Tlou ^{33g}, K. Todome ¹⁵⁵, S. Todorova-Nova ¹³⁴, S. Todt ⁵⁰, L. Toffolin ^{69a,69c}, M. Togawa ⁸⁴, J. Tojo ⁸⁹, S. Tokár ^{28a}, K. Tokushuku ⁸⁴, O. Toldaiev ⁶⁸, R. Tombs ³², M. Tomoto ^{84,112}, L. Tompkins ^{144,l}, K.W. Topolnicki ^{86b}, E. Torrence ¹²⁴, H. Torres ⁹⁰, E. Torró Pastor ¹⁶⁴, M. Toscani ³⁰, C. Tosciri ³⁹, M. Tost ¹¹, D.R. Tovey ¹⁴⁰, A. Traeet ¹⁶, I.S. Trandafir ^{27b}, T. Trefzger ¹⁶⁷, A. Tricoli ²⁹, I.M. Trigger ^{157a}, S. Trincaz-Duvoid ¹²⁸, D.A. Trischuk ²⁶, B. Trocmé ⁶⁰, L. Truong ^{33c}, M. Trzebinski ⁸⁷, A. Trzupiek ⁸⁷, F. Tsai ¹⁴⁶, M. Tsai ¹⁰⁷, A. Tsiamis ^{153,d}, P.V. Tsiareshka ³⁷, S. Tsigaridas ^{157a}, A. Tsigotis ^{153,q}, V. Tsiskaridze ¹⁵⁶, E.G. Tskhadadze ^{150a}, M. Tsopoulou ¹⁵³, Y. Tsujikawa ⁸⁸, I.I. Tsukerman ³⁷, V. Tsulaia ^{17a}, S. Tsuno ⁸⁴, K. Tsuru ¹¹⁹, D. Tsybychev ¹⁴⁶, Y. Tu ^{64b}, A. Tudorache ^{27b}, V. Tudorache ^{27b}, A.N. Tuna ⁶¹, S. Turchikhin ^{57b,57a}, I. Turk Cakir ^{3a}, R. Turra ^{71a}, T. Turtuvshin ^{38,w}, P.M. Tuts ⁴¹, S. Tzamarias ^{153,d}, E. Tzovara ¹⁰¹, F. Ukegawa ¹⁵⁸, P.A. Ulloa Poblete ^{138c,138b}, E.N. Umaka ²⁹, G. Unal ³⁶, A. Undrus ²⁹, G. Unel ¹⁶⁰, J. Urban ^{28b}, P. Urrejola ^{138a}, G. Usai ⁸, R. Ushioda ¹⁵⁵, M. Usman ¹⁰⁹, Z. Uysal ⁸², V. Vacek ¹³³, B. Vachon ¹⁰⁵, T. Vafeiadis ³⁶, A. Vaitkus ⁹⁷, C. Valderanis ¹¹⁰, E. Valdes Santurio ^{47a,47b}, M. Valente ^{157a}, S. Valentinetti ^{23b,23a}, A. Valero ¹⁶⁴, E. Valiente Moreno ¹⁶⁴, A. Vallier ⁹⁰, J.A. Valls Ferrer ¹⁶⁴, D.R. Van Arneeman ¹¹⁵, T.R. Van Daalen ¹³⁹, A. Van Der Graaf ⁴⁹, P. Van Gemmeren ⁶, M. Van Rijnbach ³⁶, S. Van Stroud ⁹⁷, I. Van Vulpen ¹¹⁵, P. Vana ¹³⁴, M. Vanadia ^{76a,76b}, W. Vandelli ³⁶, E.R. Vandewall ¹²², D. Vannicola ¹⁵², L. Vannoli ⁵³, R. Vari ^{75a}, E.W. Varnes ⁷, C. Varni ^{17b}, T. Varol ¹⁴⁹, D. Varouchas ⁶⁶, L. Variiale ¹⁶⁴, K.E. Varvell ¹⁴⁸, M.E. Vasile ^{27b}, L. Vaslin ⁸⁴, G.A. Vasquez ¹⁶⁶, A. Vasyukov ³⁸, R. Vavricka ¹⁰¹, T. Vazquez Schroeder ³⁶, J. Veatch ³¹, V. Vecchio ¹⁰², M.J. Veen ¹⁰⁴, I. Veliscek ²⁹, L.M. Veloce ¹⁵⁶, F. Veloso ^{131a,131c}, S. Veneziano ^{75a}, A. Ventura ^{70a,70b}, S. Ventura Gonzalez ¹³⁶, A. Verbytskyi ¹¹¹, M. Verducci ^{74a,74b}, C. Vergis ⁹⁵, M. Verissimo De Araujo ^{83b}, W. Verkerke ¹¹⁵, J.C. Vermeulen ¹¹⁵, C. Vernieri ¹⁴⁴, M. Vessella ¹⁰⁴, M.C. Vetterli ^{143,ad}, A. Vgenopoulos ^{153,d}, N. Viaux Maira ^{138f}, T. Vickey ¹⁴⁰, O.E. Vickey Boeriu ¹⁴⁰, G.H.A. Viehhauser ¹²⁷, L. Vigani ^{63b}, M. Villa ^{23b,23a}, M. Villaplana Perez ¹⁶⁴, E.M. Villhauer ⁵², E. Vilucchi ⁵³, M.G. Vincter ³⁴, A. Visibile ¹¹⁵, C. Vittori ³⁶, I. Vivarelli ^{23b,23a}, E. Voevodina ¹¹¹, F. Vogel ¹¹⁰, J.C. Voigt ⁵⁰, P. Vokac ¹³³, Yu. Volkotrub ^{86b}, J. Von Ahnen ⁴⁸, E. Von Toerne ²⁴, B. Vormwald ³⁶, V. Vorobel ¹³⁴, K. Vorobev ³⁷, M. Vos ¹⁶⁴, K. Voss ¹⁴², M. Vozak ¹¹⁵, L. Vozdecky ¹²¹, N. Vranjes ¹⁵, M. Vranjes Milosavljevic ¹⁵, M. Vreeswijk ¹¹⁵, N.K. Vu ^{62d,62c}, R. Vuillermet ³⁶, O. Vujinovic ¹⁰¹, I. Vukotic ³⁹, S. Wada ¹⁵⁸, C. Wagner ¹⁰⁴, J.M. Wagner ^{17a}, W. Wagner ¹⁷², S. Wahdan ¹⁷², H. Wahlberg ⁹¹, M. Wakida ¹¹², J. Walder ¹³⁵, R. Walker ¹¹⁰, W. Walkowiak ¹⁴², A. Wall ¹²⁹, E.J. Wallin ⁹⁹, T. Wamorkar ⁶, A.Z. Wang ¹³⁷, C. Wang ¹⁰¹, C. Wang ¹¹, H. Wang ^{17a}, J. Wang ^{64c}, R. Wang ⁶¹, R. Wang ⁶, S.M. Wang ¹⁴⁹, S. Wang ^{62b}, S. Wang ^{14a}, T. Wang ^{62a}, W.T. Wang ⁸⁰, W. Wang ^{14a}, X. Wang ^{14c}, X. Wang ¹⁶³, X. Wang ^{62c}, Y. Wang ^{62d}, Y. Wang ^{14c}, Z. Wang ¹⁰⁷, Z. Wang ^{62d,51,62c}, Z. Wang ¹⁰⁷, A. Warburton ¹⁰⁵, R.J. Ward ²⁰, N. Warrack ⁵⁹, S. Waterhouse ⁹⁶, A.T. Watson ²⁰, H. Watson ⁵⁹, M.F. Watson ²⁰, E. Watton ^{59,135}, G. Watts ¹³⁹, B.M. Waugh ⁹⁷, J.M. Webb ⁵⁴, C. Weber ²⁹, H.A. Weber ¹⁸, M.S. Weber ¹⁹, S.M. Weber ^{63a}, C. Wei ^{62a}, Y. Wei ⁵⁴, A.R. Weidberg ¹²⁷, E.J. Weik ¹¹⁸, J. Weingarten ⁴⁹, C. Weiser ⁵⁴, C.J. Wells ⁴⁸, T. Wenaus ²⁹, B. Wendland ⁴⁹, T. Wengler ³⁶, N.S. Wenke ¹¹¹, N. Wermes ²⁴, M. Wessels ^{63a}, A.M. Wharton ⁹², A.S. White ⁶¹, A. White ⁸, M.J. White ¹, D. Whiteson ¹⁶⁰, L. Wickremasinghe ¹²⁵, W. Wiedenmann ¹⁷¹, M. Wielers ¹³⁵, C. Wiglesworth ⁴², D.J. Wilbern ¹²¹, H.G. Wilkens ³⁶, J.J.H. Wilkinson ³², D.M. Williams ⁴¹, H.H. Williams ¹²⁹, S. Williams ³², S. Willocq ¹⁰⁴, B.J. Wilson ¹⁰², P.J. Windischhofer ³⁹,

F.I. Winkel ³⁰, F. Winklmeier ¹²⁴, B.T. Winter ⁵⁴, J.K. Winter ¹⁰², M. Wittgen ¹⁴⁴, M. Wobisch ⁹⁸, T. Wojtkowski ⁶⁰, Z. Wolffs ¹¹⁵, J. Wollrath ¹⁶⁰, M.W. Wolter ⁸⁷, H. Wolters ^{131a,131c}, M.C. Wong ¹³⁷, E.L. Woodward ⁴¹, S.D. Worm ⁴⁸, B.K. Wosiek ⁸⁷, K.W. Woźniak ⁸⁷, S. Wozniowski ⁵⁵, K. Wraight ⁵⁹, C. Wu ²⁰, M. Wu ^{14d}, M. Wu ¹¹⁴, S.L. Wu ¹⁷¹, X. Wu ⁵⁶, Y. Wu ^{62a}, Z. Wu ⁴, J. Wuerzinger ^{111,ab}, T.R. Wyatt ¹⁰², B.M. Wynne ⁵², S. Xella ⁴², L. Xia ^{14c}, M. Xia ^{14b}, J. Xiang ^{64c}, M. Xie ^{62a}, S. Xin ^{14a,14e}, A. Xiong ¹²⁴, J. Xiong ^{17a}, D. Xu ^{14a}, H. Xu ^{62a}, L. Xu ^{62a}, R. Xu ¹²⁹, T. Xu ¹⁰⁷, Y. Xu ^{14b}, Z. Xu ⁵², Z. Xu ^{14c}, B. Yabsley ¹⁴⁸, S. Yacoob ^{33a}, Y. Yamaguchi ¹⁵⁵, E. Yamashita ¹⁵⁴, H. Yamauchi ¹⁵⁸, T. Yamazaki ^{17a}, Y. Yamazaki ⁸⁵, J. Yan ^{62c}, S. Yan ⁵⁹, Z. Yan ¹⁰⁴, H.J. Yang ^{62c,62d}, H.T. Yang ^{62a}, S. Yang ^{62a}, T. Yang ^{64c}, X. Yang ³⁶, X. Yang ^{14a}, Y. Yang ⁴⁴, Y. Yang ^{62a}, Z. Yang ^{62a}, W-M. Yao ^{17a}, H. Ye ^{14c}, H. Ye ⁵⁵, J. Ye ^{14a}, S. Ye ²⁹, X. Ye ^{62a}, Y. Yeh ⁹⁷, I. Yeletsikh ³⁸, B.K. Yeo ^{17b}, M.R. Yexley ⁹⁷, T.P. Yildirim ¹²⁷, P. Yin ⁴¹, K. Yorita ¹⁶⁹, S. Younas ^{27b}, C.J.S. Young ³⁶, C. Young ¹⁴⁴, C. Yu ^{14a,14e}, Y. Yu ^{62a}, M. Yuan ¹⁰⁷, R. Yuan ^{62d,62c}, L. Yue ⁹⁷, M. Zaazoua ^{62a}, B. Zabinski ⁸⁷, E. Zaid ⁵², Z.K. Zak ⁸⁷, T. Zakareishvili ¹⁶⁴, N. Zakharchuk ³⁴, S. Zambito ⁵⁶, J.A. Zamora Saa ^{138d,138b}, J. Zang ¹⁵⁴, D. Zanzi ⁵⁴, O. Zaplatilek ¹³³, C. Zeitnitz ¹⁷², H. Zeng ^{14a}, J.C. Zeng ¹⁶³, D.T. Zenger Jr ²⁶, O. Zenin ³⁷, T. Ženiš ^{28a}, S. Zenz ⁹⁵, S. Zerradi ^{35a}, D. Zerwas ⁶⁶, M. Zhai ^{14a,14e}, D.F. Zhang ¹⁴⁰, J. Zhang ^{62b}, J. Zhang ⁶, K. Zhang ^{14a,14e}, L. Zhang ^{62a}, L. Zhang ^{14c}, P. Zhang ^{14a,14e}, R. Zhang ¹⁷¹, S. Zhang ¹⁰⁷, S. Zhang ⁹⁰, T. Zhang ¹⁵⁴, X. Zhang ^{62c}, X. Zhang ^{62b}, Y. Zhang ^{62c}, Y. Zhang ⁹⁷, Y. Zhang ^{14c}, Z. Zhang ^{17a}, Z. Zhang ^{62b}, Z. Zhang ⁶⁶, H. Zhao ¹³⁹, T. Zhao ^{62b}, Y. Zhao ¹³⁷, Z. Zhao ^{62a}, Z. Zhao ^{62a}, A. Zhemchugov ³⁸, J. Zheng ^{14c}, K. Zheng ¹⁶³, X. Zheng ^{62a}, Z. Zheng ¹⁴⁴, D. Zhong ¹⁶³, B. Zhou ¹⁰⁷, H. Zhou ⁷, N. Zhou ^{62c}, Y. Zhou ^{14b}, Y. Zhou ^{14c}, Y. Zhou ⁷, C.G. Zhu ^{62b}, J. Zhu ¹⁰⁷, X. Zhu ^{62d}, Y. Zhu ^{62c}, Y. Zhu ^{62a}, X. Zhuang ^{14a}, K. Zhukov ³⁷, N.I. Zimine ³⁸, J. Zinsser ^{63b}, M. Ziolkowski ¹⁴², L. Živković ¹⁵, A. Zoccoli ^{23b,23a}, K. Zoch ⁶¹, T.G. Zorbas ¹⁴⁰, O. Zormpa ⁴⁶, W. Zou ⁴¹, L. Zwalinski ³⁶.

¹Department of Physics, University of Adelaide, Adelaide; Australia.

²Department of Physics, University of Alberta, Edmonton AB; Canada.

^{3(a)}Department of Physics, Ankara University, Ankara; ^(b)Division of Physics, TOBB University of Economics and Technology, Ankara; Türkiye.

⁴LAPP, Université Savoie Mont Blanc, CNRS/IN2P3, Annecy; France.

⁵APC, Université Paris Cité, CNRS/IN2P3, Paris; France.

⁶High Energy Physics Division, Argonne National Laboratory, Argonne IL; United States of America.

⁷Department of Physics, University of Arizona, Tucson AZ; United States of America.

⁸Department of Physics, University of Texas at Arlington, Arlington TX; United States of America.

⁹Physics Department, National and Kapodistrian University of Athens, Athens; Greece.

¹⁰Physics Department, National Technical University of Athens, Zografou; Greece.

¹¹Department of Physics, University of Texas at Austin, Austin TX; United States of America.

¹²Institute of Physics, Azerbaijan Academy of Sciences, Baku; Azerbaijan.

¹³Institut de Física d'Altes Energies (IFAE), Barcelona Institute of Science and Technology, Barcelona; Spain.

^{14(a)}Institute of High Energy Physics, Chinese Academy of Sciences, Beijing; ^(b)Physics Department, Tsinghua University, Beijing; ^(c)Department of Physics, Nanjing University, Nanjing; ^(d)School of Science, Shenzhen Campus of Sun Yat-sen University; ^(e)University of Chinese Academy of Science (UCAS), Beijing; China.

¹⁵Institute of Physics, University of Belgrade, Belgrade; Serbia.

¹⁶Department for Physics and Technology, University of Bergen, Bergen; Norway.

- ¹⁷(*a*) Physics Division, Lawrence Berkeley National Laboratory, Berkeley CA; (*b*) University of California, Berkeley CA; United States of America.
- ¹⁸Institut für Physik, Humboldt Universität zu Berlin, Berlin; Germany.
- ¹⁹Albert Einstein Center for Fundamental Physics and Laboratory for High Energy Physics, University of Bern, Bern; Switzerland.
- ²⁰School of Physics and Astronomy, University of Birmingham, Birmingham; United Kingdom.
- ²¹(*a*) Department of Physics, Bogazici University, Istanbul; (*b*) Department of Physics Engineering, Gaziantep University, Gaziantep; (*c*) Department of Physics, Istanbul University, Istanbul; Türkiye.
- ²²(*a*) Facultad de Ciencias y Centro de Investigaciones, Universidad Antonio Nariño, Bogotá; (*b*) Departamento de Física, Universidad Nacional de Colombia, Bogotá; Colombia.
- ²³(*a*) Dipartimento di Fisica e Astronomia A. Righi, Università di Bologna, Bologna; (*b*) INFN Sezione di Bologna; Italy.
- ²⁴Physikalisches Institut, Universität Bonn, Bonn; Germany.
- ²⁵Department of Physics, Boston University, Boston MA; United States of America.
- ²⁶Department of Physics, Brandeis University, Waltham MA; United States of America.
- ²⁷(*a*) Transilvania University of Brasov, Brasov; (*b*) Horia Hulubei National Institute of Physics and Nuclear Engineering, Bucharest; (*c*) Department of Physics, Alexandru Ioan Cuza University of Iasi, Iasi; (*d*) National Institute for Research and Development of Isotopic and Molecular Technologies, Physics Department, Cluj-Napoca; (*e*) National University of Science and Technology Politehnica, Bucharest; (*f*) West University in Timisoara, Timisoara; (*g*) Faculty of Physics, University of Bucharest, Bucharest; Romania.
- ²⁸(*a*) Faculty of Mathematics, Physics and Informatics, Comenius University, Bratislava; (*b*) Department of Subnuclear Physics, Institute of Experimental Physics of the Slovak Academy of Sciences, Kosice; Slovak Republic.
- ²⁹Physics Department, Brookhaven National Laboratory, Upton NY; United States of America.
- ³⁰Universidad de Buenos Aires, Facultad de Ciencias Exactas y Naturales, Departamento de Física, y CONICET, Instituto de Física de Buenos Aires (IFIBA), Buenos Aires; Argentina.
- ³¹California State University, CA; United States of America.
- ³²Cavendish Laboratory, University of Cambridge, Cambridge; United Kingdom.
- ³³(*a*) Department of Physics, University of Cape Town, Cape Town; (*b*) iThemba Labs, Western Cape; (*c*) Department of Mechanical Engineering Science, University of Johannesburg, Johannesburg; (*d*) National Institute of Physics, University of the Philippines Diliman (Philippines); (*e*) University of South Africa, Department of Physics, Pretoria; (*f*) University of Zululand, KwaDlangezwa; (*g*) School of Physics, University of the Witwatersrand, Johannesburg; South Africa.
- ³⁴Department of Physics, Carleton University, Ottawa ON; Canada.
- ³⁵(*a*) Faculté des Sciences Ain Chock, Réseau Universitaire de Physique des Hautes Energies - Université Hassan II, Casablanca; (*b*) Faculté des Sciences, Université Ibn-Tofail, Kénitra; (*c*) Faculté des Sciences Semlalia, Université Cadi Ayyad, LPHEA-Marrakech; (*d*) LPMR, Faculté des Sciences, Université Mohamed Premier, Oujda; (*e*) Faculté des sciences, Université Mohammed V, Rabat; (*f*) Institute of Applied Physics, Mohammed VI Polytechnic University, Ben Guerir; Morocco.
- ³⁶CERN, Geneva; Switzerland.
- ³⁷Affiliated with an institute covered by a cooperation agreement with CERN.
- ³⁸Affiliated with an international laboratory covered by a cooperation agreement with CERN.
- ³⁹Enrico Fermi Institute, University of Chicago, Chicago IL; United States of America.
- ⁴⁰LPC, Université Clermont Auvergne, CNRS/IN2P3, Clermont-Ferrand; France.
- ⁴¹Nevis Laboratory, Columbia University, Irvington NY; United States of America.
- ⁴²Niels Bohr Institute, University of Copenhagen, Copenhagen; Denmark.
- ⁴³(*a*) Dipartimento di Fisica, Università della Calabria, Rende; (*b*) INFN Gruppo Collegato di Cosenza,

Laboratori Nazionali di Frascati; Italy.

⁴⁴Physics Department, Southern Methodist University, Dallas TX; United States of America.

⁴⁵Physics Department, University of Texas at Dallas, Richardson TX; United States of America.

⁴⁶National Centre for Scientific Research "Demokritos", Agia Paraskevi; Greece.

⁴⁷(^a) Department of Physics, Stockholm University; (^b) Oskar Klein Centre, Stockholm; Sweden.

⁴⁸Deutsches Elektronen-Synchrotron DESY, Hamburg and Zeuthen; Germany.

⁴⁹Fakultät Physik, Technische Universität Dortmund, Dortmund; Germany.

⁵⁰Institut für Kern- und Teilchenphysik, Technische Universität Dresden, Dresden; Germany.

⁵¹Department of Physics, Duke University, Durham NC; United States of America.

⁵²SUPA - School of Physics and Astronomy, University of Edinburgh, Edinburgh; United Kingdom.

⁵³INFN e Laboratori Nazionali di Frascati, Frascati; Italy.

⁵⁴Physikalisches Institut, Albert-Ludwigs-Universität Freiburg, Freiburg; Germany.

⁵⁵II. Physikalisches Institut, Georg-August-Universität Göttingen, Göttingen; Germany.

⁵⁶Département de Physique Nucléaire et Corpusculaire, Université de Genève, Genève; Switzerland.

⁵⁷(^a) Dipartimento di Fisica, Università di Genova, Genova; (^b) INFN Sezione di Genova; Italy.

⁵⁸II. Physikalisches Institut, Justus-Liebig-Universität Giessen, Giessen; Germany.

⁵⁹SUPA - School of Physics and Astronomy, University of Glasgow, Glasgow; United Kingdom.

⁶⁰LPSC, Université Grenoble Alpes, CNRS/IN2P3, Grenoble INP, Grenoble; France.

⁶¹Laboratory for Particle Physics and Cosmology, Harvard University, Cambridge MA; United States of America.

⁶²(^a) Department of Modern Physics and State Key Laboratory of Particle Detection and Electronics, University of Science and Technology of China, Hefei; (^b) Institute of Frontier and Interdisciplinary Science and Key Laboratory of Particle Physics and Particle Irradiation (MOE), Shandong University, Qingdao; (^c) School of Physics and Astronomy, Shanghai Jiao Tong University, Key Laboratory for Particle Astrophysics and Cosmology (MOE), SKLPPC, Shanghai; (^d) Tsung-Dao Lee Institute, Shanghai; (^e) School of Physics and Microelectronics, Zhengzhou University; China.

⁶³(^a) Kirchhoff-Institut für Physik, Ruprecht-Karls-Universität Heidelberg, Heidelberg; (^b) Physikalisches Institut, Ruprecht-Karls-Universität Heidelberg, Heidelberg; Germany.

⁶⁴(^a) Department of Physics, Chinese University of Hong Kong, Shatin, N.T., Hong Kong; (^b) Department of Physics, University of Hong Kong, Hong Kong; (^c) Department of Physics and Institute for Advanced Study, Hong Kong University of Science and Technology, Clear Water Bay, Kowloon, Hong Kong; China.

⁶⁵Department of Physics, National Tsing Hua University, Hsinchu; Taiwan.

⁶⁶IJCLab, Université Paris-Saclay, CNRS/IN2P3, 91405, Orsay; France.

⁶⁷Centro Nacional de Microelectrónica (IMB-CNM-CSIC), Barcelona; Spain.

⁶⁸Department of Physics, Indiana University, Bloomington IN; United States of America.

⁶⁹(^a) INFN Gruppo Collegato di Udine, Sezione di Trieste, Udine; (^b) ICTP, Trieste; (^c) Dipartimento Politecnico di Ingegneria e Architettura, Università di Udine, Udine; Italy.

⁷⁰(^a) INFN Sezione di Lecce; (^b) Dipartimento di Matematica e Fisica, Università del Salento, Lecce; Italy.

⁷¹(^a) INFN Sezione di Milano; (^b) Dipartimento di Fisica, Università di Milano, Milano; Italy.

⁷²(^a) INFN Sezione di Napoli; (^b) Dipartimento di Fisica, Università di Napoli, Napoli; Italy.

⁷³(^a) INFN Sezione di Pavia; (^b) Dipartimento di Fisica, Università di Pavia, Pavia; Italy.

⁷⁴(^a) INFN Sezione di Pisa; (^b) Dipartimento di Fisica E. Fermi, Università di Pisa, Pisa; Italy.

⁷⁵(^a) INFN Sezione di Roma; (^b) Dipartimento di Fisica, Sapienza Università di Roma, Roma; Italy.

⁷⁶(^a) INFN Sezione di Roma Tor Vergata; (^b) Dipartimento di Fisica, Università di Roma Tor Vergata, Roma; Italy.

⁷⁷(^a) INFN Sezione di Roma Tre; (^b) Dipartimento di Matematica e Fisica, Università Roma Tre, Roma; Italy.

- ⁷⁸(*a*) INFN-TIFPA; (*b*) Università degli Studi di Trento, Trento; Italy.
- ⁷⁹Universität Innsbruck, Department of Astro and Particle Physics, Innsbruck; Austria.
- ⁸⁰University of Iowa, Iowa City IA; United States of America.
- ⁸¹Department of Physics and Astronomy, Iowa State University, Ames IA; United States of America.
- ⁸²Istinye University, Sariyer, Istanbul; Türkiye.
- ⁸³(*a*) Departamento de Engenharia Elétrica, Universidade Federal de Juiz de Fora (UFJF), Juiz de Fora; (*b*) Universidade Federal do Rio De Janeiro COPPE/EE/IF, Rio de Janeiro; (*c*) Instituto de Física, Universidade de São Paulo, São Paulo; (*d*) Rio de Janeiro State University, Rio de Janeiro; (*e*) Federal University of Bahia, Bahia; Brazil.
- ⁸⁴KEK, High Energy Accelerator Research Organization, Tsukuba; Japan.
- ⁸⁵Graduate School of Science, Kobe University, Kobe; Japan.
- ⁸⁶(*a*) AGH University of Krakow, Faculty of Physics and Applied Computer Science, Krakow; (*b*) Marian Smoluchowski Institute of Physics, Jagiellonian University, Krakow; Poland.
- ⁸⁷Institute of Nuclear Physics Polish Academy of Sciences, Krakow; Poland.
- ⁸⁸Faculty of Science, Kyoto University, Kyoto; Japan.
- ⁸⁹Research Center for Advanced Particle Physics and Department of Physics, Kyushu University, Fukuoka ; Japan.
- ⁹⁰L2IT, Université de Toulouse, CNRS/IN2P3, UPS, Toulouse; France.
- ⁹¹Instituto de Física La Plata, Universidad Nacional de La Plata and CONICET, La Plata; Argentina.
- ⁹²Physics Department, Lancaster University, Lancaster; United Kingdom.
- ⁹³Oliver Lodge Laboratory, University of Liverpool, Liverpool; United Kingdom.
- ⁹⁴Department of Experimental Particle Physics, Jožef Stefan Institute and Department of Physics, University of Ljubljana, Ljubljana; Slovenia.
- ⁹⁵School of Physics and Astronomy, Queen Mary University of London, London; United Kingdom.
- ⁹⁶Department of Physics, Royal Holloway University of London, Egham; United Kingdom.
- ⁹⁷Department of Physics and Astronomy, University College London, London; United Kingdom.
- ⁹⁸Louisiana Tech University, Ruston LA; United States of America.
- ⁹⁹Fysiska institutionen, Lunds universitet, Lund; Sweden.
- ¹⁰⁰Departamento de Física Teórica C-15 and CIAFF, Universidad Autónoma de Madrid, Madrid; Spain.
- ¹⁰¹Institut für Physik, Universität Mainz, Mainz; Germany.
- ¹⁰²School of Physics and Astronomy, University of Manchester, Manchester; United Kingdom.
- ¹⁰³CPPM, Aix-Marseille Université, CNRS/IN2P3, Marseille; France.
- ¹⁰⁴Department of Physics, University of Massachusetts, Amherst MA; United States of America.
- ¹⁰⁵Department of Physics, McGill University, Montreal QC; Canada.
- ¹⁰⁶School of Physics, University of Melbourne, Victoria; Australia.
- ¹⁰⁷Department of Physics, University of Michigan, Ann Arbor MI; United States of America.
- ¹⁰⁸Department of Physics and Astronomy, Michigan State University, East Lansing MI; United States of America.
- ¹⁰⁹Group of Particle Physics, University of Montreal, Montreal QC; Canada.
- ¹¹⁰Fakultät für Physik, Ludwig-Maximilians-Universität München, München; Germany.
- ¹¹¹Max-Planck-Institut für Physik (Werner-Heisenberg-Institut), München; Germany.
- ¹¹²Graduate School of Science and Kobayashi-Maskawa Institute, Nagoya University, Nagoya; Japan.
- ¹¹³Department of Physics and Astronomy, University of New Mexico, Albuquerque NM; United States of America.
- ¹¹⁴Institute for Mathematics, Astrophysics and Particle Physics, Radboud University/Nikhef, Nijmegen; Netherlands.
- ¹¹⁵Nikhef National Institute for Subatomic Physics and University of Amsterdam, Amsterdam;

Netherlands.

¹¹⁶Department of Physics, Northern Illinois University, DeKalb IL; United States of America.

¹¹⁷^(a)New York University Abu Dhabi, Abu Dhabi;^(b)United Arab Emirates University, Al Ain; United Arab Emirates.

¹¹⁸Department of Physics, New York University, New York NY; United States of America.

¹¹⁹Ochanomizu University, Otsuka, Bunkyo-ku, Tokyo; Japan.

¹²⁰Ohio State University, Columbus OH; United States of America.

¹²¹Homer L. Dodge Department of Physics and Astronomy, University of Oklahoma, Norman OK; United States of America.

¹²²Department of Physics, Oklahoma State University, Stillwater OK; United States of America.

¹²³Palacký University, Joint Laboratory of Optics, Olomouc; Czech Republic.

¹²⁴Institute for Fundamental Science, University of Oregon, Eugene, OR; United States of America.

¹²⁵Graduate School of Science, Osaka University, Osaka; Japan.

¹²⁶Department of Physics, University of Oslo, Oslo; Norway.

¹²⁷Department of Physics, Oxford University, Oxford; United Kingdom.

¹²⁸LPNHE, Sorbonne Université, Université Paris Cité, CNRS/IN2P3, Paris; France.

¹²⁹Department of Physics, University of Pennsylvania, Philadelphia PA; United States of America.

¹³⁰Department of Physics and Astronomy, University of Pittsburgh, Pittsburgh PA; United States of America.

¹³¹^(a)Laboratório de Instrumentação e Física Experimental de Partículas - LIP, Lisboa;^(b)Departamento de Física, Faculdade de Ciências, Universidade de Lisboa, Lisboa;^(c)Departamento de Física, Universidade de Coimbra, Coimbra;^(d)Centro de Física Nuclear da Universidade de Lisboa, Lisboa;^(e)Departamento de Física, Universidade do Minho, Braga;^(f)Departamento de Física Teórica y del Cosmos, Universidad de Granada, Granada (Spain);^(g)Departamento de Física, Instituto Superior Técnico, Universidade de Lisboa, Lisboa; Portugal.

¹³²Institute of Physics of the Czech Academy of Sciences, Prague; Czech Republic.

¹³³Czech Technical University in Prague, Prague; Czech Republic.

¹³⁴Charles University, Faculty of Mathematics and Physics, Prague; Czech Republic.

¹³⁵Particle Physics Department, Rutherford Appleton Laboratory, Didcot; United Kingdom.

¹³⁶IRFU, CEA, Université Paris-Saclay, Gif-sur-Yvette; France.

¹³⁷Santa Cruz Institute for Particle Physics, University of California Santa Cruz, Santa Cruz CA; United States of America.

¹³⁸^(a)Departamento de Física, Pontificia Universidad Católica de Chile, Santiago;^(b)Millennium Institute for Subatomic physics at high energy frontier (SAPHIR), Santiago;^(c)Instituto de Investigación Multidisciplinario en Ciencia y Tecnología, y Departamento de Física, Universidad de La Serena;^(d)Universidad Andres Bello, Department of Physics, Santiago;^(e)Instituto de Alta Investigación, Universidad de Tarapacá, Arica;^(f)Departamento de Física, Universidad Técnica Federico Santa María, Valparaíso; Chile.

¹³⁹Department of Physics, University of Washington, Seattle WA; United States of America.

¹⁴⁰Department of Physics and Astronomy, University of Sheffield, Sheffield; United Kingdom.

¹⁴¹Department of Physics, Shinshu University, Nagano; Japan.

¹⁴²Department Physik, Universität Siegen, Siegen; Germany.

¹⁴³Department of Physics, Simon Fraser University, Burnaby BC; Canada.

¹⁴⁴SLAC National Accelerator Laboratory, Stanford CA; United States of America.

¹⁴⁵Department of Physics, Royal Institute of Technology, Stockholm; Sweden.

¹⁴⁶Departments of Physics and Astronomy, Stony Brook University, Stony Brook NY; United States of America.

- ¹⁴⁷Department of Physics and Astronomy, University of Sussex, Brighton; United Kingdom.
- ¹⁴⁸School of Physics, University of Sydney, Sydney; Australia.
- ¹⁴⁹Institute of Physics, Academia Sinica, Taipei; Taiwan.
- ¹⁵⁰^(a)E. Andronikashvili Institute of Physics, Iv. Javakhishvili Tbilisi State University, Tbilisi; ^(b)High Energy Physics Institute, Tbilisi State University, Tbilisi; ^(c)University of Georgia, Tbilisi; Georgia.
- ¹⁵¹Department of Physics, Technion, Israel Institute of Technology, Haifa; Israel.
- ¹⁵²Raymond and Beverly Sackler School of Physics and Astronomy, Tel Aviv University, Tel Aviv; Israel.
- ¹⁵³Department of Physics, Aristotle University of Thessaloniki, Thessaloniki; Greece.
- ¹⁵⁴International Center for Elementary Particle Physics and Department of Physics, University of Tokyo, Tokyo; Japan.
- ¹⁵⁵Department of Physics, Tokyo Institute of Technology, Tokyo; Japan.
- ¹⁵⁶Department of Physics, University of Toronto, Toronto ON; Canada.
- ¹⁵⁷^(a)TRIUMF, Vancouver BC; ^(b)Department of Physics and Astronomy, York University, Toronto ON; Canada.
- ¹⁵⁸Division of Physics and Tomonaga Center for the History of the Universe, Faculty of Pure and Applied Sciences, University of Tsukuba, Tsukuba; Japan.
- ¹⁵⁹Department of Physics and Astronomy, Tufts University, Medford MA; United States of America.
- ¹⁶⁰Department of Physics and Astronomy, University of California Irvine, Irvine CA; United States of America.
- ¹⁶¹University of Sharjah, Sharjah; United Arab Emirates.
- ¹⁶²Department of Physics and Astronomy, University of Uppsala, Uppsala; Sweden.
- ¹⁶³Department of Physics, University of Illinois, Urbana IL; United States of America.
- ¹⁶⁴Instituto de Física Corpuscular (IFIC), Centro Mixto Universidad de Valencia - CSIC, Valencia; Spain.
- ¹⁶⁵Department of Physics, University of British Columbia, Vancouver BC; Canada.
- ¹⁶⁶Department of Physics and Astronomy, University of Victoria, Victoria BC; Canada.
- ¹⁶⁷Fakultät für Physik und Astronomie, Julius-Maximilians-Universität Würzburg, Würzburg; Germany.
- ¹⁶⁸Department of Physics, University of Warwick, Coventry; United Kingdom.
- ¹⁶⁹Waseda University, Tokyo; Japan.
- ¹⁷⁰Department of Particle Physics and Astrophysics, Weizmann Institute of Science, Rehovot; Israel.
- ¹⁷¹Department of Physics, University of Wisconsin, Madison WI; United States of America.
- ¹⁷²Fakultät für Mathematik und Naturwissenschaften, Fachgruppe Physik, Bergische Universität Wuppertal, Wuppertal; Germany.
- ¹⁷³Department of Physics, Yale University, New Haven CT; United States of America.
- ^a Also Affiliated with an institute covered by a cooperation agreement with CERN.
- ^b Also at An-Najah National University, Nablus; Palestine.
- ^c Also at Borough of Manhattan Community College, City University of New York, New York NY; United States of America.
- ^d Also at Center for Interdisciplinary Research and Innovation (CIRI-AUTH), Thessaloniki; Greece.
- ^e Also at Centro Studi e Ricerche Enrico Fermi; Italy.
- ^f Also at CERN, Geneva; Switzerland.
- ^g Also at Département de Physique Nucléaire et Corpusculaire, Université de Genève, Genève; Switzerland.
- ^h Also at Departament de Física de la Universitat Autònoma de Barcelona, Barcelona; Spain.
- ⁱ Also at Department of Financial and Management Engineering, University of the Aegean, Chios; Greece.
- ^j Also at Department of Physics, California State University, Sacramento; United States of America.
- ^k Also at Department of Physics, King's College London, London; United Kingdom.
- ^l Also at Department of Physics, Stanford University, Stanford CA; United States of America.

- m* Also at Department of Physics, Stellenbosch University; South Africa.
- n* Also at Department of Physics, University of Fribourg, Fribourg; Switzerland.
- o* Also at Department of Physics, University of Thessaly; Greece.
- p* Also at Department of Physics, Westmont College, Santa Barbara; United States of America.
- q* Also at Hellenic Open University, Patras; Greece.
- r* Also at Institutio Catalana de Recerca i Estudis Avancats, ICREA, Barcelona; Spain.
- s* Also at Institut für Experimentalphysik, Universität Hamburg, Hamburg; Germany.
- t* Also at Institute for Nuclear Research and Nuclear Energy (INRNE) of the Bulgarian Academy of Sciences, Sofia; Bulgaria.
- u* Also at Institute of Applied Physics, Mohammed VI Polytechnic University, Ben Guerir; Morocco.
- v* Also at Institute of Particle Physics (IPP); Canada.
- w* Also at Institute of Physics and Technology, Mongolian Academy of Sciences, Ulaanbaatar; Mongolia.
- x* Also at Institute of Physics, Azerbaijan Academy of Sciences, Baku; Azerbaijan.
- y* Also at Institute of Theoretical Physics, Ilia State University, Tbilisi; Georgia.
- z* Also at Lawrence Livermore National Laboratory, Livermore; United States of America.
- aa* Also at National Institute of Physics, University of the Philippines Diliman (Philippines); Philippines.
- ab* Also at Technical University of Munich, Munich; Germany.
- ac* Also at The Collaborative Innovation Center of Quantum Matter (CICQM), Beijing; China.
- ad* Also at TRIUMF, Vancouver BC; Canada.
- ae* Also at Università di Napoli Parthenope, Napoli; Italy.
- af* Also at University of Colorado Boulder, Department of Physics, Colorado; United States of America.
- ag* Also at Washington College, Chestertown, MD; United States of America.
- ah* Also at Yeditepe University, Physics Department, Istanbul; Türkiye.
- * Deceased